

Electronic Thesis and Dissertation Repository

5-31-2017 12:00 AM

Sol-gel Derived Silica-titania Porous Coating for the Surface Modification of Dental Implants

Yili Cheng, *The University of Western Ontario*

Supervisor: Jesse Zhu, *The University of Western Ontario*

Joint Supervisor: Hiran Perinpanayagam, *The University of Western Ontario*

A thesis submitted in partial fulfillment of the requirements for the Master of Engineering Science degree in Chemical and Biochemical Engineering

© Yili Cheng 2017

Follow this and additional works at: <https://ir.lib.uwo.ca/etd>

Recommended Citation

Cheng, Yili, "Sol-gel Derived Silica-titania Porous Coating for the Surface Modification of Dental Implants" (2017). *Electronic Thesis and Dissertation Repository*. 4580.
<https://ir.lib.uwo.ca/etd/4580>

This Dissertation/Thesis is brought to you for free and open access by Scholarship@Western. It has been accepted for inclusion in Electronic Thesis and Dissertation Repository by an authorized administrator of Scholarship@Western. For more information, please contact wlsadmin@uwo.ca.

Abstract

A series of sol-gel derived silica-titania hybrid coatings for dental implants were prepared in this research project to improve the implants' bioactivities. Rosin was used as a space-occupying material to create a porous surface layer with increased roughness. The proper formulation of mixed sols and the parameters for the spin coating procedure were first tested on glass and aluminum substrates. Subsequently the most promising techniques were applied to titanium. SEM analysis was conducted to demonstrate the morphology of the coated specimens. The hardness, adhesion and abrasion resistance of the coated titanium substrates were tested out. Bioactivities of the hybrid coatings on titanium were evaluated by immersing treated specimens into simulated body fluid (1.5SBF). The porous silica-titania hybrid coatings were shown to provide the most desirable surface morphology, mechanical property and bioactivity.

Keywords

Surface modified dental implants, titanium biomaterial, sol-gel spin coating, silica-titania hybrid coating, porous coating, rosin, bioactivity

Table of Contents

Abstract	i
Table of Contents	ii
List of Tables	v
List of Figures	vi
Chapter 1	1
1 Introduction	1
1.1 Sol-gel derived silica-titania porous coating on titanium for dental implants	1
1.2 Objectives	2
Chapter 2	4
2 Literature review	4
2.1 Titanium substrate for dental implants	4
2.1.1 Dental implants made of titanium	4
2.1.2 Surface modifications of titanium substrates	5
2.2 The sol-gel coating methods on titanium substrates	8
2.2.1 The silica coating on titanium by sol-gel methods	9
2.2.2 The titania coating on titanium by sol-gel methods	12
2.2.3 The silica-titania coating on titanium by sol-gel methods	17
2.2.4 The hydroxyapatite coatings on titanium by sol-gel methods	20
2.2.5 Other coatings on titanium substrate for medical implants	26
2.3 Rosin on biomedical applications	27
Chapter 3	31
3 Materials and methods	31
3.1 Preparations and pretreatments of substrates	31
3.2 Preparations of sols	31

3.3 Spin coating procedure	32
3.4 Characterizations of coated surfaces.....	33
3.5 Mechanical properties.....	33
3.6 Bioactivities	34
Chapter 4.....	37
4 Sol-gel-derived coating on glasses.....	37
4.1 Introduction.....	37
4.2 Sol-gel-derived silica coating on glasses	37
4.3 Sol-gel-derived titania coating on glasses.....	38
4.4 Sol-gel-derived silica-titania coating on glasses.....	40
4.4.1 Silica-titania mixed sols with respective hydrolyses	41
4.4.2 Silica-titania mixed sols with titania-first hydrolysis	47
4.4.3 Silica-titania mixed sols with silica-first hydrolysis.....	55
Chapter 5.....	57
5 Sol-gel-derived silica-titania coating on Aluminum.....	57
5.1 Introduction.....	57
5.2 Sol-gel derived silica-titania coating on aluminum substrate.....	57
5.3 Comparison with coatings on glass and aluminum substrates.....	59
Chapter 6.....	62
6 Sol-gel-derived silica-titania coating on titanium.....	62
6.1 Introduction.....	62
6.2 Sol-gel derived silica-titania porous coating on titanium	62
6.2.1 Sol-gel derived silica-titania porous coating by 30% rosin	64
6.2.2 Sol-gel derived silica-titania porous coating by 40% rosin	68
6.2.3 Sol-gel derived silica-titania porous coating by 50% rosin	71
6.3 Mechanical properties of samples.....	73

6.4 Bioactivities of samples	79
Chapter 7.....	84
7 Concluding remarks and recommendations	84
7.1 Concluding remarks	84
7.2 Recommendations and limitations	86
References.....	88
Curriculum Vitae	96

List of Tables

Table 3.1 Reagents for preparation of 1.5SBF (1000 mL)	35
Table 3.2 Ion concentrations (mol/m^3) of the 1.5SBF and human blood plasma.....	35
Table 4.1 Formulations of titania sols.....	39
Table 4.2 Silica-titania coating procedure with respective hydrolyses and mixed before aging	41
Table 4.3 Silica-titania coating procedure with respective hydrolyses and mixed after aging	44
Table 4.4 Titania-silica coating procedure with respective hydrolyses and mixed after aging	46
Table 4.5 Silica-titania coating procedure with titania-first hydrolysis and mixed before aging	47
Table 4.6 Titania-silica coating procedure with titania-first hydrolysis	51
Table 4.7 Silica-titania coating procedure with titania-first hydrolysis and mixed after stirred aging.....	52
Table 4.8 Silica-titania coating procedure with silica-first hydrolysis	55
Table 5.1 Sol-gel derived silica-titania coating procedure on aluminum	57
Table 6.1 Sol-gel derived silica-titania porous coating by 30% rosin	64
Table 6.2 Sol-gel derived silica-titania porous coating by 40% rosin	68
Table 6.3 Sol-gel derived silica-titania porous coating by 50% rosin	71
Table 6.4 Sol-gel derived coating with relative promising surface morphology.....	73
Table 6.5 Different abrasion cycles on each coated sample	75

List of Figures

Figure 2.1 Diagram of the dental implant. <i>Sourced from:</i> http://www.infinitydentalcare.com/dental-implants	4
Figure 2.2 SEM micrographs of modified titanium dental implants, (a) titanium plasma-sprayed surface, (b) titanium oxide-blasted surface, (c) dual acid-etched surface, (d) fluoride treated surface, (e) plasma-sprayed hydroxyapatite surface, (f) biomimetic calcium phosphate surface (Le Guéhenec et al. 2007).	7
Figure 2.3 Scheme of the sol-gel process	9
Figure 2.4 (A) SEM picture of the cross-section of sol-gel prepared titania film coating on c.p. Ti after being soaked in SBF for 2 weeks; (B) compositional profile of the layer from 'a' to 'b' in (A), obtained by SEM-EDX. The marked area is the gap. (Li and de Groot, 1993) .	13
Figure 2.5 Different forms of titania as Anatase and Rutile (Macwan, Dave, and Chaturvedi 2011)	15
Figure 2.6 Detailed SEM images of the titania-silver coating on TiSi alloy (Horkavcová et al. 2017)	17
Figure 2.7 A rosin acid molecule with formula $C_{20}H_{30}O_2$ (Fiebach and Grimm 2000)	28
Figure 2.8 Scanning electron microscopic photographs of the rosin microparticles prepared by various solvents, (a) ethanol, (b) acetone (Lee et al. 2004).	30
Figure 4.1 SEM micrographs of sol-gel-derived silica coating on glasses with 25% rosin (a) and with 50% rosin (b). Both surfaces are porous and higher proportion of space-occupying material leads to a higher porosity.	38
Figure 4.2 SEM micrograph of sol-gel-derived titania coating on glass. No pore was observed on the treated surface.	39

Figure 4.3 Photo of sol-gel-derived titania coating on glass microscope slides with spinning speed at 1000 rpm(a), 800 rpm(b) and 600 rpm(c)separately. All coated surfaces with low spinning speed were too thick that severer cracks were observed on all specimens. 40

Figure 4.4 SEM micrographs of silica-titania coating with respective hydrolyses and with 30% rosin: (a) 3000 rpm; 150°C; (b) 3000 rpm; 120°C; (c) 2000 rpm; 150°C; (d) 2000 rpm; 120°C. Most surfaces were cracked. Phase separation was observed on specimen(c)..... 42

Figure 4.5 SEM micrographs of silica-titania coating with respective hydrolyses and with 50% rosin: (e) 3000 rpm; 150°C; (f) 3000 rpm; 120°C; (g) 2000 rpm; 150°C; (h) 2000 rpm; 120°C. Phase separation was clearly demonstrated on specimens with 150°C sintering. Cracks were shown on specimens heat-treated at 120°C. 43

Figure 4.6 SEM micrographs of silica-titania coating with respective hydrolyses and with 30% rosin: (a) 3000 rpm; 150°C; (b) 3000 rpm; 120°C; (c) 2000 rpm; 150°C; (d) 2000 rpm; 120°C. Two phases were separated seriously and most pores showed up only in one phase. 45

Figure 4.7 SEM micrographs of specimen(c) at $\times 12k$ magnification(c1) and at $\times 500$ magnification(c2). The phase separation was directly observed by the contrast under different magnifications..... 45

Figure 4.8 Photos of silica-titania coatings on glass microscope slides with titania-first hydrolysis and before aging mixing: (a) 30% rosin; 3000 rpm; 150°C; (b) 30% rosin; 3000 rpm; 120°C; (c) 30% rosin; 2000 rpm; 150°C; (d) 30% rosin; 2000 rpm; 120°C; The coating was not evenly distributed and the edge was less coated due to the spinning process on glass microscope slides. All SEM illustrations were conducted on the well-coated middle area. .. 48

Figure 4.9 SEM micrographs of silica-titania coating with titania-first hydrolysis and with 30% rosin: (a) 3000 rpm; 150°C; (b) 3000 rpm; 120°C; (c) 2000 rpm; 150°C; (d) 2000 rpm; 120°C; Evenly-distributed porous surfaces were achieved and slight phase separation was still observed. 48

Figure 4.10 SEM micrographs of the specimen (c) with the well-distributed morphology at $\times 1.5k$ magnification (c1). The scaffold-like structure could be directly observed at $\times 15k$ magnification (c2).. 49

Figure 4.11 SEM micrographs of silica-titania coating with titania-first hydrolysis and with 50% rosin: (e) 3000 rpm; 150°C; (f) 3000 rpm; 120°C; (g) 2000 rpm; 150°C; (h) 2000 rpm; 120°C. Coarse surfaces were formed on most specimens. The porous structure was only observed on sample(g). 50

Figure 4.12 SEM micrographs of different spots on the specimen(g) at ×2k magnification. The porous surface was not uniform. Coarse parts also existed as shown in (g1). Phase separation was clearly observed on (g2) spot. 50

Figure 4.13 Photos of silica-titania coatings on glass microscope slides with titania-first hydrolyses and after-aging mixing: (a) 30% rosin; 3000 rpm; 150°C; (b) 30% rosin; 3000 rpm; 120°C; (c) 30% rosin; 2000 rpm; 150°C; (d) 30% rosin; 2000 rpm; 120°C; The coating was not evenly distributed and the edge was less coated due to the spinning process on glass microscope slides. All SEM illustrations were conducted on the well-coated middle area. .. 52

Figure 4.14 SEM micrographs of silica-titania coating with titania-first hydrolysis and with 30% rosin: (a) 3000 rpm; 150°C; (b) 3000 rpm; 120°C; (c) 2000 rpm; 150°C; (d) 2000 rpm; 120°C; 53

Figure 4.15 SEM micrographs of the sample(c) and sample(d) at ×15k magnification. The scaffold-like structure on coated surface was further demonstrated. 53

Figure 4.16 SEM micrographs of silica-titania coating with titania-first hydrolysis and with 50% rosin: (e) 3000 rpm; 150°C; (f) 3000 rpm; 120°C; (g) 2000 rpm; 150°C; (h) 2000 rpm; 120°C. The porosity of coated specimens didn't increase obviously with the more space-occupying material. 54

Figure 4.17 SEM micrographs of specimens spin coated at 2000 rpm and heat-treated at 120°C with 30% rosin (d1) and 50% rosin (h1). Fine and close pores were created with higher content of rosin. 55

Figure 4.18 SEM micrographs of silica-titania coating with silica-first hydrolysis: (a) 30% rosin; 15k magnification; (b) 50% rosin; 2k magnification; No pore was observed after the coating procedure with silica-first hydrolysis. 56

Figure 5.1 SEM micrographs of sol-gel derived silica-titania porous coating on aluminum: (a) 30% titania; 30% rosin; (b) 40% titania; 30% rosin; (c) 50% titania; 30% rosin; (d) 30% titania; 50% rosin.	58
Figure 5.2 SEM micrographs of coatings with 30% titania at $\times 12k$ magnification. The specimen (d1) with 50% rosin got a higher porosity than the specimen (a1) with 30% rosin.	59
Figure 5.3 SEM micrographs of surfaces under same coating procedures with same formulations on different substrates: (a) on aluminum; 12k magnification; (e) on glass; 15k magnification; (b) on aluminum; 5k magnification; (f) on glass; 12k magnification; (c) on aluminum; 12k magnification; (g) on glass; 15k magnification;	60
Figure 6.1 Titanium substrate surface after thermal oxidation with the increased surface roughness	63
Figure 6.2 Titanium substrate surface after plasma oxidation with the increased surface roughness	63
Figure 6.3 SEM micrographs (at $\times 10k$ magnification) of porous coating by 30% rosin: (a) No pretreatment; 150°C; (b) No pretreatment; 120°C; (c) Thermal oxidized; 150°C; (d) Thermal oxidized; 120°C; (e) Plasma oxidized; 150°C; (f) Plasma oxidized; 120°C. All surfaces were porous yet slightly cracked. The micro-sized scaffold structure was observed on sample (f).	65
Figure 6.4 SEM micrographs of the same porous coating shown in Figure 6.3 but at $\times 2k$ magnification (lower than the magnifications used in Figure 6.3) [except for (c1) at $\times 1.5k$ magnification]. Cracks at uniform distribution could be easily observed at a lower magnification. Moreover, high porosity could already be observed on (f1) at $\times 2k$ magnification.	67
Figure 6.5 EDX analysis of sample (a) revealed titanium and silicon to be present in the treated surface.	68

Figure 6.6 SEM micrographs of porous coating by 40% rosin: (a) No pretreatment; 150°C; (b) No pretreatment; 120°C; (c) Thermal oxidized; 150°C; (d) Thermal oxidized; 120°C; (e) Plasma oxidized; 120°C. Severer cracks were observed compared to porous coating with lower rosin content (30% rosin)..... 70

Figure 6.7 SEM micrographs of porous coating by 50% rosin: (a) No pretreatment; 150°C; (b) No pretreatment; 120°C; (c) Thermal oxidized; 150°C; (d) Thermal oxidized; 120°C; (e) Plasma oxidized; 120°C; Serious cracking was revealed on coated surface with highest rosin content (50% rosin)..... 72

Figure 6.8 Contrastive images of sample III before and after the 6H pencil scratch with 500 magnifications: a. before the scratch; b. after the scratch. The coated surfaces were harder than 6H since no obviously scratch mark was left on the surface. 74

Figure 6.9 Comparative images of sample III before and after the cross hutch cutter test with 50 magnifications: a. before the test; b. after the test. The silica-titania surface was tightly attached to the titanium substrate..... 75

Figure 6.10 Microscope images of sample I with 500 magnifications under cycles' abrasion: a. before abrasion; b. 300 cycles; c. 500 cycles. Most of the coating was rubbed out after 500 cycles abrasion. 76

Figure 6.11 Microscope images of sample II with 500 magnifications under cycles' abrasion: a. before abrasion; b. 300 cycles; c. 500 cycles. Half of the coating was rubbed out after 500 cycles abrasion. 77

Figure 6.12 Microscope images of sample III with 500 magnifications under cycles' abrasion: a. before abrasion; b. 100 cycles; c. 200 cycles; d. 300 cycles. Most of the coating was rubbed out after only 200 cycles abrasion. 78

Figure 6.13 SEM micrographs of samples immersed in 1.5 SBF for 3 days: a. sample I; b. sample II; c. sample III; d. cp Ti substrate. More crystal deposits were found on coated silica-titania surfaces compared to the commercially pure titanium substrate. 79

Figure 6.14 SEM micrographs of samples immersed in 1.5 SBF for 10 days: a. sample I; b. sample II; c. sample III; d. cp Ti substrate. More mineral deposition were found on coated silica-titania surfaces compared to the commercially pure titanium substrate. 80

Figure 6.15 SEM micrographs of samples immersed in 1.5 SBF for 30 days: a. sample I; b. sample II; c. sample III; d. cp Ti substrate. More calcium phosphate was generated on coated silica-titania surfaces compared to the commercially pure titanium substrate. 81

Figure 6.16 EDX analysis of the deposited mineral crystal on sample III after 10 days' incubation in 1.5SBF. The presence of calcium and phosphorus was detected. The low Ca/P atomic ratio (lower than 1.40) revealed the amorphous-stated calcium phosphate after 10 days incubation. 82

Chapter 1

1 Introduction

1.1 Sol-gel derived silica-titania porous coating on titanium for dental implants

Titanium is widely used for orthopedic and dental implants because of its excellent mechanical properties, good corrosion resistance and favorable biocompatibility (He et al. 2014). It also offers bone implants impressive inertness due to the formation of a titanium dioxide layer on their surfaces. The naturally titania-coated titanium could be characterized as anti-corrosion and rust-proof for bone implants. However, the post-surgical stability of a bone implant could still be seriously affected by an imperfect tissue-implant interface, which means that more research is still needed to improve their efficacy.

Silica and titania coating are both widely studied for coatings on dental and orthopedic implants. As a principal component of the bioactive glass-ceramics, silica has demonstrated a significant effect on forming an apatite layer. Amorphous titanium oxide with a good biocompatibility and unique osseointegration also functions well within the bone-titanium interface. Their ability to induce an apatite layer and guide bone regeneration could be illustrated by immersing coated samples in simulated body fluid (SBF) (Li et al. 1994). The detection of apatite formation on the coated surface after incubation in SBF is usually carried out by scanning electron microscopy (SEM) (Michelina Catauro, Bollino, and Papale 2014). Surface roughness is another primary parameter of a coated surface that affects the performance of a modified substrate. The rough-surfaced implants favor both bone anchoring and biomechanical stability (Le Guéhennec et al. 2007) and could be adequate for functionalization, mineral nucleation, and growth of a continuous bonelike mineral layer within the pores (Murphy, Kohn, and Mooney 2000).

In order to create a coated layer on the surface of implants, the sol-gel technique of coating has already been shown to be quite effective. (Velten et al. 2002). The sol-gel

coating procedure may involve either dipping, spinning or spraying techniques, and their parameters can be readily modulated in order to control the chemical composition, the microstructure and finally the properties of the surface (Catauro et al. 2015). In this project, dental implants of commercially pure titanium were spin-coated with silica and titania synthesized via the sol-gel method. Space-holder material was used in this process to leave a porous layer with a higher surface roughness and to thereby further improve their biocompatibility and bioactivity.

1.2 Objectives

The overall objective of this research is to create highly porous surface coatings on titanium implants. These coatings would provide larger surface areas and deep porosities that would enhance their osseointegration. The specific objective of this research project was to create a silica-titania porous coating on titanium by using a sol-gel spin coating technique for dental implants.

In a preliminary investigation, standard glass slides used in light microscopy were served as the substrate for refining the sol-gel technique and to identify an appropriate range of parameters for the creation of the porous layer of silica-titania. Rosin, which has a wide range of pharmaceutical applications, was applied in the original sols as a space-holder material and was soaked off in the end by ethanol leaving a porous coating on the substrate. Silica sol and titania sol were prepared to form a coated surface using basic spin coating procedures. Subsequently the two types of sols were mixed together in different ways to create a silica-titania coating with a homogeneous porous structure. Optimal coating conditions were revealed through these experiments.

The aluminum as the substrate was tested to further study the coating process. Optimized experimental conditions were confirmed in these experiments. The differences between distinct substrates under the same sol formulation and the same coating procedure were investigated.

Eventually, the optimized spin coating procedure was applied to titanium substrates. Thermal oxidation and plasma oxidation were conducted on titanium substrates before

coating procedures, to evaluate the effects of pretreatments on the titanium. The surface morphology of coated samples were characterized by scanning electron microscopy. Coated samples with a desirable porous surface were selected, and their mechanical properties such as hardness and abrasion resistance were also evaluated. The bioactivities of chosen samples were observed by incubating these samples in simulated body fluids and observing mineral deposition on the coated surfaces.

This master's research project aimed to develop a porous silica-titania coating on titanium substrates for dental and orthopedic implants, which could enhance their bioactivity and performance.

Chapter 2

2 Literature review

2.1 Titanium substrate for dental implants

2.1.1 Dental implants made of titanium

Dental and orthopedic implants are very effective medical devices which based a lot on the development and use of biomaterials for fulfilling or replacing some important human body functions. The number of dental implant procedures has mounted up steadily worldwide and the success of a particular orthopedic implant highly depends on its ability to survive and function as foreign bodies within the living human system (Wang et al. 2011). The way that dental implants function in the human body is demonstrated in Figure 2.1. A portion of the dental implant is anchored within the patient's bone, while rest of the implant is connected to other functional parts to enhance or replace damaged body tissue. (Hou 2015).

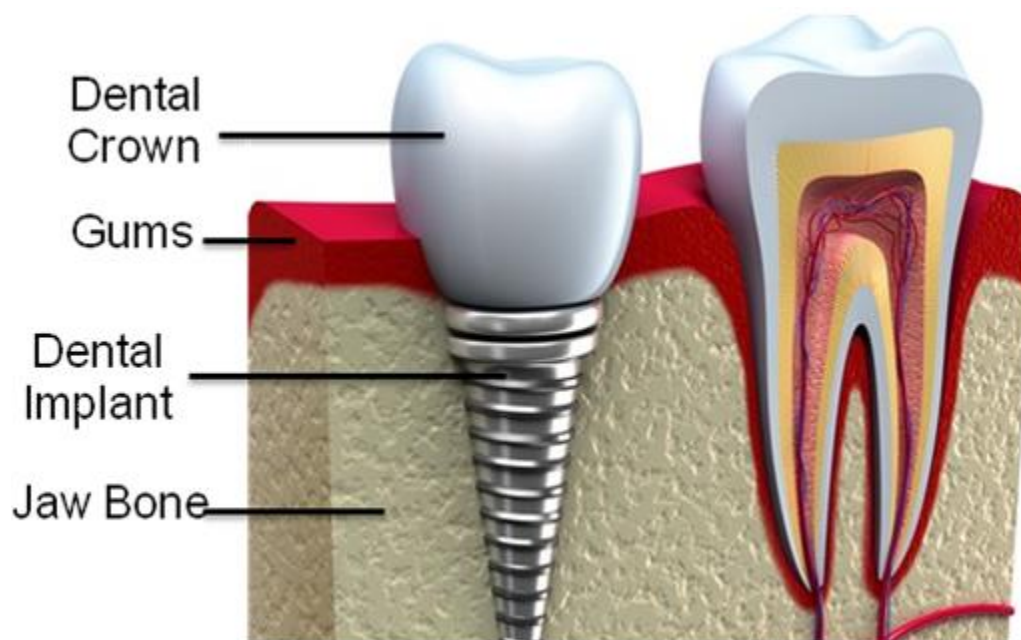


Figure 2.1 Diagram of the dental implant. *Sourced from:*

<http://www.infinitydentalcare.com/dental-implants>

Titanium and its alloys have been through a great development in past decades with their excellent superiorities over other biomaterials. Their properties like extraordinary strength to weight ratio, thermal conductivity and biocompatibility are quite ideal in the medical engineering field. Once it has been implanted into the human body, the titanium implants interact with body fluids and tissues with an impressive friendly physiologically and induce the bone deposition onto the surface. The direct bone deposit on the surface of implants without an intervening connective tissue layer is quite significant as the initial stage of osseointegration for the implants rapid loading (Le Guéhennec et al. 2007). Moreover, not only implants itself but also the surgical conditions and the patient all play crucial roles as to the long-term success of a particular dental implant (Wang et al. 2011).

2.1.2 Surface modifications of titanium substrates

Even though the orthopedic implants form a significant portion of the worldwide biomedical industry with their simplicity and effectiveness, there are still requests to further improve the performance of the applications. Take the titanium substrate as the example, the rate and quality of the direct bone–implant contact after implantation in titanium substrates are related to their surface properties. Parameters such as surface roughness, suitable mechanical properties, wettability, hydrophilicity and the element composition all affect the implant–tissue interaction and have a further impact on the osseointegration and the post-surgical stability of implants (Le Guéhennec et al. 2007). That's why the surface modification methods should be conducted on titanium substrate to improve the interactions between implants and surrounding tissues.

The surface roughness of titanium implants plays a significant role in the rate and quality of osseointegration. Certain surface roughness could improve both the early fixation and long-term mechanical stability of the implants (Buser et al. 1991). The common surface roughness scale can be divided into macro-sized, micro-sized and nano-sized. The macro-sized morphology is in the range of millimeters to tens of microns. The surface roughness of microtopography is considered as in the range 1-10 μm . The micro-sized surface would be beneficial for the bone-to-implant contact (Wennerberg et al. 1998). Otherwise, the nanometer range of the surface could result in better adsorption of proteins and stronger

adhesion of osteoblastic cells and lead to a faster rate of osseointegration (Brett et al. 2004).

There are a lot of mechanical methods being studied to process and modify the surface roughness of titanium dental implants. The grit-blasting methods with hard ceramic particles have been used to roughen the titanium implant surfaces. Ceramic particles such as alumina, titanium oxide, and calcium phosphate particles could be used for grit-blasting since they are both biocompatible and chemically stable. Another technique for roughening the titanium implants is acid-etching. Strong acids such as hydrochloric acid, sulfuric acid, nitric acid and hydrofluoric acid could be used for acid-etching and could usually produce micro cavities in the size range from 0.5 to 2 μ m in diameter (Zinger et al. 2004). Titanium implants could also be treated in fluoride solutions to react with fluoride ions to form soluble TiF_4 species. The micro-rough topography created on the surface has shown to further improve the osseointegration of implants and surrounding body tissues (Wong et al. 1995). Titanium thermal plasma-spraying is another method to roughen the titanium implants substrate. In this method, the titanium powders are injected into a plasma torch and are projected onto substrate where they could fuse and condense to form a uniform thick film. Scanning electron microscopy could be used to evaluate the roughness of the modified titanium dental implants (Figure 2.2). The coating with higher roughness would be beneficial to the implant-surrounding interface (Buser et al. 1991).

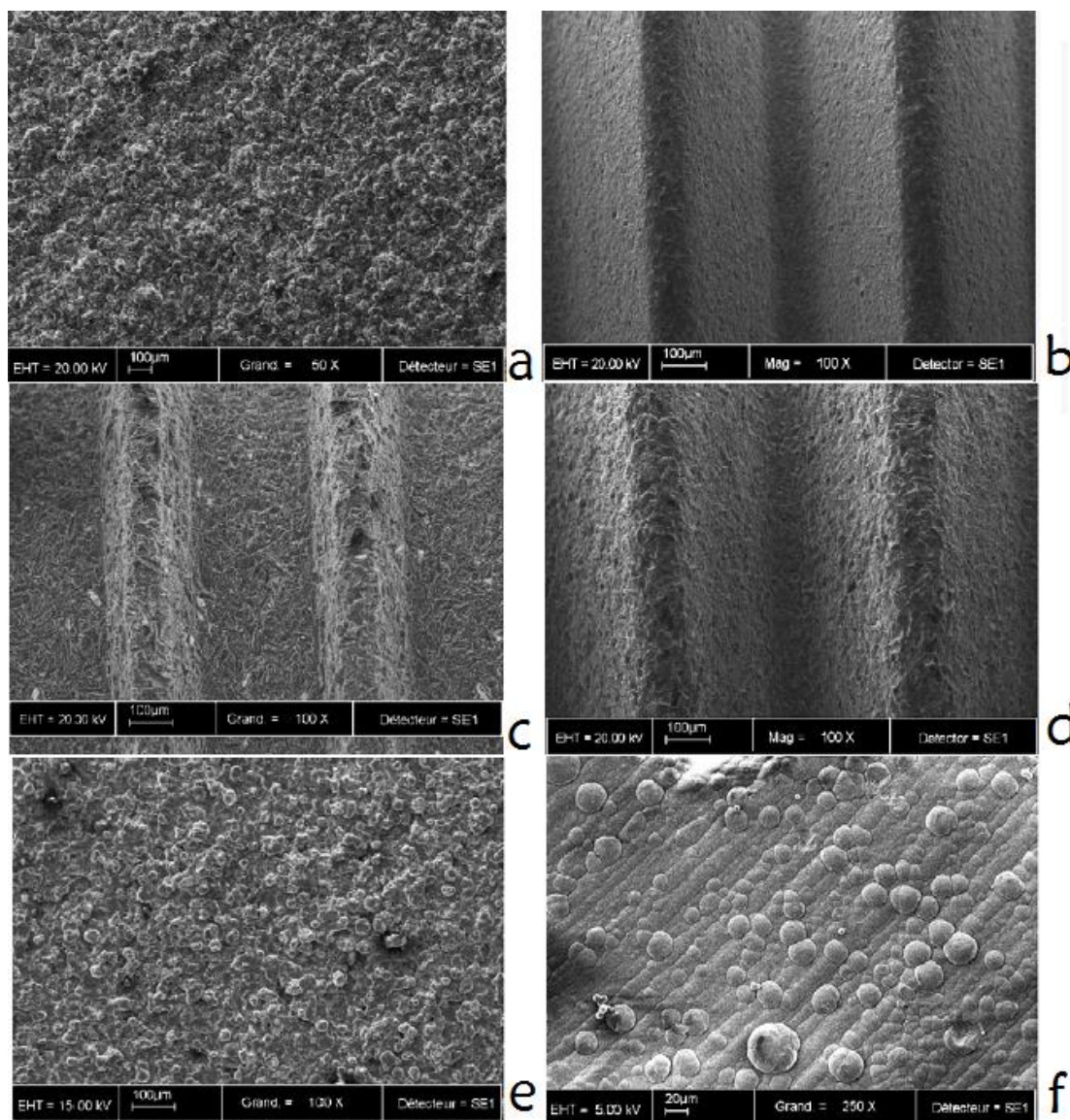


Figure 2.2 SEM micrographs of modified titanium dental implants, (a) titanium plasma-sprayed surface, (b) titanium oxide-blasted surface, (c) dual acid-etched surface, (d) fluoride treated surface, (e) plasma-sprayed hydroxyapatite surface, (f) biomimetic calcium phosphate surface (Le Guéhenec et al. 2007).

In order to achieve a superior initial rate of osseointegration and to improve the bonding strength between implants and surrounding tissues, lots of physicochemical methods have been used to process a modified surface through moderate physical and chemical reactions. Sol-gel coatings are widely used in modifying the surfaces of dental implants as a chemical coating method. It offers a good result in thin ceramic deposited coating with a

better control of the chemical component and microstructure of the coating. Titanium substrates could also be chemically treated using acid, alkali, hydrogen peroxide and even heat based on correspondingly chemical reactions. For example, the alkali and following heat treatment could induce the formation of apatite and on the surface of bioactive ceramics (Hench 1993). Oxidation on titanium substrate offers a mesoporous bioactive titania layer with a promising structure for implants applications that generate a biological apatite on the coated surface (Yang et al. 2004). Chemical vapor deposition is also widely adopted in the industry to modify the medical and biological properties of titanium substrates. Certain chemicals in the gas phase are reacted with the sample surfaces and deposited as a non-volatile compound on implants surfaces. Besides, physical vapor deposition is considered as a coating process with high coating density and strong coating-substrate adhesion. The multi-layers coating could also be achieved by physical vapor deposition as evaporation, ion plating, sputtering in order (Liu, Chu, and Ding 2004). Coated materials could also be thermally melted and the liquid droplets stick and condense on the surface after energetically introduced. This coating process is named as thermal spraying which is often divided into flame spraying and plasma spraying based on the achievable maximum temperature (Liu, Chu, and Ding 2004). In a word, physicochemical surface modifications would generally increase the surface roughness and morphologically improve the implants performance.

2.2 The sol-gel coating methods on titanium substrates

The sol-gel process has been researched for decades and it offers certain advantages as the high purity of the metal alkoxide precursors, the homogeneity of the components at the molecular level, better control of the chemical composition and microstructure and also the low processing temperature (Bradley 1989). A sol is a stable suspension of solid particles in a liquid usually achieved from hydrolysis of the precursor solution. A supporting solvent that contains a continuous solid network enclosing a continuous liquid phase could be formed after the polycondensation of the sol. Metal alkoxides and alkoxy silanes are usually used as the precursor and are solved in a suitable solvent to form a homogeneous solution (Bradley 1989). A gel containing the hydrated metal oxide with macroscopic dimensions molecule could be produced through the hydrolysis and the

rapid evaporation of the solvent under particular controlled conditions. The process of the gel is called gelation and the processed wet gel could be transformed into dry gel through a polycondensation and following dissolution and reprecipitation of monomers or oligomers (Liu, Chu, and Ding 2004). The produced gel could then produce a ceramic or glassy material (as shown in Figure 2.3) with densification and crystallization under a carefully designed process and usually at lower temperature (Bradley 1989). The achieved microstructure is mostly decided by the performed treatment on the precursors and also the relative process parameters during condensation and evaporation (Liu, Chu, and Ding 2004).

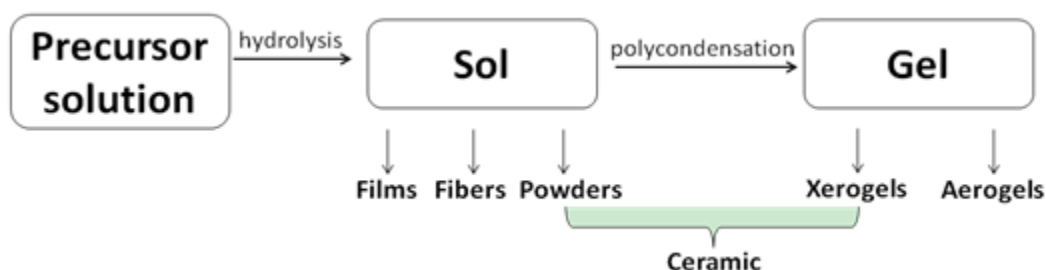


Figure 2.3 Scheme of the sol-gel process

Spin-coating, dip-coating and their variants are widely used processing methods for the sol-gel applications. The spin coating process usually contains deposition, spin up, spin off and evaporation (Liu, Chu, and Ding 2004). The dip coating technique is more suitable for coatings on complex shaped substrates. In a dip coating process, the substrate is dipped into the precursor solution and then withdrawal at certain speeds which play a significant role in the thickness of the coating (Catauro et al. 2015). The solvent evaporation with condensation reactions is also needed for a deposition of a solid coating (Liu, Chu, and Ding 2004).

2.2.1 The silica coating on titanium by sol-gel methods

As a primary component of the bioactive glasses and glass-ceramics, the bioactivity of silica has been studied for decades (Li et al. 1994). It's been confirmed that hydrated silica plays an important role in developing an active hydroxyapatite layer on the surface

which leads to an improved adhesion and bonding between implants and surrounding bone tissue (Li et al. 1992).

Li et al. (1992) reported that a pure hydrated silica gel could induce bioactive hydroxyapatite formation on the coated surface in a simulated body fluid with pH from 7.2 to 7.4. The silica coating was prepared by the hydrolysis and polycondensation of tetraethoxysilane (TEOS) and the silica coating had interconnected pores in both nanometer and micrometer scale on the surface (Li et al. 1992). Yoshida et al. (1999) evaluated the properties of a thin silica film generated by the sol-gel dipping process. The solid silicon-oxygen network was transformed from the liquid silicon alkoxide as an isopropylalcohol solution containing 10 wt% 3-aminopropyl trimethoxysilane. The substrate was dipped into the precursor for 5 min, withdrawn at 2 mm/min and gravitationally drained with solvent evaporation. The deposited solid silica coating was strongly bonded to the titanium substrate with the bonding strength above 55MPa measured by a tensile test. The coated silica surface also increased the hydrophobization of the implants with a higher contact angle of water. A silica/fluorine-hybrid film was also created on the titanium substrate using sol-gel dipping process by Yoshida et al. (1999). The specimen was dipped into fluoride polymer solution containing 7 wt% perfluoroalkane after coated by silica. The thickness of the silica/fluorine-hybrid film was achieved approximately 0.6 μ m. The silica/fluorine coated specimen was also strongly bonded to the titanium substrate and enhanced the hydrophobization of the coated surface. Both silica and silica/fluorine hybrid coated surface significantly prevented the release of titanium ions and reduced the accumulation of dental plaque attaching to intraoral dental restorations (Yoshida et al. 1999).

To modify the biological properties of the implant, Catauro et al. (2015) prepared a silica-calcium oxide/PCL hybrid coating to finally provide a solid fixation of the implants. The dip coating technique was used to obtain a sol-gel synthesized organic/inorganic hybrid coated surface. A biodegradable polymer (poly- ϵ -caprolactone, PCL) had been incorporated into an inorganic 0.7silica- 0.3calcium oxide based matrix in different percentages to process homogeneous and transparent coatings on titanium substrates. The entrapped PCL interacted with the silica-calcium by H-bond between the C=O groups of

the polymer and the –OH groups of the inorganic matrix. PCL had been proved to be able to optimize the morphology and the further biological properties of the coated surface. Biological tests had been conducted to prove that the bioactivity and the osseointegration ability of the coated surface were improved even though the different content of PCL didn't make a significant effect on the bioactivity of the coatings. However, the cell viability did vary with the PCL amount that the coatings containing no PCL or 6 wt% PCL were more biocompatible than coatings with high PCL contents (Catauro et al. 2015).

Catauro et al. (2015) investigated a PEG functional coating produced on titanium substrate by the sol-gel technique to overcome the drawback of metallic implants as tissue tolerance and osseointegration ability. They studied the synthesis and characteristics of a silica/polyethylene glycol (PEG) hybrid coating through the dip-coating process. The hydrogen bonds between the inorganic sol-gel matrix and the organic component were formed and the ratio between the organic and inorganic phases was tested to generate various hybrid systems to improve the biological properties. The morphology of the coated surface was evaluated that high PEG content enables to obtain a crack-free coating. The formation of hydroxyapatite on the silica/PEG-coated surface after immersing in a simulated body fluid was tested to illustrate the bioactivity of the hybrid coatings. Both bioactivity and biocompatibility were improved and the PEG amount affected more on the biocompatibility than the bioactivity of the coating films (Catauro et al. 2015).

Si nanoparticles have also been found to inhibit bacterial adherence to oral biofilms and it could be used as antimicrobial agents in the biomedical applications due to its non-toxic properties. Besides, the combination of Si nanoparticles and others biocidal metals like Ag or Au has been studied. The Ag/silica nanocomposite has been proved to be able to improve certain antimicrobial properties (Cousins et al. 2007). Babapour et al. (2011) prepared a low-temperature sol-gel derived silver nanocomposite coating with silane-based matrices as the biofilm inhibitor. The incorporation of a silver salt into the sol-gel phenyltriethoxysilane (PhTEOS) matrix resulted in a desired silver release rate as high initial release rate followed by a lower sustained release for more than 15 days. The prevention of the biofilm formation for over 30 days was demonstrated by scanning

electron microscopy (SEM) morphology investigation on coated samples before and after 30 days immersion in a nutrient-rich bacterial suspension. The silver nanocomposite embedded in silane coating was quite effective in killing *E.coli* bacteria (Babapour et al. 2011).

2.2.2 The titania coating on titanium by sol-gel methods

The bioactivity of sol-gel derived silica coating as inducing apatite formation is resulted from the high concentration of acidic SiOH groups on the silica surface (Li and De Groot 1993). The induced bone-like apatite layer has been found to be responsible for the bonding of the glass-ceramics to living bones. Certain hydroxyl groups such as TiOH are also capable of starting hydroxyapatite generation by providing the initial nucleation sites (Li et al. 1994). The sol-gel process could be well applied in the inorganic oxide ceramics preparation from colloidal and polymeric sols to speed up the osseointegration (Li and De Groot 1993). In a typical sol-gel process, the titanium alkoxides are commonly used as the titania precursors. The reactions are more difficult to control than reactions of corresponding silica precursors due to the faster kinetics of the transition metals. Coating conditions like the composition of the sol, coating speed, and the sintering temperature should be carefully controlled to achieve a proper surface structure to further improve the apatite-forming ability (Jokinen et al. 1998).

Li and de Groot (1993) prepared a bioactive sol-gel-derived titania film on commercially pure titanium using a dip coating technique. The titania sol was prepared using tetraisopropylorthotitanat as the precursor and anhydrous ethanol as the solvent with mono-ethylether, hydrochloric acid and distilled water. The cpTi specimen was dipped into the prepared sol and withdrawn both at the speed of 10-15 mm/min and then was heated to evaporate the dissolvent. The coated samples were immersed in simulated body fluid for two weeks at 37°C to demonstrate the bioactivity (Panjian Li and De Groot 1993).

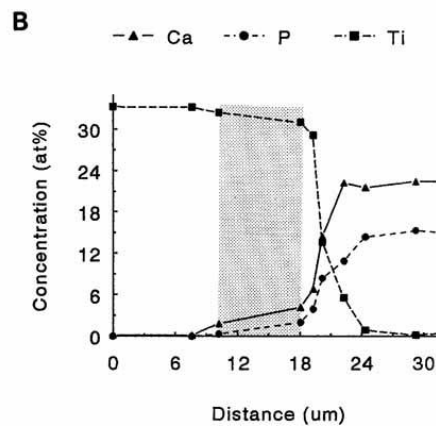
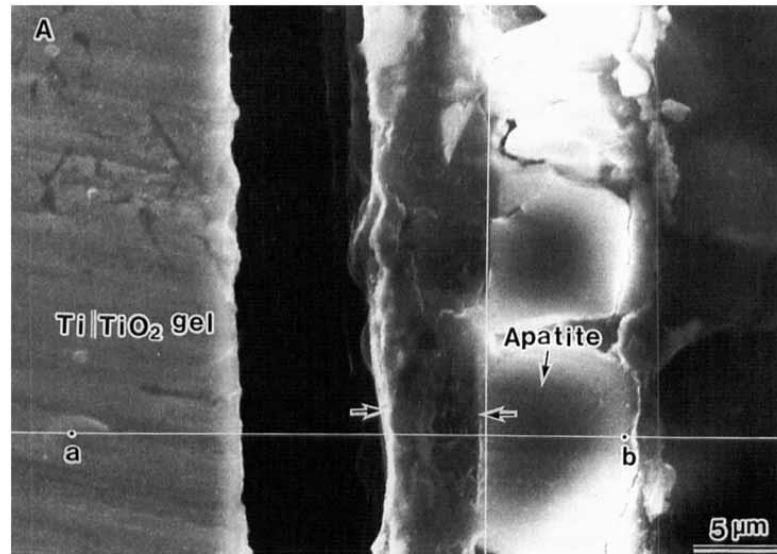


Figure 2.4 (A) SEM picture of the cross-section of sol-gel prepared titania film coating on c.p. Ti after being soaked in SBF for 2 weeks; **(B)** compositional profile of the layer from 'a' to 'b' in (A), obtained by SEM-EDX. The marked area is the gap. (Li and de Groot, 1993)

SEM and EDX were applied to analysis the sectional coated layers. The calcium phosphate was proved to be initiated and incorporated within the sol-gel-derived titania and the considerable growth of calcium phosphate allowed the whole surface to become covered with apatite (Li and De Groot 1993). The same coating process was also applied on commercially available TiAl6V4 and was used to produce implant plugs 5.0mm in diameter. The coated specimens were implanted into the femurs of mature female goats for 12 weeks after ultrasonically cleaning in anhydrous and sterilization in an autoclave.

The implant-bone interfacial zone (about 5 μ m thick) 12 weeks postoperatively was distinguished from both bone and implants (Figure 2.4). The intermediate zone was illustrated to contain titania and calcium phosphate and to provide a smooth transition in composition from the titania gel layer to the bone (Li and De Groot 1993). Their experimental result proved that the sol-gel coating process left TiOH groups on the substrate accelerate the hydrolysis of titania and to take up calcium and phosphate from the surrounding calcium phosphate solution.

The rate of bone-like apatite formation on a coated implant is considered as a descriptive parameter of the bioactive potential and the apatite-forming ability is highly decided by the coating morphology. Peltola et al. (1998) found out that the change in sintering temperature affected more on the apatite-forming ability compared to the composition of the sol and the number of coating layers (Peltola et al. 1998). The sintering procedure was carried out at 400°C, 450°C, 500°C, 550°C, 600°C and the fastest apatite-forming of all coatings was achieved at 500°C. The gel sintered at 500°C might have the optimum nanostructure, such as porosity, surface area, and polycondensation, for calcium and phosphate adsorption and apatite nucleation (Peltola et al. 1998). Velten et al. (2002) also studied the effects of sintering temperature on the morphology of the coatings in the sol-gel process. They used tetran-butyl orthotitanate (TBOT, $\text{Ti}(\text{OC}_4\text{H}_9)_4$) as the metal precursor and ethanol as the solvent without any stabilizing agents. All samples were spin coated at the speed of 6000 rpm and dried in a laboratory furnace in the atmosphere at 130°C for 30min. The solvent evaporated right after the spin coating with the following alkoxide hydrolysis and the polycondensation of the hydrolyzed particles through the elimination of water. The nano-sized amorphous titania was generated with a three-dimensional network after repeated above processes. The gel formation happened during the drying with the evaporation of ethanol, butanol, and water resulting in the agglomeration of the titania network. All samples were annealed at temperatures between 300 and 750°C for an hour as the final process. The structure of the coated surfaces was tested by X-ray diffractometry and was found to be successively amorphous, anatase and rutile with increasing temperature of the heat treatment. Structures of anatase and rutile are discussed in Figure 2.5. The experimental results showed that higher temperature

might accelerate the transitions of the structure of the films from amorphous to anatase and even to rutile (Velten et al. 2002).

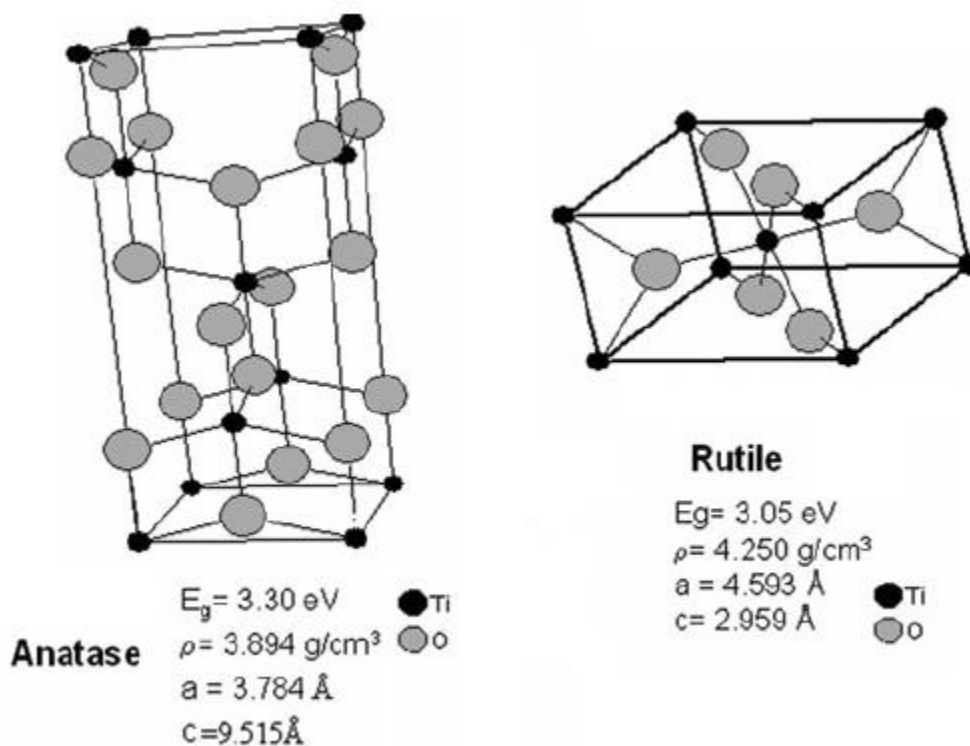


Figure 2.5 Different forms of titania as Anatase and Rutile (Macwan, Dave, and Chaturvedi 2011)

To further improve the bioactivity and biocompatibility of the modified surfaces of implants, M. Catauro et al. (2015) investigated an organic-inorganic nanocomposite surface with an inorganic titania matrix incorporating a biocompatible polymer (Catauro, Papale, and Bollino 2015). The poly- ϵ -caprolactone (PCL) was mixed with the titania matrix in sol phase and was used to dip-coat titanium grade 4 substrates to improve the biological response. The C=O of PCL chains was connected with the —OH groups of the sol-gel titania matrix through H-bonds detected by Fourier transform infrared spectroscopy. The morphological analysis of the hybrid coating was conducted by scanning electron microscopy (SEM) and showed that adding PCL into titania inorganic matrix allowed a homogeneous, porous and crack-free titania-based coating (Catauro, Papale, and Bollino 2015). The ability of the hybrid surface to induce the formation of

hydroxyapatite as bioactivity property was evaluated via immersing in SBF and the hybrid coating was proved to be more bioactive than a whole titania coating. The presence of Ti-OH groups on the coated surface may explain the hydroxyl-apatite nucleation on the modified titanium substrate (Ohtsuki, Kokubo, and Yamamuro 1992). WST-8 assay, moreover, was performed using 3T3 cells to demonstrate the biocompatibility of all the hybrid coating, the wholly inorganic titania coating, and the uncoated titanium substrate. The experimental results showed that all coated surfaces were able to induce an increase in cell viability. Besides, the porous hybrid coating could promote the cell proliferation more since it could simulate better the cellular natural environment (Webster, Siegel, and Bizios 1999). All their tests showed that the obtained titania-PCL hybrid layers could be used to modify the surface of titanium implants to enhance their biological properties and overall performances (Catauro, Papale, and Bollino 2015).

Titania coated films on implants could also be incorporated with silver for the antibacterial application. D. Horkavcová et al. (2017) proposed that newly developed TiSi alloys were dip-coated with titania sol-gel containing either AgNO_3 or Ag_3PO_4 . Scanning electron microscopy was applied to detect the size and distribution of the particles in the hybrid layers as well as layer compactness. Interconnected fissures were observed at all the coatings after sintering as shown in Figure 2.6. Embedded silver particles ranged from tens of nm to $2\mu\text{m}$ and were distributed mainly in the coating claws. The fissures didn't cause a negative effect on other measured properties of the coated surface. Moreover, the coatings containing silver (even with a low concentration as $0.06\text{ mol}\cdot\text{l}^{-1}$ in the sol) showed positive antibacterial effects against both *E. coli* and *S. epidermidis* after 24 h of interaction. Besides, the titania-silver coated surface demonstrated no cytotoxicity towards both L929 and U-2 OS cell lines during a 24h test with extracts from those materials. All the results illustrated that the sol-gel derived titania coating containing silver could be a promising candidate for the potential use of dental and orthopedic implants (Horkavcová et al. 2017).

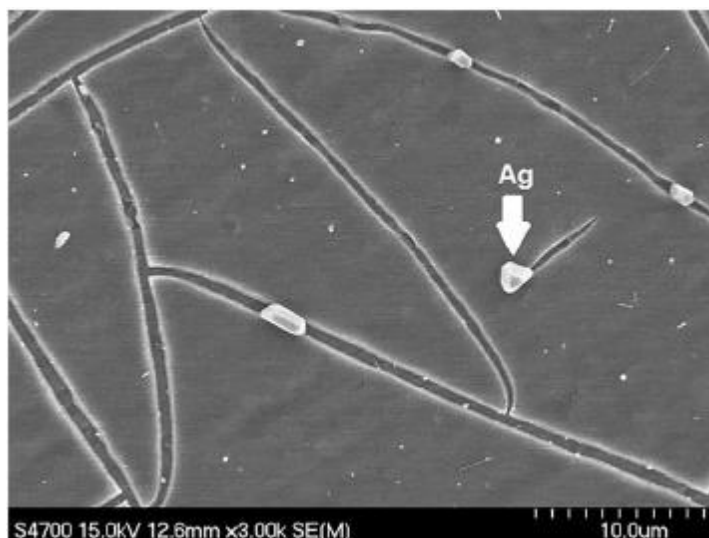


Figure 2.6 Detailed SEM images of the titania-silver coating on TiSi alloy (Horkavcová et al. 2017)

2.2.3 The silica-titania coating on titanium by sol-gel methods

Multi-component systems like sol-gel derived titania-silica system are studied to achieve better bioactivity and other essential material properties in dental and orthopedic applications. Jokinen et al. (1998) produced a titania-silica coating as well as a titania coating using the sol-gel dip-coating method to achieve the same goal. $\text{Ti}(\text{i-PrO})_4$ was used as the precursor of the titania sol and TEOS was used for silica. The mole ratios of titania-silica as 7:3 and 3:7 were both obtained for the titania-silica mixed sols. The particle size and particle size distribution were monitored by a dynamic light scattering technique. The temperature during the dip-coating process was kept at 0°C for every produce and every specimen. Five subsequent coated layers on titanium substrate were obtained through five times repeated coating procedures. Meanwhile, only one layer was prepared on a glass substrates to analyze the surface topography and roughness via atomic force microscopy (AFM). Fourier transform infrared spectroscopy was performed to characterize the calcium phosphate phases after immersing in simulated body fluid and XRD analysis was also applied to the obtained coating to check the crystallinity. The bulk properties of the single coated layer on glass substrate like thickness and refractive indexes were evaluated by fitting transmittance spectra. The coating thickness was affected by parameters such as dipping speed during the coating procedure and the oxide

content or viscosity of the original sol. The porosity of the obtained films was also calculated approximately through the Lorentz-Lorenz equation. The *in vitro* bioactivity tests were conducted in simulated body fluid (SBF) as an indication of the *in vivo* bioactivity. Bone-like hydroxyapatite was formed on all the titania coatings instead of the hybrid titania-silica coatings. The *in vitro* bioactivity results indicated that the rougher titania coated surfaces compared to the titania-silica surfaces were bioactive while the hybrid surfaces were not. The results could be explained through the topography or the roughness of the bioactive surface. The uniform-sized small particles (with diameter around 2nm) without any aggregation formed smooth surfaces which were not suitable for hydroxyapatite formation. The structure of the generated hydroxyapatite deposit as amorphous with little anatase structure was evaluated and observed by XRD. Overall, their experimental results showed that the topography of the outermost surface is of importance for the bioactivity. The local chemical properties like charge density and reactive groups were also proved to be essential to the bioactivity. However, bulk properties such as thickness and porosity didn't seem to have any influence on the bioactivity (Jokinen et al. 1998).

Aaritalo et al. (2007) also prepared the sol-gel derived titania-silica mixed oxide coatings on titanium substrate to enhance the direct tissue attachment of implants. The obtained coatings had chemically stable titania to maintain the desired nanoscale dimension and also had the silica releasing consequence under *in vitro* conditions. The bone tissue attachment ability of the sol-gel derived titania-silica coatings was evaluated by their ability to induce a bone-like calcium phosphate (CaP) layer on the coated surfaces *in vitro* and *in vivo* (Ääritalo et al. 2007). To prepare the titania and silica sols, they chose tetraisopropylorthotitanate [TIPT, $\text{Ti}((\text{CH}_3)_2\text{CHO})_4$] as the precursor of titania and chose the tetraethyl orthosilicate (TEOS, $\text{Si}(\text{OC}_2\text{H}_5)_4$). The prepared titania-silica sols were aged together at 40°C for 24 h and then were cooled down and kept at 0°C for the dip-coating procedure. During the dipping process, the titanium discs were dipped into the prepared titania-silica sols and then were withdrawn both at the speed of 0.3 mm/s at ambient atmosphere. With the following heat-treating, cooling and washing, the dipping process was finished and the whole cycle was repeated for four more times to obtain thicker coatings. Immersing the coatings in simulated body fluid (SBF) was performed to

illustrate both the bioactivity and the silica release rate of the sol-gel derived hybrid coating (Ääritalo et al. 2007).

Theoretically, the chemical homogeneity of the hybrid oxide materials is highly affected by the parameters in synthesis steps since the Ti-alkoxide and Si-alkoxide have different hydrolysis and condensation rates. With the sol-gel derived dip-coating procedure, the homogeneous surface was achieved by two-stage hydrolysis as the addition of Ti-alkoxide to prehydrolysed Si-alkoxide was followed by the addition of water and acid to complete the reaction. Besides, the homogeneous titania-silica oxides were only obtained at low titania content since the higher concentration of Ti atoms didn't react with the silica and titania tended to form as a separate phase (Jokinen et al. 1998). However, the objective of this study was to obtain silica-releasing coatings consisting of particle having the suitable size range for biological applications. Since heterogeneous titania-silica materials were more potential in biological applications, the aim of the coating procedure was to obtain a heterogeneous sol that the colloidal titania particles could crystallize into TiO₂ surrounded by an amorphous SiO₂ connected by Ti–O–Si bonds during drying and calcination. The XPS results proved that the titania-silica interface was obtained consisting of isolated titania particles surrounded by an amorphous silica possibly cross-linked by Ti-O-Si bonds in a continuous structure. Moreover, the XPS analysis showed that all coatings were able to nucleate CaP in simulated body fluid even with a smoother surface obtained by a higher amount of silica. The silica release was mostly influenced by the silica amount present in the coatings, although their surface porosity and chemical structure were slightly different. The EDS and XPS analysis illustrated that the silica was released from all the coatings from both the bulk and surface structures. Furthermore, silica did not dissolve completely from the coatings indicating that the titania and silica species are linked together by Ti–O–Si bonds and not appearing as separate particles (Ääritalo et al. 2007).

According to the study from Graig and LeGeros (1999), osseointegration, fibro-osseous integration, and periodontal connective tissue attachment are three types of biomaterial/connective tissue interfaces that are essential for the success of endosseous dental implants. Osseointegration is used to describe the direct implant to bone contact.

The indirect contact was described by fibro-osseous as the presence of an intervening fibrous connective tissue layer between the bone and the implant surface in an otherwise clinically successful implant. Moreover, the presence of a viable periodontal ligament is significant to the deposition of dental cementum which is considered as the critical initial events of periodontal connective tissue formation (Craig and LeGeros 1999). Since the poor implant performance is often caused by the non-integration of the implant with the surrounding tissue or infection, the silica-releasing sol-gel derived titania-silica coatings with tailored nanostructure prepared by Aaritalo's group was further evaluated in fibroblast and osteoblast cell cultures for cell response and direct tissue attachment by Areva et al. (2007). Their results demonstrated that the titania-silica coating containing 70% titania performed good cell responses in both fibroblast and osteoblast cultures and the titania-silica coating containing 30% titania performed prolonged osteoblast activity and calcified nodule formation. Several factors that might mainly affect the cell response were explained by the research group as stimulating effect of released silica, protein adsorption enhancement, a more suitable nanoscale topography and the coating ability to nucleate calcium phosphide. Their sol-gel derived titania-silica coatings could be used as a template for bone formation *in vitro* in tissue engineer and are quite potential in dental implants (Areva et al. 2007).

2.2.4 The hydroxyapatite coatings on titanium by sol-gel methods

Hydroxyapatite coatings, with its proved good fixation to the host bone and the increased bone ingrowth to the implants, are considered as a widely studied method to modify the titanium substrate implants and to improve the implant-tissue osseointegration (McPherson et al. 2017). To achieve the improved biocompatibility as well as the osteoconductivity, lots of techniques were attempted to carry out the optimized hydroxyapatite layers. For examples, the plasma-spraying method is a traditional way to coat a hydroxyapatite layer. However, the plasma-sprayed hydroxyapatite layer is known to be inhomogeneous in structure and have low bonding strength (20–30 MPa) due to the high-temperature processing and resultant thick coating layer (Overgaard et al. 1996). The physical vapor deposition may obtain a hydroxyapatite film with thickness less than several μm having high purity and relatively higher strength (Kim et al. 2005). The sol-

gel coating method is also widely utilized with the benefits of phase and structural homogeneity due to the low processing temperature. Moreover, it is simple, cost efficient, and beneficial for complex shaped material (Choi and Ben-Nissan 2007).

Tredwin et al. (2013) prepared the sol-gel derived hydroxyapatite coating on commercially pure titanium substrate using the spin coating technique. To synthesize the original hydroxyapatite sol, calcium nitrate and triethyl phosphite were used as precursors under an ethanol–water based solution. Parameters of the spin coating procedure were characterized and optimized for the optimum spinning speed as 3615 rpm and the optimum sol-gel form set distance as 20mm. Any rotating speed less than 2430 rpm was inadequate to centrifuge the sols while any rotating speed higher than 4010 rpm was too fast to keep the sols on the substrate. The coated surfaces were crystallized at various temperatures to evaluate the different effects of temperature on bonding strength. Scanning electron microscopy (SEM) was conducted to demonstrate the surface characteristics like the thickness and the interaction between the titanium substrate and the coated hydroxyapatite. The cross-section analysis of the hydroxyapatite-coated substrate showed the diffusion of both calcium and phosphorous into the titanium dioxide layer with approximately 1 μ m in thickness which also suggested the possible occurrence of chemical bonds between the hydroxyapatite coating and the titanium substrate. The bonding strength of the coating to the substrate was evaluated through an Instron Universal Load Testing Machine. The mean shear bond strength of the sol-gel derived hydroxyapatite layer was nearly 40 MPa, which is higher than the bonding strength of plasma-sprayed hydroxyapatite coating. Increased bonding strength was also observed with increased sintering temperature due to a greater diffusion across the coating-substrate interface. All their studies on the sol-gel synthesized hydroxyapatite coatings offered a superior potential as bone grafting materials (Tredwin et al. 2013).

However, the weak bonding capability between hydroxyapatite as ceramic and titanium as metal usually leads to a limited bonding strength of the sol-gel derived hydroxyapatite layer on a titanium substrate. Due to the high chemical affinity of titania with respect to both hydroxyapatite and titanium, a titania layer could be properly inserted into the hydroxyapatite coating system on titanium to improve the bonding ability (Kim et al.

2004). Lots of deposited hydroxyapatite-titania composite coatings on titanium substrate have been studied based on this point of view. The hydroxyapatite-titania coatings could be prepared using plasma-spraying technology or the hydroxyapatite powder mixed with titania sol yet the resultant layers were mostly thick, rough, and inhomogeneous. The sol-gel coating technology might be executable due to the chemical homogeneity and fine grain size of the coating layer, as well as the low crystallization temperature and mass producibility of the processing (Brinker and Scherer 1990).

Kim et al. (2014) coated a hydroxyapatite coating onto the titanium substrate with the insertion of a titania buffer layer using the sol-gel technique. The hydroxyapatite could enhance the bioactivity and osteoconductivity of the titanium substrate and the titania medium buffer layer was employed to improve the bonding strength between the hydroxyapatite layer and the substrate, as well as to prevent the corrosion of the titanium substrate. The thicknesses of the sol-gel derived titania film and the hydroxyapatite film in typical apatite phase was approximately 200 and 800 nm respectively. In addition, the bonding strength of the double layer increased steadily with increasing the heat treatment temperature and the highest bonding strength of the hydroxyapatite/titania double layer as 55MPa was achieved after heat treatment at 500°C. The potentiodynamic polarization test was performed to confirm the corrosion resistance improvement of the coated double layer on titanium substrate. The cellular response to this hydroxyapatite/titania double layer coating system in terms of their proliferation and differentiation behaviors was assessed by in vitro tests using human osteoblast-like HOS cells. Cells were cultured on the coated surface and were proliferated in a similar manner compared to those cells cultured on the pure titanium surfaces. However, the alkaline phosphatase activity of the cells on the hydroxyapatite/titania double layer coating was expressed to a higher degree than that on the titania single coating and pure titanium surfaces. Overall this hydroxyapatite/titania double layer coating system could be a promising material to modify the titanium substrate for dental implants (Kim et al. 2004).

Moreover, Kim et al. (2005) also prepared the chemical and thermal stable hydroxyapatite and titania sols respectively prior to making hybrid sols and corresponding sol-gel derived coating. Calcium nitrate tetrahydrate and triethyl phosphite

were hydrolyzed separately as the precursor and were mixed at a Ca/P ratio of 1.67. Titanium propoxide was hydrolyzed within an ethanol-based solution to produce the titania sol. The prepared hydroxyapatite and titania sols were mixed together at various molar ratios and were stirred as the mixture to finally obtain the hydroxyapatite/titania composite sols. The titanium substrate disc polished with silicon carbide paper was dipped into the hybrid sols and then spin-coated at 2000 rpm for 10s to obtain the homogeneous and highly dense composite coating layers with a thickness of around 800-900 nm measured by scanning electron microscopy (SEM). The adhesion strength of the composite coating layers with added titania got improved to 56MPa compared to 37MPa of pure hydroxyapatite coating using an adhesion test apparatus. Moreover, the roughness parameters such as Ra (average height above center line), Rq (root mean square of Ra), and Rz (average of the highest peaks and the lowest valleys on five measurement lengths) were all measured and obtained using a surface profiler. The composite coatings had all three roughness parameters higher than those of pure hydroxyapatite and titania coatings and the increase in titania addition also increased the roughness. The *in vitro* cellular responses to this hydroxyapatite/titania composite coating system were assessed in terms of osteoblast-like cell proliferation and ALP activity. The osteoblast-like cells grew and spread actively on the hybrid hydroxyapatite/titania coatings. The proliferation and alkaline phosphatase (ALP) activity of the cells grown on the hydroxyapatite/titania composite coatings were proved to be much higher than those on the bare titanium substrate. In conclusion, the sol-gel derived hydroxyapatite/titania hybrid coatings were proved to be favorable in terms of both mechanical strengths and *in vitro* cellular responses. All the study results suggested that the sol-gel derived hydroxyapatite/titania hybrid coatings possessed excellent properties for hard tissue applications from the mechanical and biological perspective (Kim et al. 2005).

Except for the homogenous hydroxyapatite/titania coating, a thin, stable, clean and bioactive hybrid coating could be obtained by investigating a titania matrix encapsulating a hydroxyapatite particulate phase using the sol-gel coating technique, according to the research from Milella et al. (2001). Titanium isopropoxide as the precursor was dissolved in acetyl, nitric acid n-propane alcohol and distilled water to prepare the titania sol solution and the obtained titania sol was mixed into the commercially available

hydroxyapatite-anhydrous ethanol solution to prepare the composite sol-gel solution. Plates of commercially pure titanium were coated by dipping the substrates in the mixture at a speed of 15 cm/min under certain controlled temperature (25°C) and humidity (<40%). The X-ray diffraction spectrum of the hydroxyapatite/titania coating confirmed the defined crystalline phases of hydroxyapatite incorporated in the titania matrix. The initial amorphous titania was also crystallized to anatase phase during the heating process so that no amorphous phase was observed. The coating morphology appeared homogeneous, rough and with pores with a size in the range of 250-300 nm through investigation from scanning electron microscopy (SEM). Cracks on the coating surface were observed at a higher magnification due to the shrinkage occurring during the thermal process and could be considered as points of 'mechanical interlocking' to promote osteointegration (Li, Groot, and Kokubo 1996). The interface observation through SEM also evidenced a well-deposited thin film with thickness less than 10µm. EDS analysis was performed to demonstrate that calcium and phosphorous are present in the coating in a typical ratio 1.6 of hydroxyapatite. Besides, the titania-hydroxyapatite composite coated surface was chemically clean and the presence of hydroxylic groups as Ti-OH was confirmed by XPS. Finally, the adhesion strength of the hybrid film to the titanium substrate was evaluated by a pull-test with the value approximately 40MPa, indicating that a good adherent composite film could be obtained using the sol-gel dipping coating procedure (Milella et al. 2001).

Another hydroxyapatite/fluoro-hydroxyapatite/titania coating on orthopedic implants was prepared by He et al. (2014) to improve the efficacy of the titanium substrate in bioactivity and speed of osseointegration. The multistep sol-gel technique was conducted to provide a novel triple-layered functional graded coating consisting of a titania innermost layer, a fluoro-hydroxyapatite (FHA) intermediate layer, and a porous hydroxyapatite (HA) outermost layer. Scratch test and morphological analysis performed by scanning electron microscopy proved the favorable adhesion strength between the composite coating and substrate with the thickness approximately as 2µm. The titania anatase and apatite crystallization were both detected by X-ray diffraction analysis. Furthermore, the excellent bioactivity as well as *in vitro* cell response was suggested as higher osteoblast cells proliferation and ALP activity compared to pure titanium and

hydroxyapatite coating. In conclusion, their functional graded three-layer coating may be able to integrate both short-term bioactivity and long-term stability into one. All the experimental results indicated that the novel titania/fluoro-hydroxyapatite/hydroxyapatite coating had promising prospects in surface modification for orthopedic and dental implants (He et al. 2014).

Titanium and its alloys have already been demonstrated to be well accepted by human tissue compared to other metal materials (Brunette et al. 2017). Moreover, zirconium (Zr) is also a quite favorable non-toxic metal with strong glass-forming ability, high mechanical strength, high fracture, good corrosion resistance and good biocompatibility (Inoue 2000). The TiZr alloy could have a high biomedical potential for the implant materials due to the unique combination of biocompatibility and biomechanical properties. Wen et al. (2007) investigated a hydroxyapatite/titania double-layer film on the non-toxic titanium-zirconium (TiZr) alloy for biomedical applications using the sol-gel technique. Tetrabutylorthotitanate was chosen as the precursor of titania sol while triethyl phosphate and calcium nitrate (with molar ratio Ca/P = 1.67) were chosen to prepare the hydroxyapatite sol. The first titania layer was conducted using the spin-coating technique at the speed of 3000 rpm for 15s and the second hydroxyapatite layer was subsequently spin-coated at the same speed, followed by heat treatment at various temperatures. This coating procedure was repeated for several more times to make the total thickness of the hydroxyapatite/titania double-layer get to 50 μm . XRD and SEM-EDS were performed to evaluate the morphology of the coated specimens. The titania layer exhibited a cracked surface and an anatase structure and the HA layer displayed a uniform dense structure. Moreover, the in vitro assessment was carried out by soaking the hydroxyapatite/titania-coated TiZr alloy specimens in simulated body fluid and incubating them at 37 °C in a humidified atmosphere of 95% air and 5% CO₂ which is the simulated body environment. The hydroxyapatite/titania modified TiZr alloy displayed excellent bone-like apatite-forming ability through the above experiment and could be anticipated to be a promising load-bearing biomedical material (Wen et al. 2007).

2.2.5 Other coatings on titanium substrate for medical implants

Some other coatings have also been studied to modify the surface of dental implants. To prepare a modified surface-reactive coating with a firm fixation, Catauro, Bollino and Papale (2014) investigated a zirconia/PCL organic-inorganic nanocomposite coating on a titanium grade4 (Ti-4) substrate using the dip-coating technique. The synthesized hybrid coatings had an inorganic zirconium-based matrix incorporating with different percentages of a biodegradable polymer, poly- ϵ -caprolactone (PCL) (Catauro, Bollino, and Papale 2014). Zirconium propoxide $[\text{Zr}(\text{OC}_3\text{H}_7)_4]$ and poly- ϵ -caprolactone (molecular weight = 5 65,000) were used as inorganic and organic precursors respectively to prepare the uniform and homogeneous solution of the original sols. The hybrid zirconia/PCL coated films were synthesized by dipping the substrate specimen into the mixed sols before the gelation as the hydrolysis and polycondensation of the metal alkoxides. The coated specimens were withdrawn from the sol with the speed 25 cm/min and were heat treated at 45°C for 1 day to promote a partial densification of the film without any polymer degradation. The dip-coating technique was repeated for two more times until a transparent, uniform, amorphous and cracks free surface was obtained and was confirmed by scanning electron microscopy (SEM). Besides, some interference fringes were observed toward the edges with a thinner film due to the edge effect. The obtained crack-free zirconia/PCL system proved that the thin coatings had a low susceptibility to thermal shock cracking and facilitated the ease of gas removal. The biological proprieties were investigated through *in vitro* tests as immersing samples in simulated body fluid (SBF). The formation of crystals treated specimens surfaces were evaluated with SEM and the chemical nature was further confirmed by the EDS analysis. All incubated Zr systems showed crystal deposition of apatite on the surface and the ratio between the atomic content of calcium and phosphorus as 1:6 further confirmed the chemical formula of hydroxyapatite. The presence of zirconium hydroxide could be able to explain the formation of apatite since the zirconium hydroxide groups combined with the calcium ions present in the fluid originate the increase of positive charge on the surface which has the trend to combine with the negative charge of the phosphate ions to form amorphous phosphate that would spontaneously transform into hydroxyapatite. Moreover, the human osteosarcoma cell line (Saos-2) has been seeded on specimens in

biological tests to evaluate cells–materials interaction. The cell viability was evaluated by WST-8 assay and was expressed as the ratio between the absorbance values of cells in contact with the films and cells placed on the bottom of a well in polystyrene. The result illustrated that all hybrid coating increased the biocompatibility of the uncoated titanium substrate. Overall, their sol-gel dip-coated functional hybrid zirconia/PCL could be a promising modified surface of dental implants to improve the biocompatibility and the overall performance (Catauro, Bollino, and Papale 2014).

Apart from the sol-gel technique, lots of other techniques have also been used to modify the surfaces of dental implants as different substrate materials. Pardun et al. (2015) prepared a wet powder-sprayed zirconia/calcium phosphate mixed coating for dental implants with a firm adhesion to the zirconia substrate. The hydroxyapatite coating was utilized to achieve a better osseointegration with a high bioactivity potential. Yttria-stabilized zirconia was added into the coating system to provide the mixture a chemically stable surface and a stronger bonding to the substrate with its low toxicity and beneficial mechanical properties. The hybrid coating produced through wet powder spraying (WPS) exhibited a porous morphology with a surface roughness of about 4 mm and a total porosity of 17%. The ball on three balls test (B3B) was conducted to evaluate the mechanical strength of the WPS treated surface. Scratch tests, as well as insertion experiments (zirconia dental implant screws were coated and inserted in a biomechanical test block and bovine rib bone), evidenced an intact hybrid coating on the zirconia substrate (Pardun et al. 2015).

2.3 Rosin on biomedical applications

Rosin, as a renewable resource with the ability to be modified in many different ways of differing compositions, is the most important industrially natural resin by far. It is a solid form of resin obtained from pines, conifers and some other plants and is also called colophony or Greek pitch. Rosin is usually produced by heating fresh liquid resin to vaporize the volatile liquid terpene components.

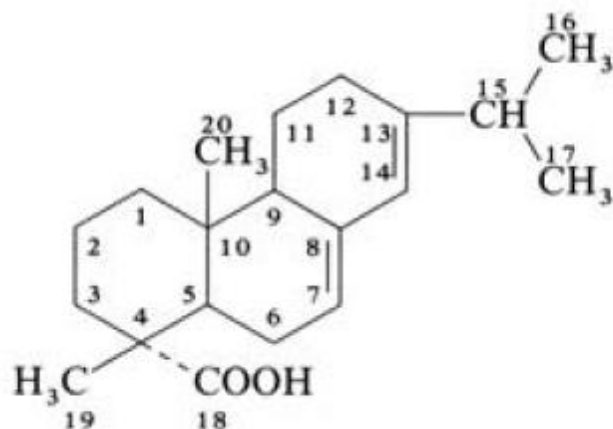


Figure 2.7 A rosin acid molecule with formula $C_{20}H_{30}O_2$ (Fiebach and Grimm 2000)

Rosin consists predominantly of rosin acids belonging to the terpene group (Figure 2.7). A large number of isomeric tricyclic rosin acids exist that differ in the position of the two double bonds and all the acids are in equilibrium with each other. Depending on the country of origin and plant species, native rosin contains between 30 and 50% levopimaric acid, which is the most sensitive isomer. On the other hand, due to the refining method, wood and tall-oil rosins are practically free of levopimaric acid. Correspondingly, they have a high content of abietic acid, neoabietic acid, palustric acid and dihydroabietic acid. (Fiebach and Grimm 2000). Rosin is brittle at room temperature with a melting point of 70 C and varies in color from bright yellow to brownish and black. It is soluble in alcohol, ether, benzene and chloroform. Rosin exhibits a typical conchoidal fracture and the double bonds in the rosin acid molecules are prone to oxidation. However, modified types such as polymerized and hydrogenated rosin types are less easily oxidized with a higher resistance to oxidation. Moreover, the polymerized and hydrogenated types of rosin virtually have no tendency to crystallize at all (Fiebach and Grimm 2000).

Native rosin, as well as its derivatives and modified rosins, could be regarded as harmless and nontoxic. The legal licensing of modified rosins in foods is governed by a large number of national regulations, which are also recognized internationally. Rosin and rosin derivatives are widely used in paints, varnishes, cosmetics, printing inks, and

chewing gums. They also exhibit wide-ranging pharmaceutical applications with its ability to form tablet films and enteric coatings (Satturwar, Fulzele, and Dorle 2005). For example, polymerized rosin has been demonstrated with an excellent film-forming property with sustained release applications which is essential in drug delivery system to prolong the drug release (Fulzele, Satturwar, and Dorle 2002). Satturwar, Fulzele, and Dorle (2005) investigated smooth flexible films produced using polymerized rosin with improved tensile strength and percentage elongation. Fulzele, Satturwar, and Dorle (2003) also prepared two rosin-based biomaterials, the glycerol ester of maleic rosin and the pentaerythritol ester of maleic rosin, by using *in vivo* and *in vitro* degradation behavior tests and biocompatibility studies that were useful for drug delivery applications. In addition, Lee et al. formulated a sustained release system for indomethacin with rosin micro particles prepared by a dispersion and dialysis method without the addition of surfactant. The release behaviors of indomethacin from the rosin micro particles were significantly affected by the solvents used to dissolve rosin and were also dependent on the drug content and the rosin content. Their overall results showed that the rosin micro particles had the potential to generate the sustained release system (Lee et al. 2004). Besides, they did another research on nano-sized rosin particles also prepared by a dispersion and dialysis method without addition of surfactant. The hydrocortisone-loaded rosin nanoparticles were demonstrated to be potentially useful as a drug delivery system (Lee et al. 2005).

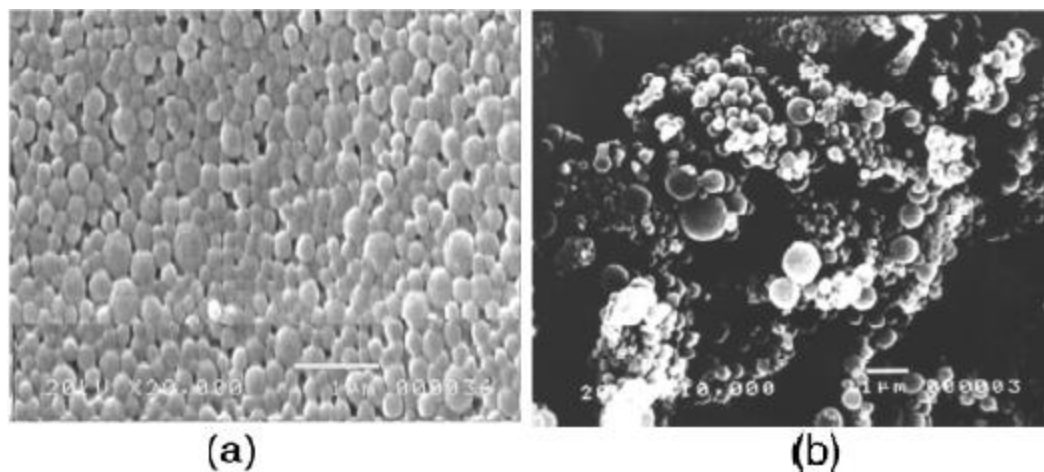


Figure 2.8 Scanning electron microscopic photographs of the rosin microparticles prepared by various solvents, (a) ethanol, (b) acetone (Lee et al. 2004).

Due to its nontoxic property and the solubility in ethanol (Figure 2.8), rosin may also have the potential to be used as a space-occupying material to create a porous surface for medicinal applications. This hypothesis was demonstrated in this study since no much research has been conducted on this field.

Chapter 3

3 Materials and methods

3.1 Preparations and pretreatments of substrates

Glass microscope slides (Technologist Choice Superior Quality Microscope Slides, 26mm by 76mm by 1mm, 0.5 gross) were used as the substrate at the beginning to test the sol-gel coating process. Their surfaces were pre-cleaning by washing with a glass detergent and rinsing with deionized water. Aluminum (3003 H14 Aluminum; 0.6×51×89 mm, Q-PANEL A-2×3.5, Westlake, OH, USA) was used subsequently to demonstrate the sol-gel coating process on a metal substrate. Commercially pure titanium (cp-Ti; Grade 2, thickness = 0.5 mm, McMaster-Carr, Cleveland, OH) discs were used ultimately to find the most appropriate sol-gel formula for creating a porous coating. All substrates were ultrasonically cleaned for 5 min in ethanol (97%, Commercial Alcohols, Brampton, Ontario) and 5 min in acetone (Assay min. 99.5%, Caledon Laboratories Ltd. Georgetown, Ont., Canada) before drying in an air stream to get ready for the following spin coating procedure. Two sizes of the commercially pure titanium substrates of 1cm by 1cm and 2cm by 4cm were used for the coating to complete different assessments. Some of the titanium substrates were thermally oxidized at 600°C in a laboratory furnace (Barnstead Thermolyne 6000 Muffle Furnace, Minnesota, US) for an hour, and some were pretreated by plasma oxidation (CTP-2000K Plasma Generator, Corona Lab. Nanjing, China) for 3 minutes.

3.2 Preparations of sols

Initially, separate silica (SiO₂) and titania (TiO₂) sols were prepared, and subsequently mixed silica-titania sols were prepared to create the porous coatings on substrates.

For the silica (SiO₂) sol, the precursor of SiO₂ was tetraethoxysilane (TEOS, Si(OC₂H₅)₄, Alfa Aesar, Ward Hill, MA), which was dissolved in ethanol (97%), deionized water and hydrochloric acid (HCl, 37%) consecutively at room temperature, with mechanical

stirring (5 minutes) before the addition of each next agent. This sol was aged (25°C) with mechanical stirring overnight and under static conditions for an additional 72 hours.

The titania sol was prepared as follows: Titanium butoxide (TNBT, $\text{Ti}(\text{OCH}_2\text{CH}_2\text{CH}_2\text{CH}_3)_3$, Alfa Aesar, Ward Hill, MA) was dissolved in Acetic acid (CH_3COOH , 99.7%) and ethanol (97%) with mechanical stirring for 20 minutes to form solution (A). Nitric acid (HNO_3 , 69%), ethanol (97%) and deionized water were mixed to form solution (B). Solution (B) was added dropwise to solution (A) at a speed of 1-2 drops/second with stirring. After solutions (A) and (B) were mixed, the sol was aged (25°C) for one hour with mechanical stirring and an additionally 24 h under static conditions

The silica-titania ($\text{SiO}_2\text{-TiO}_2$) sols were prepared by mixing the silica and titania sols at different molar ratios of silica and titania, in different orders and at different formative stages. The parameters for the process were carefully controlled and the details of their compositions and mixing times are listed and discussed in Chapter 4.

Rosin (Zhengshunxing chemical industry limited company, Chengdu, Sichuan, China) was added to prepared and aged sols as a placeholder material in different molar ratios (detailed discussion in chapter 4). It was soaked off in ethanol after the coating formation to leave a porous surface.

3.3 Spin coating procedure

The spin coating procedure was accomplished with a spin coater (KW-4A Spin Coater, SETCAS Electronics Co., Ltd, Beijing, China). The substrate was mounted on the plate by vacuum adsorption. Aged sols were put in an ultrasonic water bath (Ultrasonic Cleaner model 75D, VWR International, West Chester, PA) for 5 minutes immediately before the coating procedure, to ensure uniform dispersion. Sols were dropped onto the substrate and were spread quickly until they evenly covered the surface. The coatings were performed by spinning the sols at a specified speed for a specified time. Then each substrate was heat-treated at temperatures ranging from 100°C to 150°C, in a high performance air flow oven (Sheldon manufacturing, Inc., Cornelius, OR) for an hour, and

cooled to room temperature in a fume hood. Each coating was immersed in ethanol (20% or 97%) for a specified time that ranged from 5 seconds to 2 minutes, washed with deionized water, dried in an air stream and then cooled in air (Hinczewski et al. 2005)

3.4 Characterizations of coated surfaces

All coated surface were thoroughly inspected and were characterized by scanning electron microscopy (SEM) using a Hitachi S-4000 SEM (Hitachi, Pleasanton, CA) to evaluate their surface morphology and porosity. Microscope slides (26mm by 76mm) with coated surface were cut into a smaller size of around 10mm by 26mm, which was done carefully without disrupting the attached coating. This step was unnecessary for Aluminum (2cm by 2cm) and titanium samples (1cm by 1cm) that were already at an acceptable size for scanning electron microscopy (SEM). The coated samples with a proper size were mounted onto metal stubs using adhesive black carbon tape and were sputter coated with nano-sized (10 nm) gold particles. Observations with SEM were performed under 5kV working voltage and 6mm working distance.

The elemental composition of the coated sheets were analyzed by energy dispersive X-ray spectroscopy (EDX) using the same Hitachi S-4000 SEM, with working voltage 15kV and working distance 15 mm. The EDX analyses were repeated at three different spots on each surface to clearly identify the presence of the elements across the entire surface.

3.5 Mechanical properties

The hardness and scratch resistance of the coatings on titanium were assessed by a commercial pencil hardness tester (Elcometer 501 pencil hardness tester, Elcometer Instruments Ltd. Edge Lane, Manchester, England). Pencils with different hardness grades (from 6B to 6H) were constant-load scratched over the coated titanium and the same normal load and angle were applied on every scratch. Each specimen was then observed under a microscope to see if there was a scratch or cut that had been caused by the pencil. The hardest pencil grade that did not cause damage to the coating was

identified as the pencil hardness of the coated surface (Lakshmi, Bharathidasan, and Basu 2011).

Elcometer 107 Cross Hutch Cutter (Elcometer Ltd., Windsor, Canada) was applied to evaluate the adhesion strength of the coated surface to the underlying substrate according to the ASTM protocol, D3359. A blade (11 mm by 1.5 mm) was used to cut the coated film down to the substrate and several perpendicular cuts were made to create a grid of small squares, as specified in ASTM D3359. This lattice was cleaned by blowing an airstream, and covered with adhesive tape (SEMico CHT, direct substitute for Permacel P99, M.E. Taylor Engineering, INC., Rockville, Maryland, US) that was firmed with a pencil eraser. The tape was withdrawn by a single smooth pull within 2 minutes of application. The remaining lattices were then assessed for retention and scored (scale: 0-5) for adhesion according to the ASTM standard D3359. The optical microscope (Mitutoyo WF Microscope, Opti-tech Scientific Inc. Scarborough, Ont.) with $\times 50$ magnification was used to examine the tested surfaces.

An abrasion resistance test was also conducted on the surface coatings that were on titanium substrates, by using the rubbing tester. The coated samples (with size 2cm by 4cm) were fixed onto a plate with binder clips, and were subjected to the movement of a reciprocating arm that was mounted with a square bit (1cm by 1cm) wrapped by glass cloth (Shinex, Fonora Textile Inc.), under a specified load of 1Kg. The bit was oscillated back and forth to create a 1cm by 2cm wear pattern at a frequency of each cycle per second (Thomas, Stoks, and Buegman 2001). The glass fiber paper covering the bit was replaced by a new piece of paper after 200 cycles' of abrasion. The test was stopped when a specific number of cycle were complete (detailed discussion in Chapter 6). The abrasion degree on coated surface was observed under an optical microscope (Mitutoyo WF Microscope, Opti-tech Scientific Inc. Scarborough, Ont.) with $\times 500$ magnification.

3.6 Bioactivities

The bioactivity of the coatings on titanium were studied by immersing the samples (1cm by 1cm) in stimulated body fluids (SBF) using consistent sized disks (cp-Ti with 24 mm

diameter) at 37°C. Different incubation times were used that ranged from 3 days to 4 weeks.

Stimulated body fluid (SBF) which had an inorganic ion concentration that is similar to human extracellular fluid was used. 1.5SBF with an ionic concentration that is 1.5 times that of SBF was utilized in this experiment to accelerate apatite formation on the coated surface. It was prepared by dissolving reagent chemicals of NaCl, NaHCO₃, KCl, K₂HPO₄, MgCl₂.6H₂O, CaCl₂ and Na₂SO₄ into ultra-pure water with continuous stirring at 37°C. After these reagents had dissolved, the solution was buffered at physiological pH 7.20 at 37°C with tris (hydroxymethyl) aminomethane [Tris, (HOCH₂)₃CNH₂] and hydrochloric acid (1 kmol/m³ HCl) (Tanahashi et al. 1994).

Table 3.1 Reagents for preparation of 1.5SBF (1000 mL)

Reagent		Amount
NaCl	Assay min. 99.0%, Caledon Laboratories Ltd. Georgetown, Ont., Canada	12.017 g
NaHCO ₃	Assay min. 99.7%, Caledon Laboratories Ltd. Georgetown, Ont., Canada	0.526 g
KCl	Assay min. 99.0%, Caledon Laboratories Ltd. Georgetown, Ont., Canada	0.339 g
K ₂ HPO ₄	Assay min. 98.0%, Caledon Laboratories Ltd. Georgetown, Ont., Canada	0.261 g
MgCl ₂ .6H ₂ O	Assay min. 99.0%, Caledon Laboratories Ltd. Georgetown, Ont., Canada	0.454 g
1 kmol/m ³ HCl	87.28 mL of 35.4% HCl is diluted to 1000 mL with volumetric flask	60 cm ³
CaCl ₂	Assay min. 96.0%, Caledon Laboratories Ltd. Georgetown, Ont., Canada	0.420 g
Na ₂ SO ₄	Assay min. 99.0%, Caledon Laboratories Ltd. Georgetown, Ont., Canada	0.109 g
(HOCH ₂) ₃ CNH ₂	Assay min. 99.9%, Life Technologies, Inc, Gaithersburg, MD US	9.094 g
1 kmol/m ³ HCl	87.28 mL of 35.4% HCl is diluted to 1000 mL with volumetric flask	Appropriate amount

Table 3.2 Ion concentrations (mol/m³) of the 1.5SBF and human blood plasma

	Na ⁺	K ⁺	Mg ²⁺	Ca ²⁺	Cl ⁻	HCO ₃ ⁻	HPO ₄ ²⁻	SO ₄ ²⁻
1.5SBF	213.0	7.5	2.3	3.8	221.7	6.3	1.5	0.8
Plasma	142.0	5.0	1.5	2.5	103.0	27.0	1.0	0.5

Each specimen in separated disks was rinsed in 97% EtOH before fully soaked in 3 mL of 1.5SBF and the simulated body fluid was replaced by fresh solution every 24 hrs during the experiment. The coatings were removed from the solution after immersion and were gently rinsed with distilled water, dried at fume hood before surface analysis.

Scanning electron microscopy was utilized to characterize the crystallization on the coated surfaces after immersion in 1.5SBF. Energy dispersive X-ray spectroscopy (EDX) (Hitachi S-4000 SEM, Pleasanton, CA) was used to detect the elemental composition of the mineral crystals that formed on the coated surfaces.

Chapter 4

4 Sol-gel-derived coating on glasses

4.1 Introduction

Sol-gel derived silica-titania coating was accomplished by spin coating procedure in this chapter. Glass microscope slides were firstly used as the substrate to demonstrate the possibility and practicability of this idea. Rosin was used as the space-occupying materials to create a porous character of the surface. Both silica and titania sols were experimented respectively at first. After that two types of sols were mixed together in different ways and were tested by scanning electron microscopy under different coating circumstances to derive a desired homogeneous porous coating.

4.2 Sol-gel-derived silica coating on glasses

Silica sol-gel derived coating was first carried out on glass microscope slides to demonstrate the potential of a porous coating. Rosin was used as space occupying material to form a porous coating at the end. The average molecular weight of rosin was considered as 300. The molar ratio of silica/rosin as 3:1 (25% rosin) and 1:1 (50% rosin) were tested in the case. The rotating speed for spin coating was 3500 rpm. The coated specimen was heat-treated at 150°C for 20 min and cooled to room temperature. After sintering, the specimen was soaked in 20% ethanol for 2 min to soak rosin off and leaving a porous surface on the substrate.

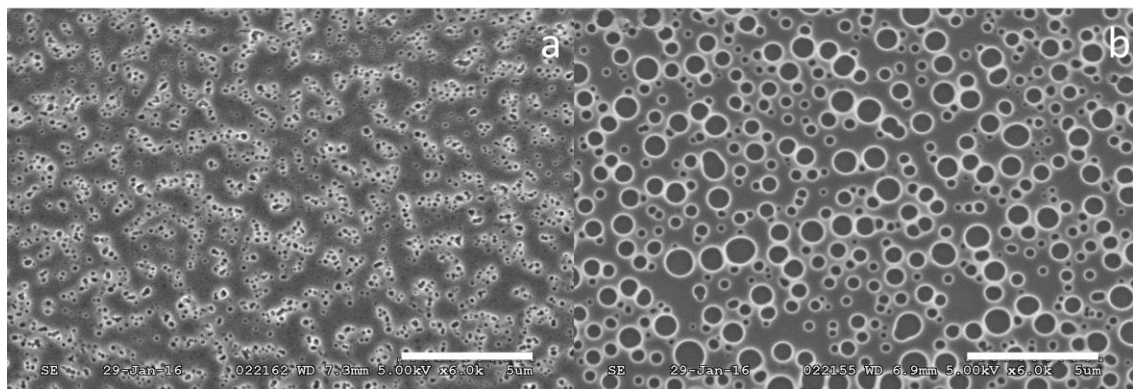


Figure 4.1 SEM micrographs of sol-gel-derived silica coating on glasses with 25% rosin (a) and with 50% rosin (b). Both surfaces are porous and higher proportion of space-occupying material leads to a higher porosity.

The coated surfaces as porous silica were illustrated by the SEM, as shown in Figure 4.1. Pores were evenly distributed and larger pores were formed with using a higher proportion of rosin.

4.3 Sol-gel-derived titania coating on glasses

Sol-gel derived titania coating was tried out also using rosin as a space occupying material to form a porous surface. The molar ratio of titania/rosin as 7:3 (30% rosin) was tested for the maiden attempt. The coating process parameters were the same as silica coating process parameters, with 3500 rpm rotating speed, heat-treated at 150°C for 20 min and soaked in 20% ethanol for 2 min. The coated surface was examined by scanning electron microscopy.

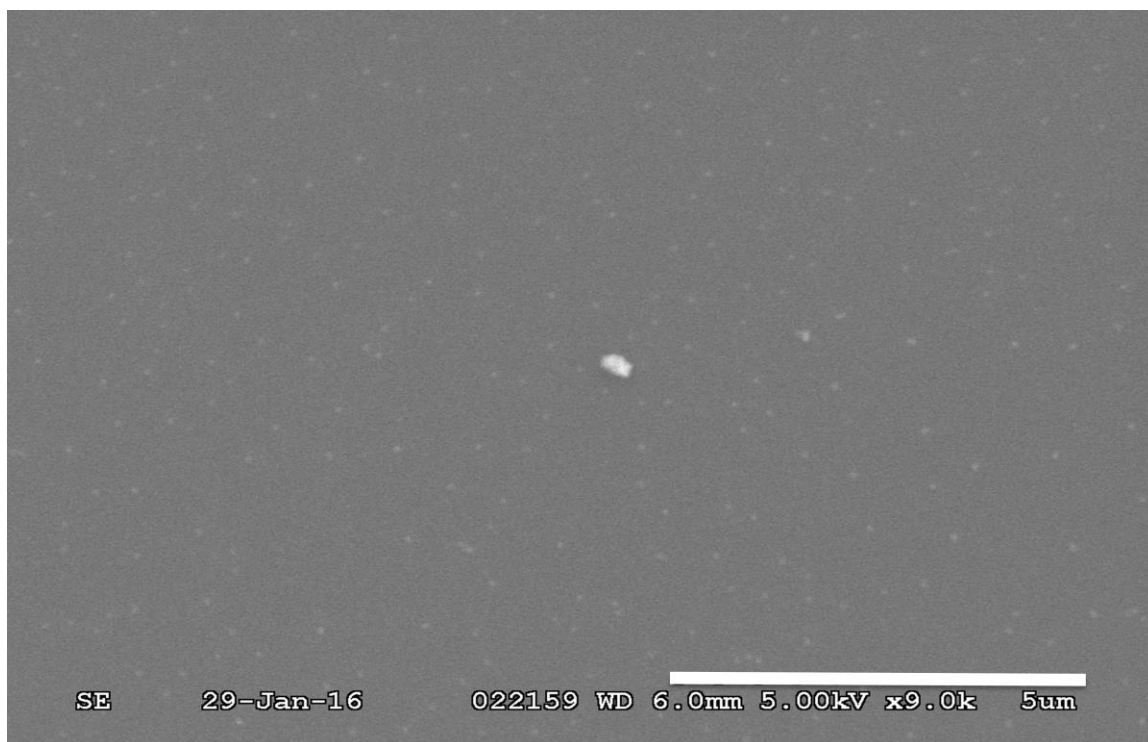


Figure 4.2 SEM micrograph of sol-gel-derived titania coating on glass. No pore was observed on the treated surface.

As shown in Figure 4.2, the attempt to create a porous surface was failed through the same coating procedure with titania sol-gel under scanning electron microscopy. Concentrated titania sols might be needed since the original concentration of titania in titania sols was not high enough to form the scaffold.

Table 4.1 Formulations of titania sols

	Solution (A)			Solution (B)		
	Titanium butoxide	Acetic acid	Ethanol	Nitric acid	Ethanol	Deionized water
Original	10 mL	2 mL	30 mL	0.5 mL	10 mL	1 mL
Modified	10 mL	2 mL	20 mL	0.5 mL	7 mL	1 mL

Modifications were also made during the coating procedure. The rotation rates were decreased (600rpm, 800rpm, 1000rpm, 1200rpm, 2000rpm, 3000rpm) to increase the thickness of the coating accordingly. Different heat-treat temperatures (100°C, 120°C, 150°C) were applied for coating sintering. And also 97% ethanol instead of diluted

ethanol was used to soak rosin off for 10 sec instead of 2 min. That's because water in diluted ethanol with increased surface tension may break apart the porous coating.

Most coatings under modification were cracked after heat-treatment and could be easily wiped off. Some coatings were even more fragile after rosin soaked off. It could be due to the concentrated titania in formulation and harsh experimental conditions. Figure 4.3 shows a group of failed coatings under this circumstance. 30% rosin was added into the titania sols with this group. The slides were coated with 1000 rpm, 800 rpm and 600 rpm rotating speed separately, heat-treated at 100°C for 1 hr and soaked in 97% ethanol for 10 sec. As shown in the picture, lower rotating speed led to a thicker surface (the color was darker) which was severely cracked.

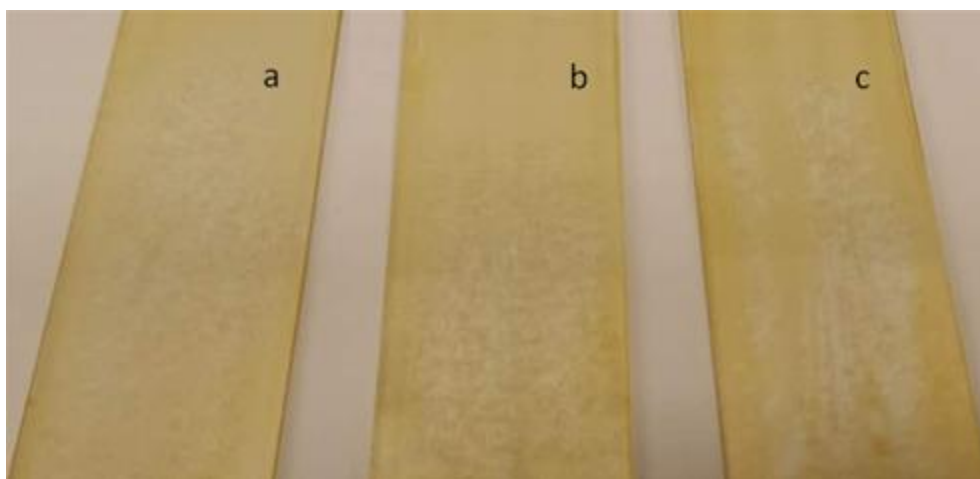


Figure 4.3 Photo of sol-gel-derived titania coating on glass microscope slides with spinning speed at 1000 rpm(a), 800 rpm(b) and 600 rpm(c) separately. All coated surfaces with low spinning speed were too thick that severer cracks were observed on all specimens.

4.4 Sol-gel-derived silica-titania coating on glasses

Sol-gel derived titania coatings with above procedure were mostly fragile and porous less. Given the facts that titania was an essential bioactive agent and sol-gel derived silica porous coatings were evenly distributed and stable, it's exercisable to combine silica and titania sols together to create a silica-titania coating on substrates. Silica and titania have

the strong potential to link together by Ti–O–Si bonds (Jokinen et al. 1998). Glass microscope slides were used again at the first to demonstrate the potential of a sol-gel derived silica-titania porous coating.

4.4.1 Silica-titania mixed sols with respective hydrolyses

In this group, alkoxide of Ti and alkoxide of Si were separately hydrolyzed at the beginning and were mixed together to form the silica-titania sols. Two types of sols could be mixed together before or after aging process with their respective hydrolyses.

4.4.1.1 Silica-titania sols mixed before aging

In the first case, two types of sols were mixed before aging process. The mixed silica-titania sols were aged together with stirring overnight and were further reacted under static conditions for 3 days before the spin coating process. Process parameters for each coating steps were listed in table 4.2.

Table 4.2 Silica-titania coating procedure with respective hydrolyses and mixed before aging

	Si / Ti (mol)	Si+Ti / Rosin (mol)	Rotating speed (rpm)	Heating temperature /Time	Soaking
a.	2:1	7:3	3000	150°C/1hr	97% EtOH/10s
b.	2:1	7:3	3000	120°C/1hr	97% EtOH/10s
c.	2:1	7:3	2000	150°C/1hr	97% EtOH/10s
d.	2:1	7:3	2000	120°C/1hr	97% EtOH/10s
e.	2:1	1:1	3000	150°C/1hr	97% EtOH/10s
f.	2:1	1:1	3000	120°C/1hr	97% EtOH/10s
g.	2:1	1:1	2000	150°C/1hr	97% EtOH/10s
h.	2:1	1:1	2000	120°C/1hr	97% EtOH/10s

The molar ratio of silica/titania in this group was 2:1 and higher proportion of silica was used to make sure a relatively higher porosity could be achieved. The molar ratio of centre elements (silicon plus titanium) and rosin as 7:3 (30% rosin) and 1:1 (50% rosin) were tested in this group. Different rotating speed during the spinning producer and different heat-treated temperatures were applied on distinct slides. All substrates in this group were soaked in 97% ethanol for 10 second after coating and sintering. The scanning electron microscopy (SEM) was employed at the end to observe all 8 types of coated surfaces.

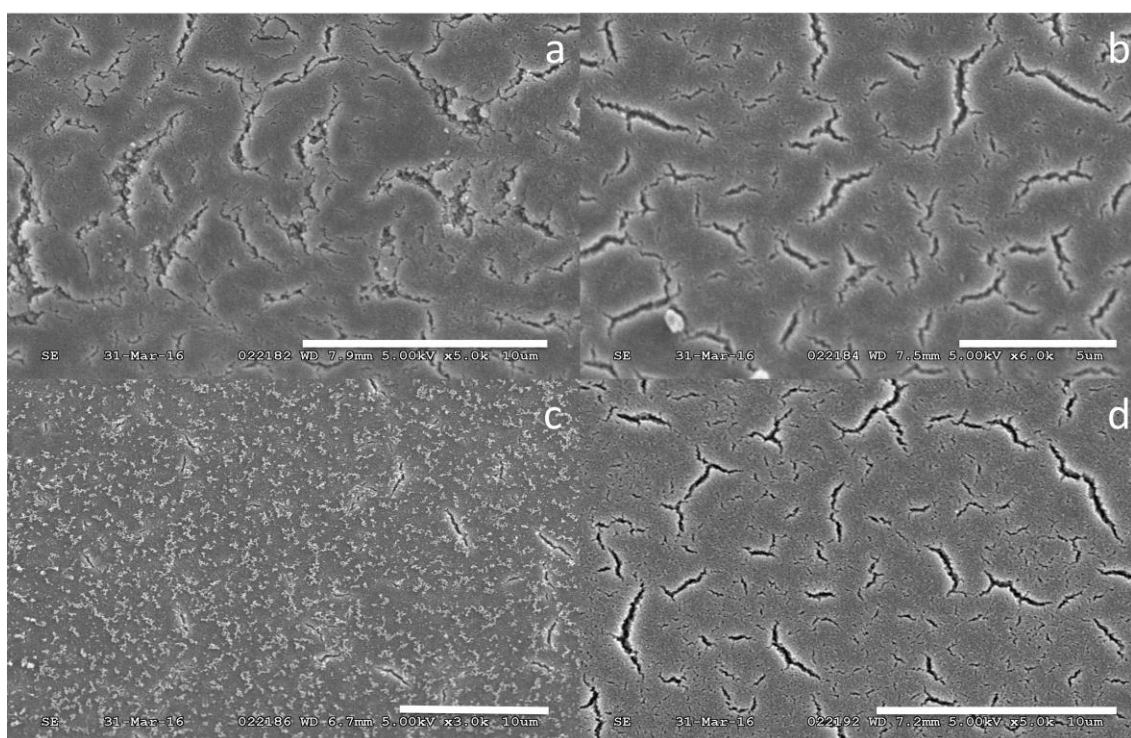


Figure 4.4 SEM micrographs of silica-titania coating with respective hydrolyses and with 30% rosin: (a) 3000 rpm; 150°C; (b) 3000 rpm; 120°C; (c) 2000 rpm; 150°C; (d) 2000 rpm; 120°C. Most surfaces were cracked. Phase separation was observed on specimen(c).

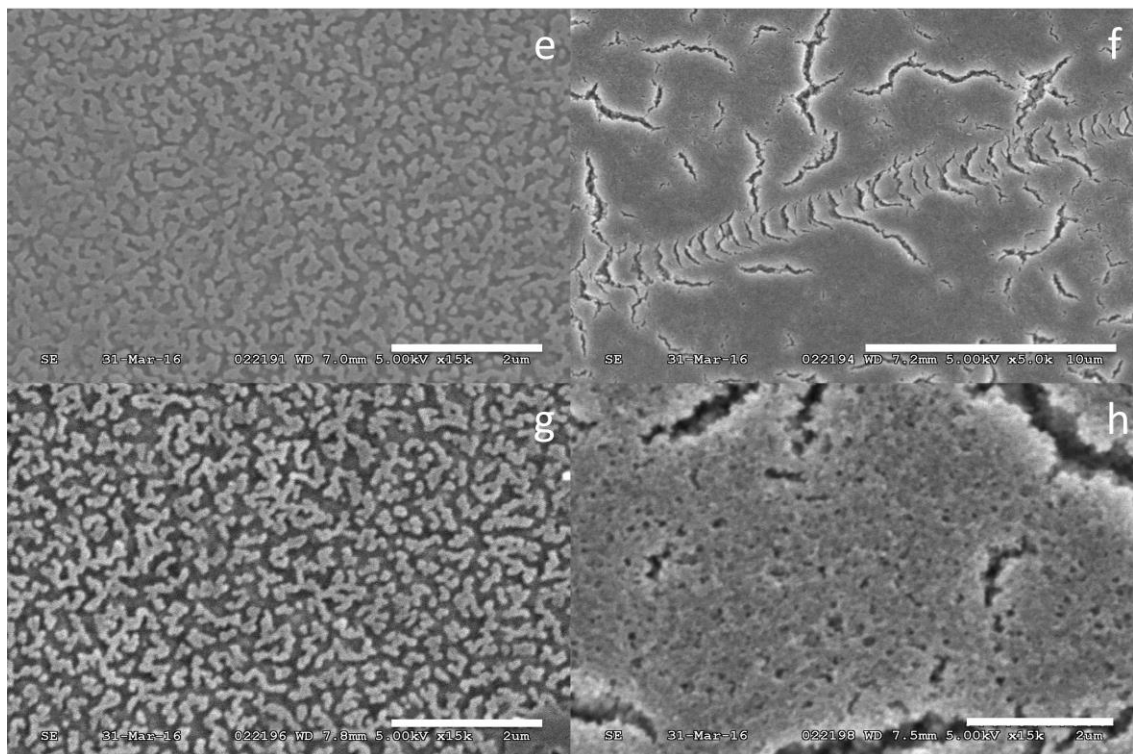


Figure 4.5 SEM micrographs of silica-titania coating with respective hydrolyses and with 50% rosin: (e) 3000 rpm; 150°C; (f) 3000 rpm; 120°C; (g) 2000 rpm; 150°C; (h) 2000 rpm; 120°C. Phase separation was clearly demonstrated on specimens with 150°C sintering. Cracks were shown on specimens heat-treated at 120°C.

As shown in Figure 4.4 and Figure 4.5, most coatings were cracked and no uniformly distributed pore was observed. Surfaces under 120°C heat-treatment had flaws in length from sub-microns to a few microns with irregular distribution. Few flaw but two separated phases were observed clearly on most surfaces under 150°C heat-treatment. Different rotating speeds in spinning procedure did cause a huge impact on the results in this group. Silica-titania mixed with respective hydrolyses was not a proper solution to leave a sol-gel derived porous coating on glass microscope slides.

4.4.1.2 Silica-titania sols mixed after aging

In the second case, two types of sols were mixed after aging process. Silica-titania sol was mixed after 3 days static aging for silica sol and overnight static aging for titania. Process parameters for each coating steps, in this case, were listed in table 4.3.

Table 4.3 Silica-titania coating procedure with respective hydrolyses and mixed after aging

	Si / Ti (mol)	Si+Ti / Rosin (mol)	Rotating speed (rpm)	Heating temperature /Time	Soaking
a.	7:3	7:3	3000	150°C/1hr	97% EtOH/10s
b.	7:3	7:3	3000	120°C/1hr	97% EtOH/10s
c.	7:3	7:3	2000	150°C/1hr	97% EtOH/10s
d.	7:3	7:3	2000	120°C/1hr	97% EtOH/10s

Higher proportion of silica (the molar ratio of silica and titania as 7:3) was used again to improve the possibility to achieve a porous surface. The molar ratio of centre elements (silicon plus titanium) and rosin as 7:3 (30% rosin) was tested in this group. Rotating speed as 3000 rpm or 2000 rpm and heat-treatment temperature as 150°C and 120°C were also applied. 97% ethanol was used again for 10 sec to soak rosin off. SEM micrographs were taken to demonstrate the surface morphology of the coatings.

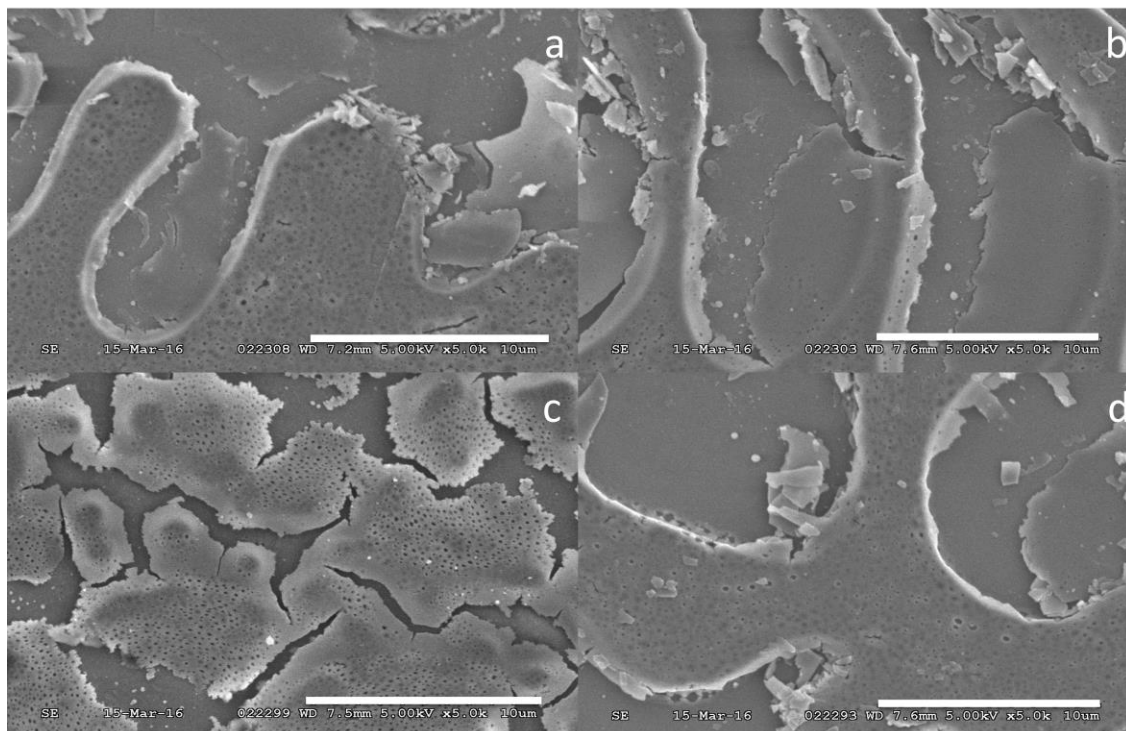


Figure 4.6 SEM micrographs of silica-titania coating with respective hydrolyses and with 30% rosin: (a) 3000 rpm; 150°C; (b) 3000 rpm; 120°C; (c) 2000 rpm; 150°C; (d) 2000 rpm; 120°C. Two phases were separated seriously and most pores showed up only in one phase.

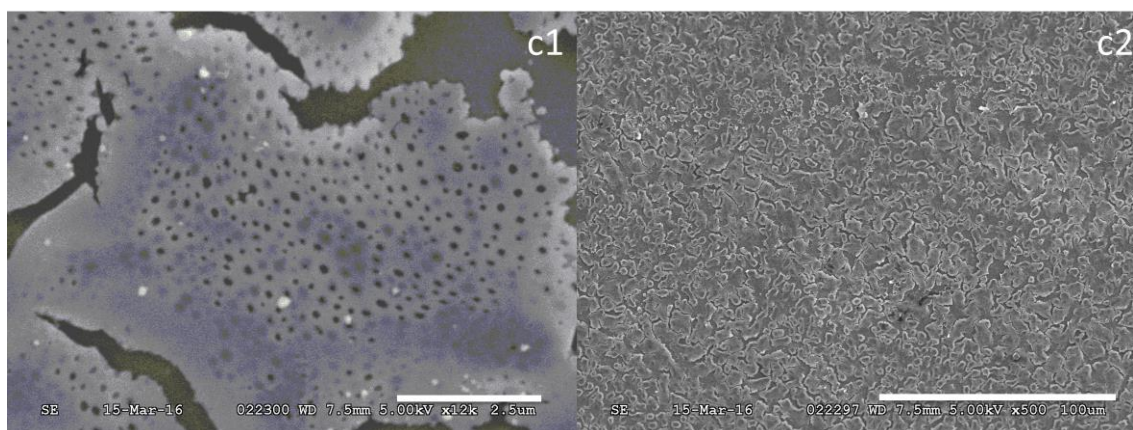


Figure 4.7 SEM micrographs of specimen(c) at $\times 12k$ magnification(c1) and at $\times 500$ magnification(c2). The phase separation was directly observed by the contrast under different magnifications

As shown in Figure 4.6 and Figure 4.7, severely phase separation was observed and relative uniform distributed pores were showed up in only one phase. The diameters of the pores ranged from dozens to hundreds nanometers. Reasonable speculation could be that silica and titania were not well mixed after respective hydrolyses and two phase were cracked and separated eventually on the substrate. Pores could only be on the silica phase due to the experimental results of sol-gel derived silica coating and titania coating.

Instead of a high proportion of silica in the formulation of silica-titania sols, the formulation of titania-silica sols with half silica and half titania was also tested out. The molar ratio of silica and titania was 1:1 and the molar ratio of center elements (silicon plus titanium) and rosin were kept in 7:3 (30% rosin) in this group testing. Process parameters for each coating steps such as rotating speeds and heat-treatment temperatures, in this case, were listed in table 4.4.

Table 4.4 Titania-silica coating procedure with respective hydrolyses and mixed after aging

	Si / Ti (mol)	Si+Ti / Rosin (mol)	Rotating speed (rpm)	Heating temperature /Time	Soaking
e.	1:1	7:3	3000	150°C/1hr	97% EtOH/10s
f.	1:1	7:3	3000	120°C/1hr	97% EtOH/10s
g.	1:1	7:3	2000	150°C/1hr	97% EtOH/10s
h.	1:1	7:3	2000	120°C/1hr	97% EtOH/10s

Just like other groups' coating, four types of coated surfaces were all observed under scanning electron microscopy (SEM). No pore, flaw, crack or phase separation was found out on the surface. The coatings in this test group were quite as plain as the sol-gel derived titania coatings described in chapter 4.2.

4.4.2 Silica-titania mixed sols with titania-first hydrolysis

Silica-titania sols could also be mixed together with titania-first hydrolyses. There were also two ways to achieve this goal.

4.4.2.1 Silica-titania sols mixed before aging

In the first case, titania sol was first prepared and silica sol was added into titania right before aging. The mixed sol was stirring aged overnight together followed by standing together for additional 72 hrs aging at 25°C under static conditions.

Table 4.5 Silica-titania coating procedure with titania-first hydrolysis and mixed before aging

	Si / Ti (mol)	Si+Ti / Rosin (mol)	Rotating speed (rpm)	Heating temperature /Time	Soaking
a.	7:3	7:3	3000	150°C/1hr	97% EtOH/10s
b.	7:3	7:3	3000	120°C/1hr	97% EtOH/10s
c.	7:3	7:3	2000	150°C/1hr	97% EtOH/10s
d.	7:3	7:3	2000	120°C/1hr	97% EtOH/10s
e.	7:3	1:1	3000	150°C/1hr	97% EtOH/10s
f.	7:3	1:1	3000	120°C/1hr	97% EtOH/10s
g.	7:3	1:1	2000	150°C/1hr	97% EtOH/10s
h.	7:3	1:1	2000	120°C/1hr	97% EtOH/10s

The molar ratio of silica/titania in this group was 7:3 and a higher proportion of silica were used once again. The molar ratio of center elements (silicon plus titanium) and rosin as 7:3 (30% rosin) and 1:1 (50% rosin) were both tested. Different rotating speeds and different heat-treated temperatures were applied and listed in table 4.5 and the photos are shown in Figure 4.8.

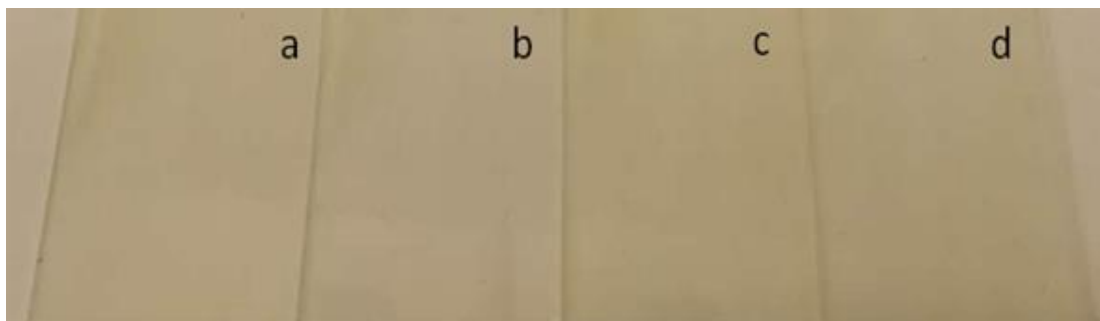


Figure 4.8 Photos of silica-titania coatings on glass microscope slides with titania-first hydrolysis and before aging mixing: (a) 30% rosin; 3000 rpm; 150°C; (b) 30% rosin; 3000 rpm; 120°C; (c) 30% rosin; 2000 rpm; 150°C; (d) 30% rosin; 2000 rpm; 120°C; The coating was not evenly distributed and the edge was less coated due to the spinning process on glass microscope slides. All SEM illustrations were conducted on the well-coated middle area.

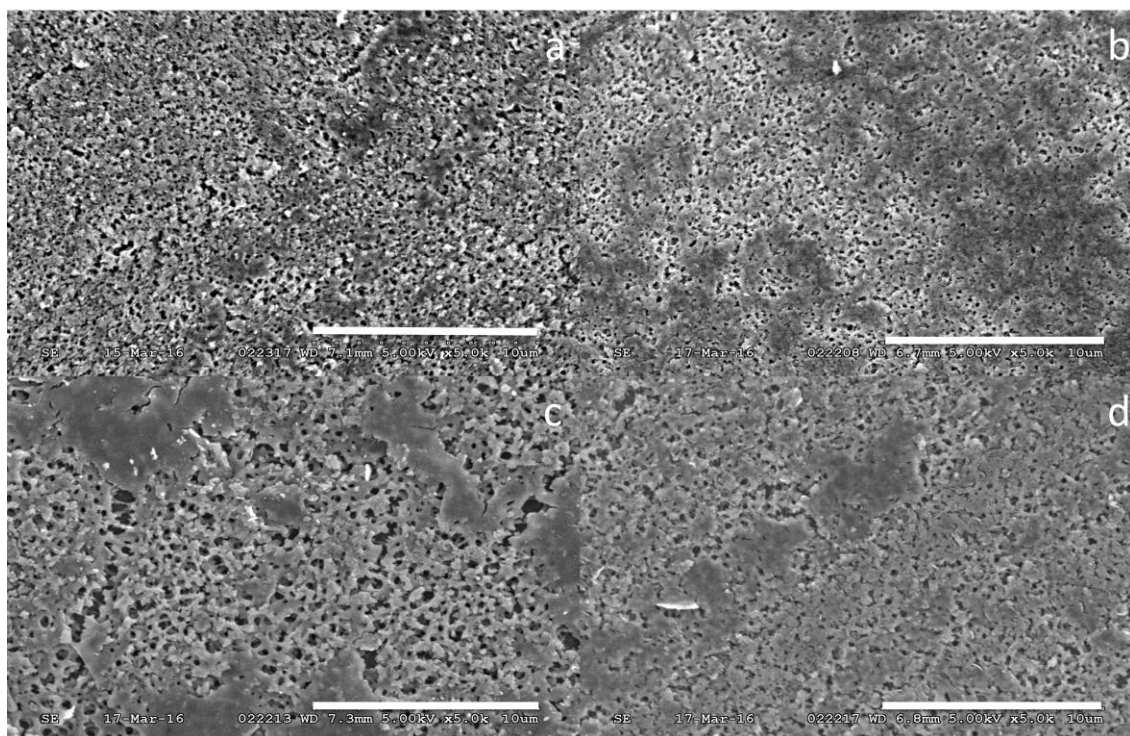


Figure 4.9 SEM micrographs of silica-titania coating with titania-first hydrolysis and with 30% rosin: (a) 3000 rpm; 150°C; (b) 3000 rpm; 120°C; (c) 2000 rpm; 150°C; (d) 2000 rpm; 120°C; Evenly-distributed porous surfaces were achieved and slight phase separation was still observed.

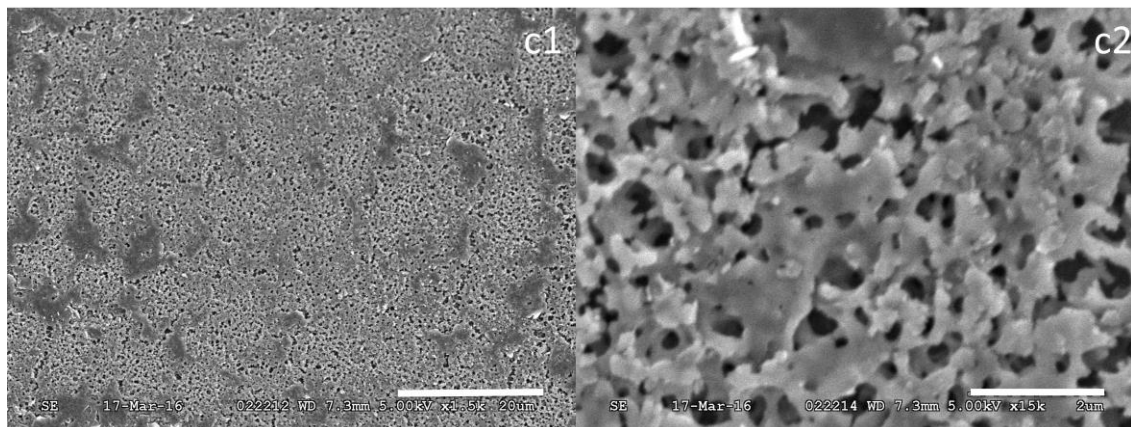


Figure 4.10 SEM micrographs of the specimen (c) with the well-distributed morphology at $\times 1.5k$ magnification (c1). The scaffold-like structure could be directly observed at $\times 15k$ magnification (c2).

SEM micrographs were taken to demonstrate the morphology of coated surfaces (Figure 4.9). Pores with diameters in the range of tens or hundreds nanometers were observed on all coatings. Slight phase separation could still be observed on the thicker surfaces with 2000 rpm rotating speed in spinning procedure. Scaffold-like structure with several micro-sized pores was achieved on sample(c) with a thicker coating and the heat-treatment at a higher temperature (Figure 4.10).

Increased rosin content was applied from 30% to 50%. Rosin was working as space-occupying material in the formulation but higher porosity wasn't observed with more added rosin. As shown in Figure 4.11, only one coated surface [sample (g)] out of four had open porous structure and it had fewer pores than sample (c) with same coating procedure and even less space-occupying material had. Other three coatings in this group had a much rougher surface instead of a porous one and the slight phase separation. It may due to the falling of too many voids left by too much space-occupying material mostly stayed in only one phase of the coating.

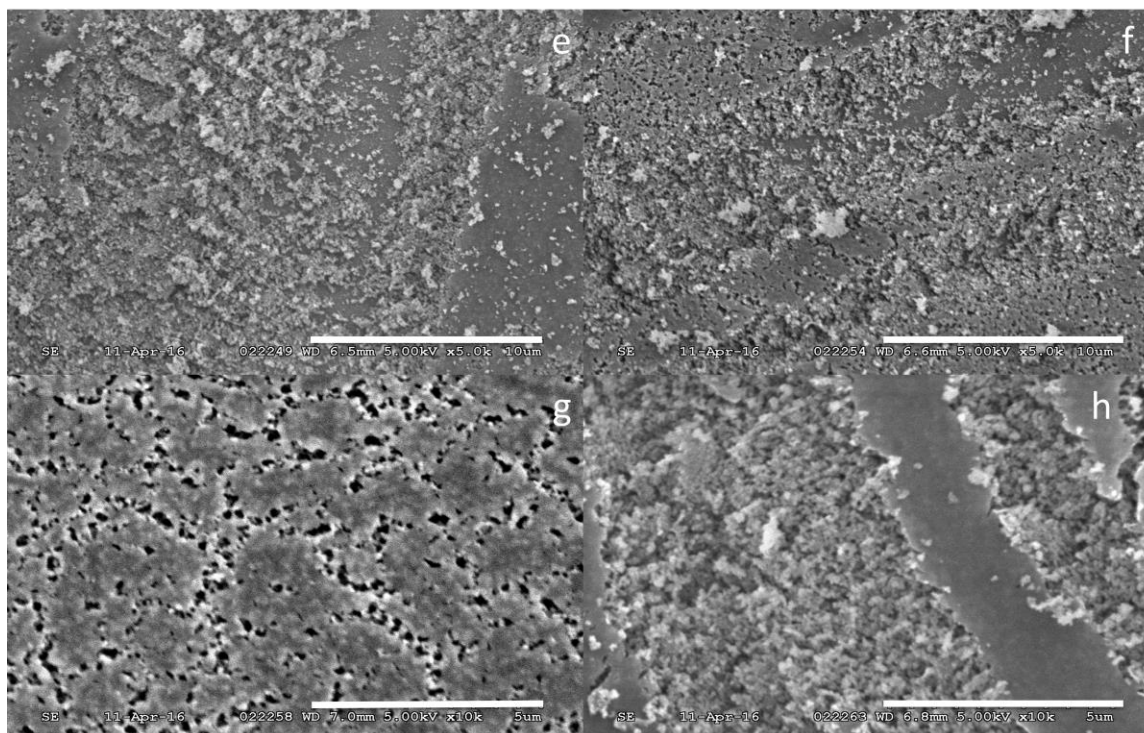


Figure 4.11 SEM micrographs of silica-titania coating with titania-first hydrolysis and with 50% rosin: (e) 3000 rpm; 150°C; (f) 3000 rpm; 120°C; (g) 2000 rpm; 150°C; (h) 2000 rpm; 120°C. Coarse surfaces were formed on most specimens. The porous structure was only observed on sample(g).

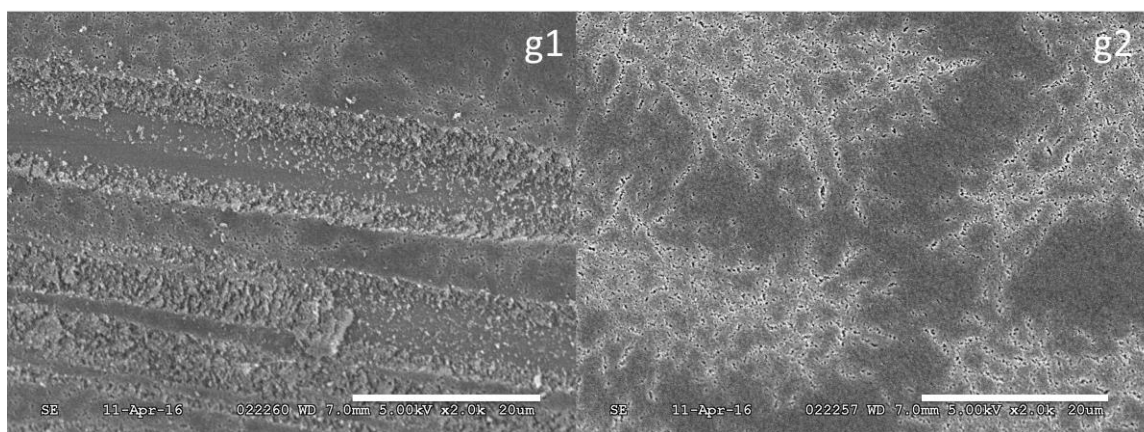


Figure 4.12 SEM micrographs of different spots on the specimen(g) at $\times 2k$ magnification. The porous surface was not uniform. Coarse parts also existed as shown in (g1). Phase separation was clearly observed on (g2) spot.

4.4.2.2 Silica-titania sols mixed before aging with higher proportion of titania

The molar ratio of silica and titania from above samples was all 7:3 with only 30% titania. A higher proportion of titania was also tested out because of the good bioactivity and biocompatibility of titania.

Table 4.6 Titania-silica coating procedure with titania-first hydrolysis

	Si / Ti (mol)	Si+Ti / Rosin (mol)	Rotating speed (rpm)	Heating temperature /Time	Soaking
a.	1:1	7:3	2000	150°C/1hr	97% EtOH/10s
b.	1:1	1:1	2000	150°C/1hr	97% EtOH/10s
c.	3:7	7:3	2000	150°C/1hr	97% EtOH/10s
d.	3:7	1:1	2000	150°C/1hr	97% EtOH/10s

The proportion of titania in this group experiment was increased to 50% and even 70%. Space-occupying rosin content as 30% and 50% were both detected. Parameters as 2000 rpm for rotating speed and 150°C heat-treatment for an hour were processed in coating procedure since coated samples under certain conditions in previous experiments all had good outcomes. It turns out that no pore was detected under scanning electron microscopy with up to 15k magnification. The attempt to applying more titania than silica in the sol-gel formulation with titania-first hydrolysis failed.

4.4.2.3 Silica-titania sols mixed after aging

The second way to mix sols with titania-first hydrolyses was to add silica into prepared titania right after its overnight stirred aging. The mixed sol was only statically aged together for the last 3 days. The molar ratio of silica/titania in this group was 7:3 and higher proportion of silica was still used. The molar ratio of centre elements (silicon plus titanium) and rosin as 7:3 (30% rosin) and 1:1 (50% rosin) were still both tested. Different rotating speeds and different heat-treated temperatures were applied and listed in table 4.7.

Table 4.7 Silica-titania coating procedure with titania-first hydrolysis and mixed after stirred aging.

	Si / Ti (mol)	Si+Ti / Rosin (mol)	Rotating speed (rpm)	Heating temperature /Time	Soaking
a.	7:3	7:3	3000	150°C/1hr	97% EtOH/10s
b.	7:3	7:3	3000	120°C/1hr	97% EtOH/10s
c.	7:3	7:3	2000	150°C/1hr	97% EtOH/10s
d.	7:3	7:3	2000	120°C/1hr	97% EtOH/10s
e.	7:3	1:1	3000	150°C/1hr	97% EtOH/10s
f.	7:3	1:1	3000	120°C/1hr	97% EtOH/10s
g.	7:3	1:1	2000	150°C/1hr	97% EtOH/10s
h.	7:3	1:1	2000	120°C/1hr	97% EtOH/10s

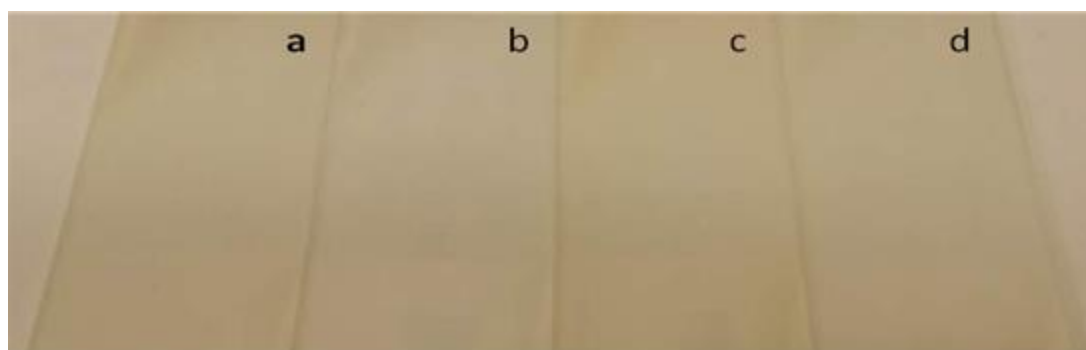


Figure 4.13 Photos of silica-titania coatings on glass microscope slides with titania-first hydrolyses and after-aging mixing: (a) 30% rosin; 3000 rpm; 150°C; (b) 30% rosin; 3000 rpm; 120°C; (c) 30% rosin; 2000 rpm; 150°C; (d) 30% rosin; 2000 rpm; 120°C; The coating was not evenly distributed and the edge was less coated due to the spinning process on glass microscope slides. All SEM illustrations were conducted on the well-coated middle area.

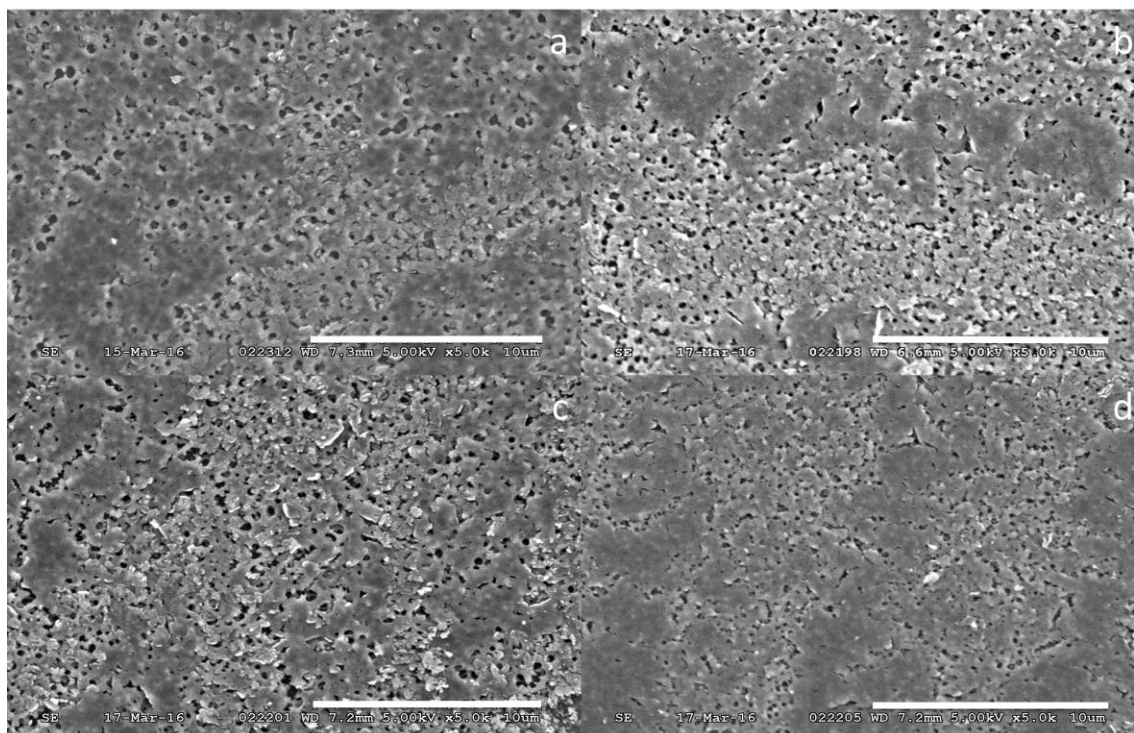


Figure 4.14 SEM micrographs of silica-titania coating with titania-first hydrolysis and with 30% rosin: (a) 3000 rpm; 150°C; (b) 3000 rpm; 120°C; (c) 2000 rpm; 150°C; (d) 2000 rpm; 120°C;

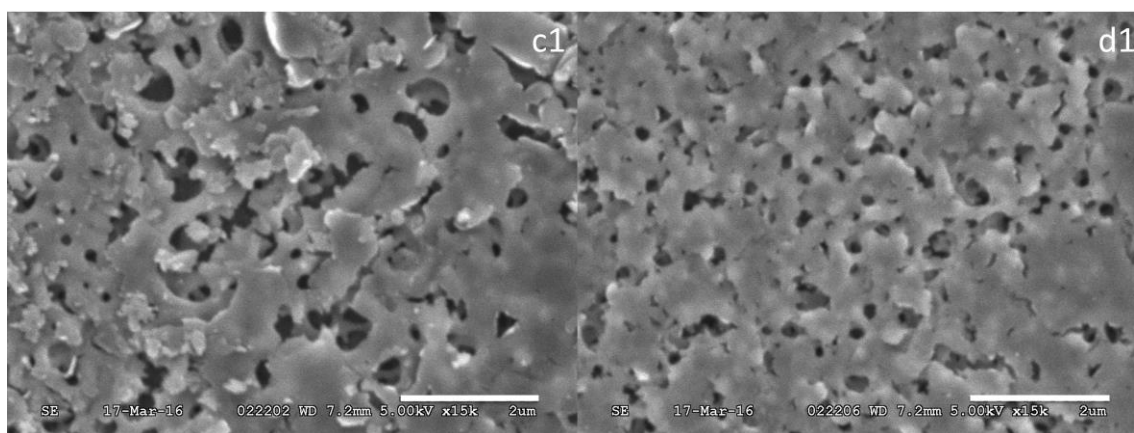


Figure 4.15 SEM micrographs of the sample(c) and sample(d) at $\times 15k$ magnification. The scaffold-like structure on coated surface was further demonstrated.

Coated surfaces were characterized by scanning electron microscopy. As shown in Figure 4.14, Pores were observed again on all coatings with the same size of the pores achieved by before-stirring mixing procedure. Slight phase separation was observed on all four surfaces and one phase always had more pores than the other phase had. Sample (c) with a thicker coating and the heat-treatment at a higher temperature still had the bigger sized pores but no distinctly scaffold-like structure (Figure 4.15).

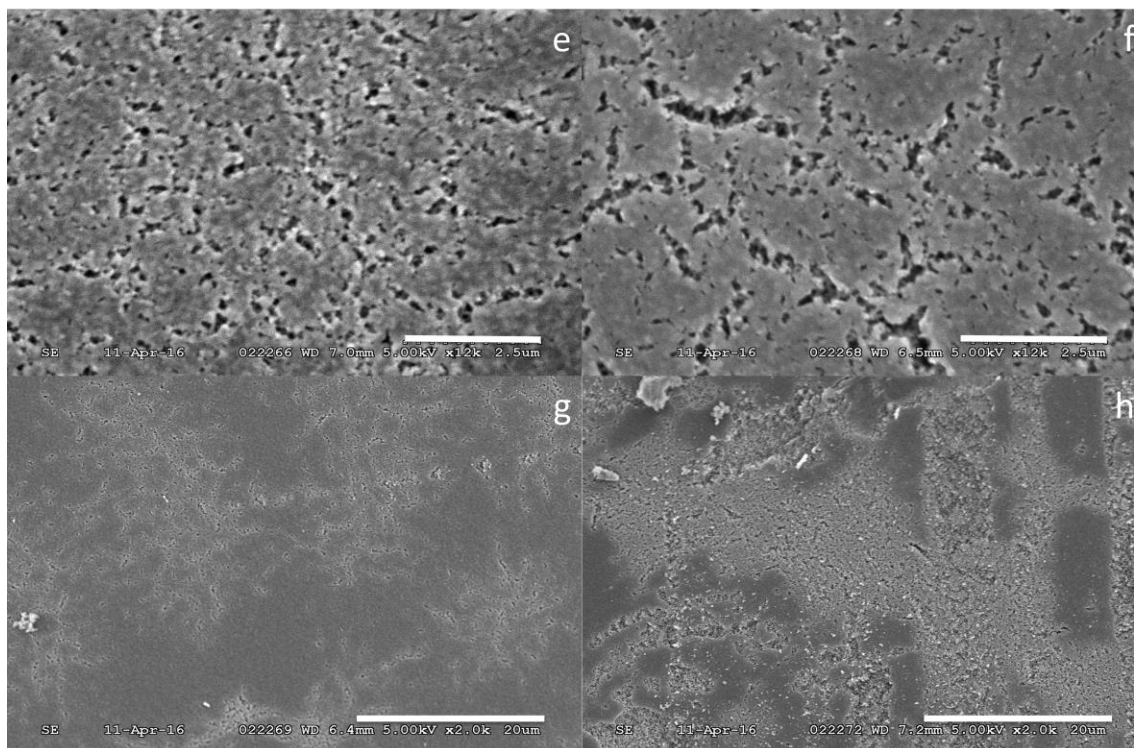


Figure 4.16 SEM micrographs of silica-titania coating with titania-first hydrolysis and with 50% rosin: (e) 3000 rpm; 150°C; (f) 3000 rpm; 120°C; (g) 2000 rpm; 150°C; (h) 2000 rpm; 120°C. The porosity of coated specimens didn't increase obviously with the more space-occupying material.

Applied rosin content was increased to 50% again. Yet the surface porosity didn't increase with increasing content of the space-occupying material. As shown in Figure 4.16, all four surfaces are porous compared to the rough surfaces in Figure 4.11 that mixed before aging. Coatings in this group had fewer pores but almost the same size of

the pores made by 30% rosin soaked off. A convincing show of anomalous phase separation was noticed on all four coatings in this group.

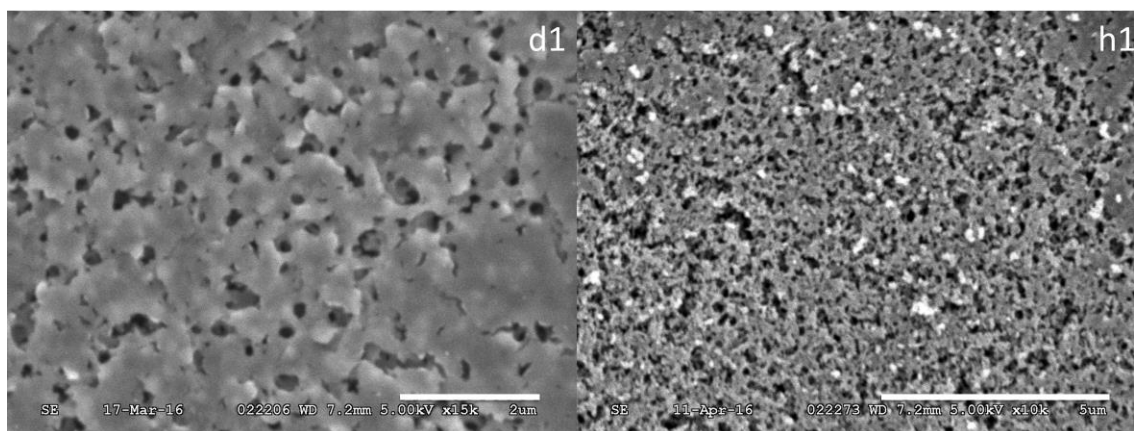


Figure 4.17 SEM micrographs of specimens spin coated at 2000 rpm and heat-treated at 120°C with 30% rosin (d1) and 50% rosin (h1). Fine and close pores were created with higher content of rosin.

4.4.3 Silica-titania mixed sols with silica-first hydrolysis

Silica-titania sols could also be mixed together with silica-first hydrolysis. In this case, silica sol was fully prepared at the beginning and was added into stirring aged titania sols. The mixed sols were further reacted and aged together under static conditions overnight. The molar ratio of silica and titania was 7:3 still with a higher proportion of silica. Rosin content as 30% and 50% were both tested out. During the coating procedure, 2000 rpm for rotating speed and 150°C heat-treatment for an hour were applied again as process parameters due to previous good results under certain conditions. Detailed coating procedure parameters were listed in Table 4.8. Scanning electron microscopy was used to demonstrate the surface morphology of coated substrate.

Table 4.8 Silica-titania coating procedure with silica-first hydrolysis

	Si / Ti (mol)	Si+Ti / Rosin (mol)	Rotating speed (rpm)	Heating temperature / Time	Soaking
a.	7:3	7:3	2000	150°C/1hr	97% EtOH/10s

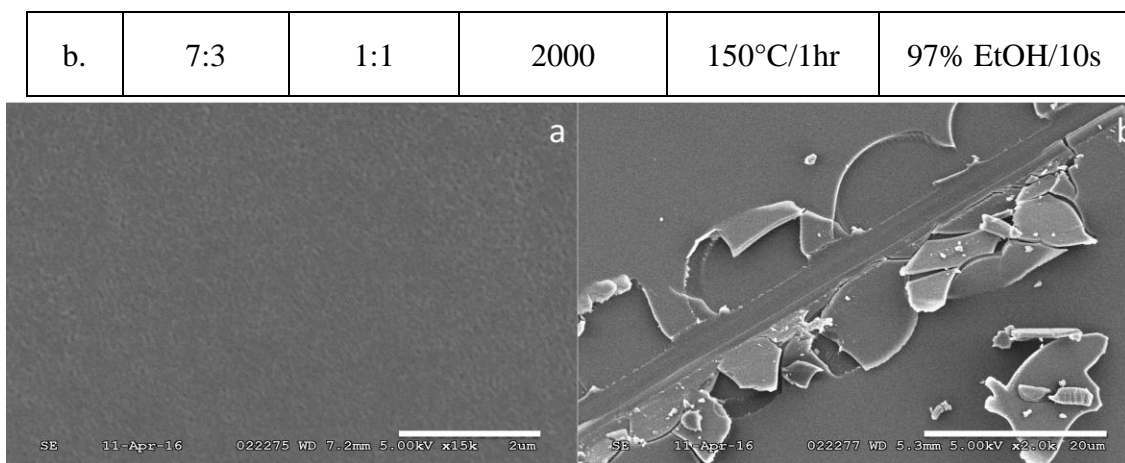


Figure 4.18 SEM micrographs of silica-titania coating with silica-first hydrolysis: (a) 30% rosin; 15k magnification; (b) 50% rosin; 2k magnification; No pore was observed after the coating procedure with silica-first hydrolysis.

As shown in Figure 4.18, a relatively plain surface without any pore was observed even with 15k magnification on the sample (a) made through 30% rosin. Sample (b) had a quite plain surface with no pore as well. Yet somehow it had a few sharp aged cracks that were most likely caused by some external mechanical force. No obvious phase separation was observed on both coatings. Silica-first hydrolysis was not a proper method to create a sol-gel derived porous silica-titania coating according to this experimental result.

To sum up, the titania-first hydrolysis and at least 70% silica sols were necessary to form a porous coating on glass microscope slides. The surface with highest porosity was achieved through 30% rosin instead of 40% or even 50% rosin. Modified process parameters such as 2000 rpm rotating speed, an hour heat-treatment at 150°C, and 97% ethanol for rosin soaking off in 10s could be used to achieve the desired results. All the original sol formulations and spin coating process parameters could be further estimated on different substrates in following chapters.

Chapter 5

5 Sol-gel-derived silica-titania coating on Aluminum

5.1 Introduction

Aluminum, usually considered as a bio-inert material (Li et al. 1994), was secondly used as the coating substrate after glass microscope slides to further demonstrate the practicability of sol-gel derived porous coatings on metal. Experimental parameters during the coating procedure that gave the relatively better coating results on glass microscopes slides were selected and performed again on aluminum substrates. Different surface morphologies on different substrates with the same coating procedure were also evaluated in the end of this chapter.

5.2 Sol-gel derived silica-titania coating on aluminum substrate

In this group of experiments, the molar ratios of silica and titania as 7:3, 6:4, 1:1 (the proportion of titania as 30%, 40%, 50%) were all tested. Titania sol was first hydrolyzed and was then added into after-stirred silica sol to age statically for 3 days together. Rosin content was 30% for most samples but 50% rosin was also tested once in this group. Other parameters of the coating procedures were listed in Table 5.1.

Table 5.1 Sol-gel derived silica-titania coating procedure on aluminum

	Si / Ti (mol)	Si+Ti / Rosin (mol)	Rotating speed (rpm)	Heating temperature / Time	Soaking
a.	7:3	7:3	2000	150°C/1hr	97% EtOH/10s
b.	6:4	7:3	2000	150°C/1hr	97% EtOH/10s
c.	5:5	7:3	2000	150°C/1hr	97% EtOH/10s
d.	7:3	1:1	2000	120°C/1hr	97% EtOH/10s

SEM micrographs were taken to demonstrate the surface morphology of coated samples. As shown in Figure 5.1, most attempt in this group failed to achieve a porous surface on samples. Only few pores were observed on sample (a) and no pore was observed on sample (b) and (c). Comparison of picture (a), (b) and (c) showed that the proportion of titania in the original formulation to create a porous coating on aluminum was up to 30%. Higher percent of titania was not capable of forming a porous surface. Combined with the results from chapter 4, we'd come to the conclusion that 30% titania was the highest proportion of titania sol in the original sol-gel formulation to form a evenly-distributed porous surface on both glass and aluminum substrates.

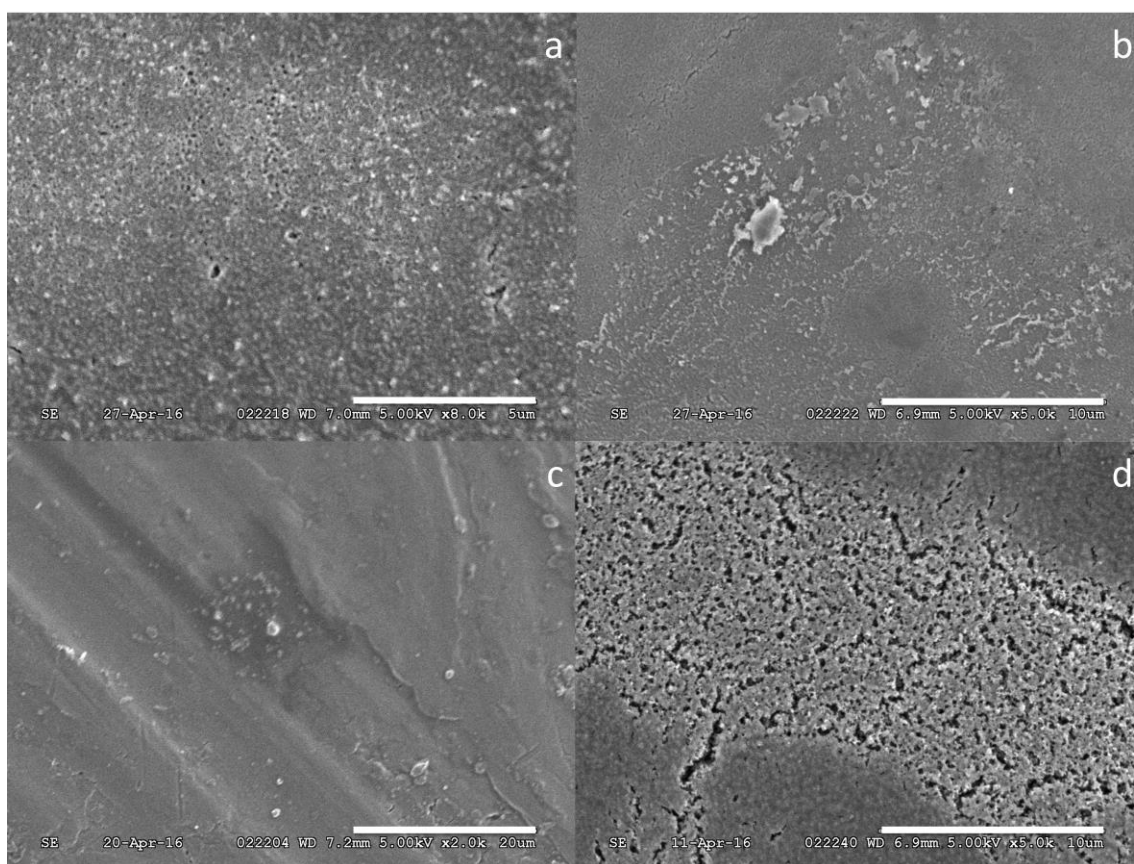


Figure 5.1 SEM micrographs of sol-gel derived silica-titania porous coating on aluminum: (a) 30% titania; 30% rosin; (b) 40% titania; 30% rosin; (c) 50% titania; 30% rosin; (d) 30% titania; 50% rosin.

At the same time, the contrast between picture (a) and picture (d) showed us that more soaked off rosin left more pores or flaws on coated aluminum. Some flaws on sample (d) were in the length of micron size. Sample (a) and sample (d) were also observed under a higher magnification using scanning electron microscopy as shown in Figure 5.2. Distinguished from sol-gel derived porous coatings on glass microscope slides, porous coating with a higher porosity could be achieved by using a higher proportion of rosin as the space-occupying material. However, severer phase separation was observed on sample (d) than sample (a) accompanied by higher porosity.

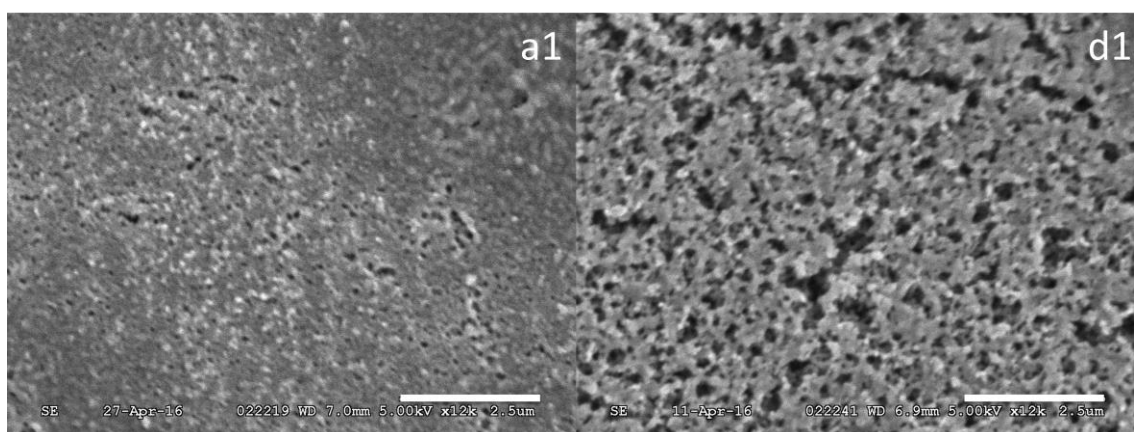


Figure 5.2 SEM micrographs of coatings with 30% titania at $\times 12k$ magnification. The specimen (d1) with 50% rosin got a higher porosity than the specimen (a1) with 30% rosin.

5.3 Comparison with coatings on glass and aluminum substrates

Same formulation with same spin coating procedure was conducted on both glass and aluminum substrate and the surface topographies on two substrates were observed and compared. Three groups of comparisons were finished and were illustrated in Figure 5.3. All coatings demonstrated in Figure 5.3 had 30% titania and 70% silica and the pores were formed using 97% ethanol to soak off 30% rosin. Both coatings were spin-coated at 2000 rpm and were heat-treated at 150°C for an hour. The only difference between the left and right column in Figure 5.3 is the different substrates as aluminum for the left column and glass for the right.

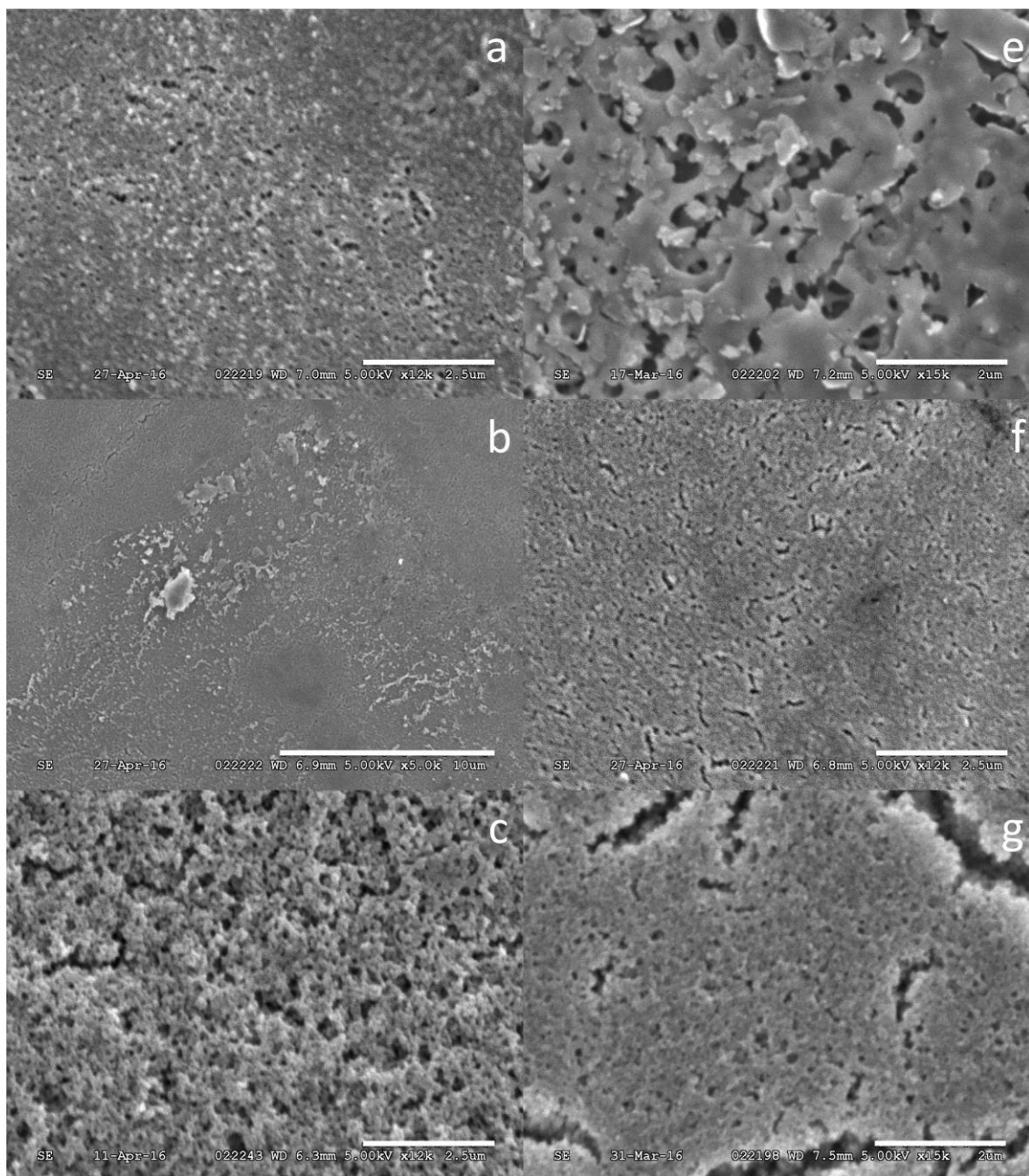


Figure 5.3 SEM micrographs of surfaces under same coating procedures with same formulations on different substrates: (a) on aluminum; 12k magnification; (e) on glass; 15k magnification; (b) on aluminum; 5k magnification; (f) on glass; 12k magnification; (c) on aluminum; 12k magnification; (g) on glass; 15k magnification;

In Figure 5.3, two pictures in the same row showed the coatings with the same formulation and coating procedure on different substrates with the left column for

aluminum substrate and the right column for glass microscope slides. Picture (a) and (e) were both with 30% titania and 30% rosin listed as sample (a) in Table 5.1. Higher porosity (even scaffold-like structure) was seen in picture (e) compared to picture (a). Meanwhile, only few pores in the size of tens of hundreds of nanometer were observed on picture (a). Picture (b) and (f) were both with 40% titania and 30% rosin listed as sample (b) in Table 5.1. None of these two samples were created with a desired porous surface. Picture 'c' and (g) were both with 50% titania and 30% rosin listed as sample (c) in Table 5.1. Close distributed small holes were observed on picture (c) with 12k magnification. Barely pores but crevices were found on picture (g) even with 15k magnification.

Given all that, starkly contrast was observed between coatings on different substrates, as observed under the same sol-gel formulation and the same coating process. The nature of substrates did have a considerable influence on the characters of coatings. The aluminum substrate and glass microscope slides may had a quite different reactions and characteristics under different coating circumstances and there was no better one substrate under all the different coating procedure. On the other hand, different groups of sol-gel formulations and spin coating procedures with a higher probability of success should still be all carried out on titanium itself as the most widely used substrate of dental implants.

Chapter 6

6 Sol-gel-derived silica-titania coating on titanium

6.1 Introduction

Titanium as the most widely used material for dental implants was finally used as the substrate in this chapter. Some titanium substrates were pretreated to change the original surface morphologies of substrates before the spin coating procedure. The experimental parameters of the processed spin coating were mostly discussed and selected in previous chapters. The achieved sol-gel derived silica-titania coatings with desired porous surface morphologies were further tested for their mechanical properties like hardness and abrasion resistance. The bioactivities of the promising samples were also characterized by immersing coated samples in simulated body fluid for certain time and detecting the mineral deposition (Murphy, Kohn, and Mooney 2000).

6.2 Sol-gel derived silica-titania porous coating on titanium

For titanium as the substrate, certain pretreatments were accomplished on titanium substrates right before the coating procedure to prepare a titanium oxide layer so as to increase the surface roughness and the final coating performance. All titanium substrate were grounded by silicon carbide paper and were then ultrasonically washed for 5 minutes in ethanol before pretreatment. After cleaning and drying in a fume hood, some substrates were placed in a 600°C laboratory furnace in the atmosphere for an hour as the thermal oxidation pretreatment. Some substrates were plasma oxidized in the atmosphere for 3 min. The oxide layers from pretreatments may contain some incidental elements since the layers were carried out by the reaction between the substrate and the surrounding atmosphere. Surface morphology of pretreated titanium substrates was demonstrated by scanning electron microscopy as shown in Figure 6.1 and Figure 6.2.

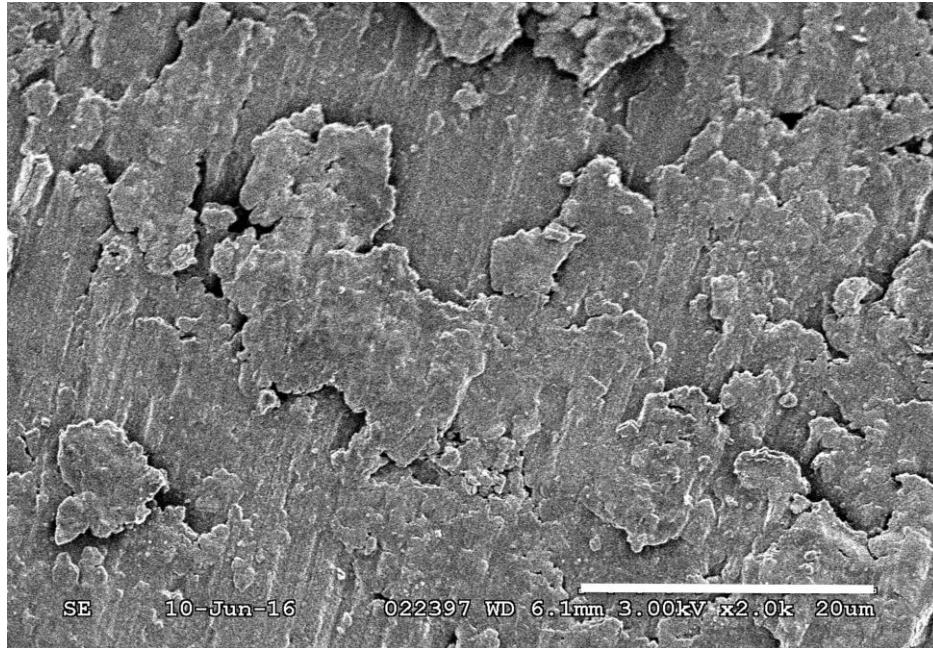


Figure 6.1 Titanium substrate surface after thermal oxidation with the increased surface roughness

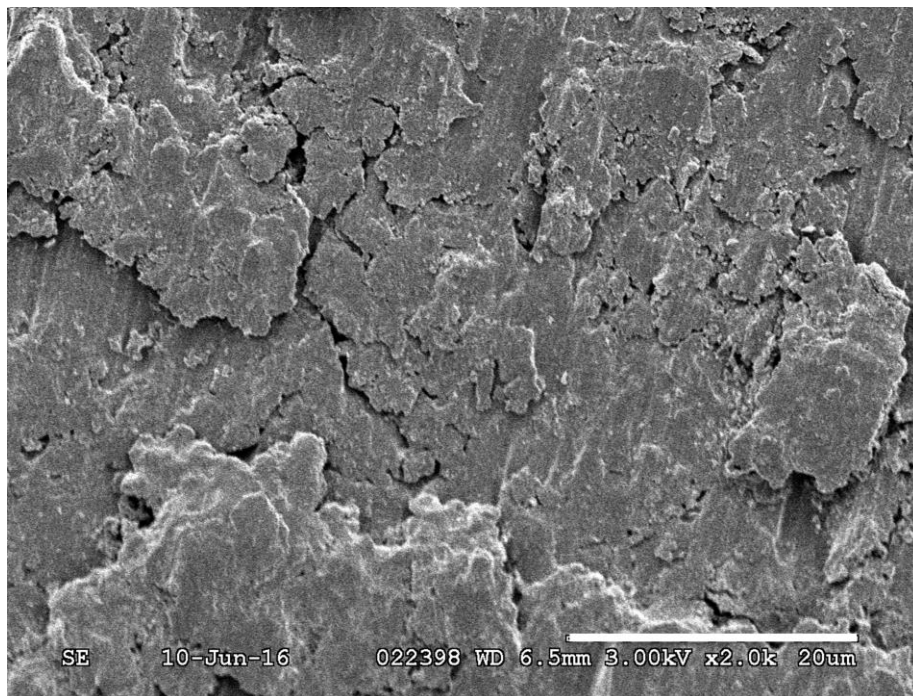


Figure 6.2 Titanium substrate surface after plasma oxidation with the increased surface roughness

6.2.1 Sol-gel derived silica-titania porous coating by 30% rosin

As discussed in the last chapter, the highest proportion of titania in original sol was only 30% which meant at least 70% of silica was needed to make sure the porous coating could be achieved. 30% rosin was tried out as the space-occupying material in this group. Both thermal oxidation and plasma oxidation were accomplished as pretreatment and were compared to the samples with no pretreatment. Detailed spin coating procedure parameters were listed in Table 6.1. The rotating speed of spinning remained in 2000 rpm. Heat-treating temperature as 150°C and 120°C were both tested out for an hour.

Table 6.1 Sol-gel derived silica-titania porous coating by 30% rosin

	Si / Ti (mol)	Si+Ti / Rosin (mol)	Pretreatment	Rotating speed (rpm)	Heating temperature /Time
a.	7:3	7:3	-	2000	150°C/1hr
b.	7:3	7:3	-	2000	120°C/1hr
c.	7:3	7:3	Thermal oxidation	2000	150°C/1hr
d.	7:3	7:3	Thermal oxidation	2000	120°C/1hr
e.	7:3	7:3	Plasma oxidation	2000	150°C/1hr
f.	7:3	7:3	Plasma oxidation	2000	120°C/1hr

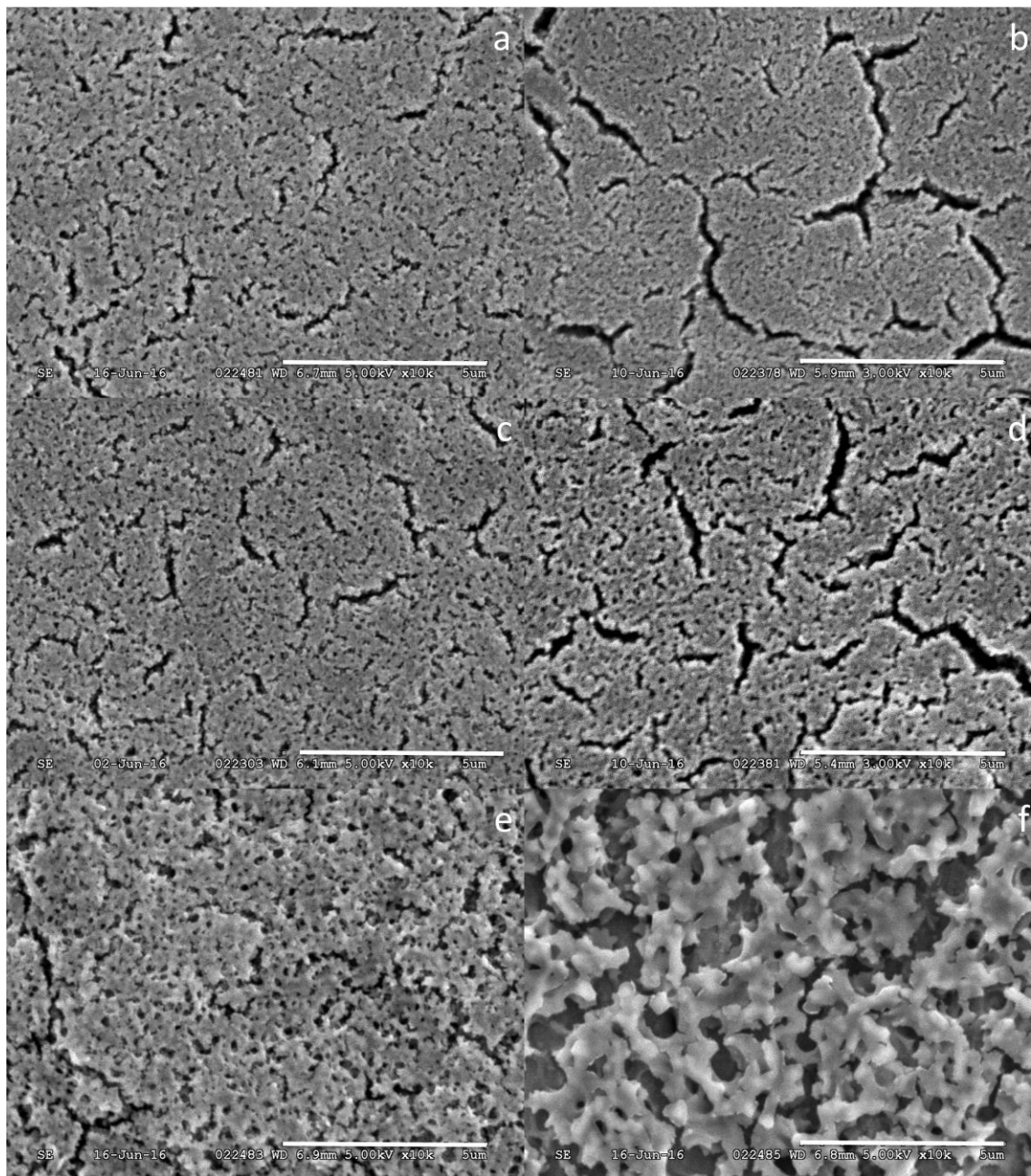


Figure 6.3 SEM micrographs (at $\times 10k$ magnification) of porous coating by 30% rosin: (a) No pretreatment; 150°C ; (b) No pretreatment; 120°C ; (c) Thermal oxidized; 150°C ; (d) Thermal oxidized; 120°C ; (e) Plasma oxidized; 150°C ; (f) Plasma oxidized; 120°C . All surfaces were porous yet slightly cracked. The micro-sized scaffold structure was observed on sample (f).

SEM micrographs were taken to demonstrate the surface morphologies of the coated samples. As shown in Figure 6.3, substrate pretreated by plasma oxidation had the most uniform porous surfaces. Plasma oxidized and 120°C heat-treated sample even had the micro-sized scaffold structure which should be perfect for a bioactive surface. Evenly distributed flaws were observed on substrates with no pretreatment and with thermal oxidation. Compared to 150°C heat-treatment, 120°C heat-treated samples brought out the less cracked surfaces. No phase separation was revealed in all six samples.

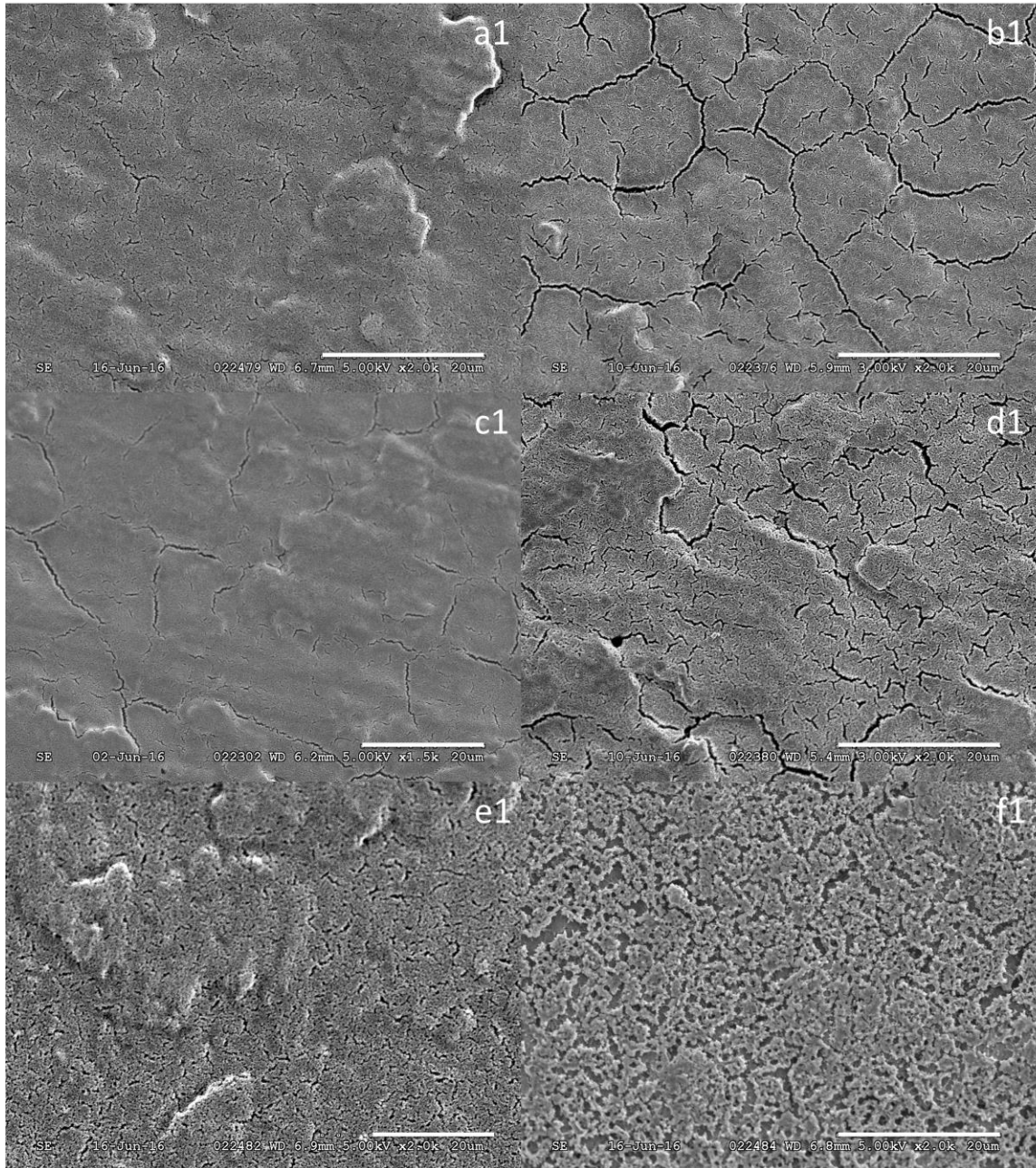


Figure 6.4 SEM micrographs of the same porous coating shown in Figure 6.3 but at $\times 2k$ magnification (lower than the magnifications used in Figure 6.3) [except for (c1) at $\times 1.5k$ magnification]. Cracks at uniform distribution could be easily observed at a lower magnification. Moreover, high porosity could already be observed on (f1) at $\times 2k$ magnification.

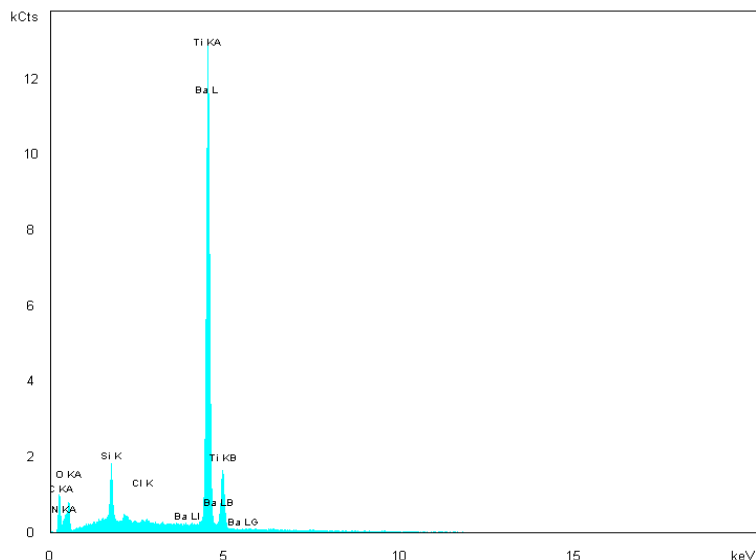


Figure 6.5 EDX analysis of sample (a) revealed titanium and silicon to be present in the treated surface.

Energy dispersive X-ray spectroscopy (EDX) illustrated the actual composition of the surfaces in Figure 6.5. The coated surface of sample (a) exhibited titanium as the predominant element and silicon, carbon and oxygen were also present on the surface in smaller proportions.

6.2.2 Sol-gel derived silica-titania porous coating by 40% rosin

The content of rosin as the space-occupying material was increased to 40% in this group of the experiment. The molar ratio of silica and titania remained in 7:3. Both thermal oxidation and plasma oxidation were still used as the pretreatment of substrates. Plasma oxidized substrate was only heat-treated at 120°C this time since the plasma oxidized substrate heated at 120°C [Figure 6.3 (f)] had an obvious advantage over the one heated at 150°C [Figure 6.3 (e)]. All parameters for the procedure were listed in Table 6.2.

Table 6.2 Sol-gel derived silica-titania porous coating by 40% rosin

	Si / Ti (mol)	Si+Ti / Rosin (mol)	Pretreatment	Rotating speed (rpm)	Heating temperature /Time
a.	7:3	6:4	-	2000	150°C/1hr

b.	7:3	6:4	-	2000	120°C/1hr
c.	7:3	6:4	Thermal oxidation	2000	150°C/1hr
d.	7:3	6:4	Thermal oxidation	2000	120°C/1hr
e.	7:3	6:4	Plasma oxidation	2000	120°C/1hr

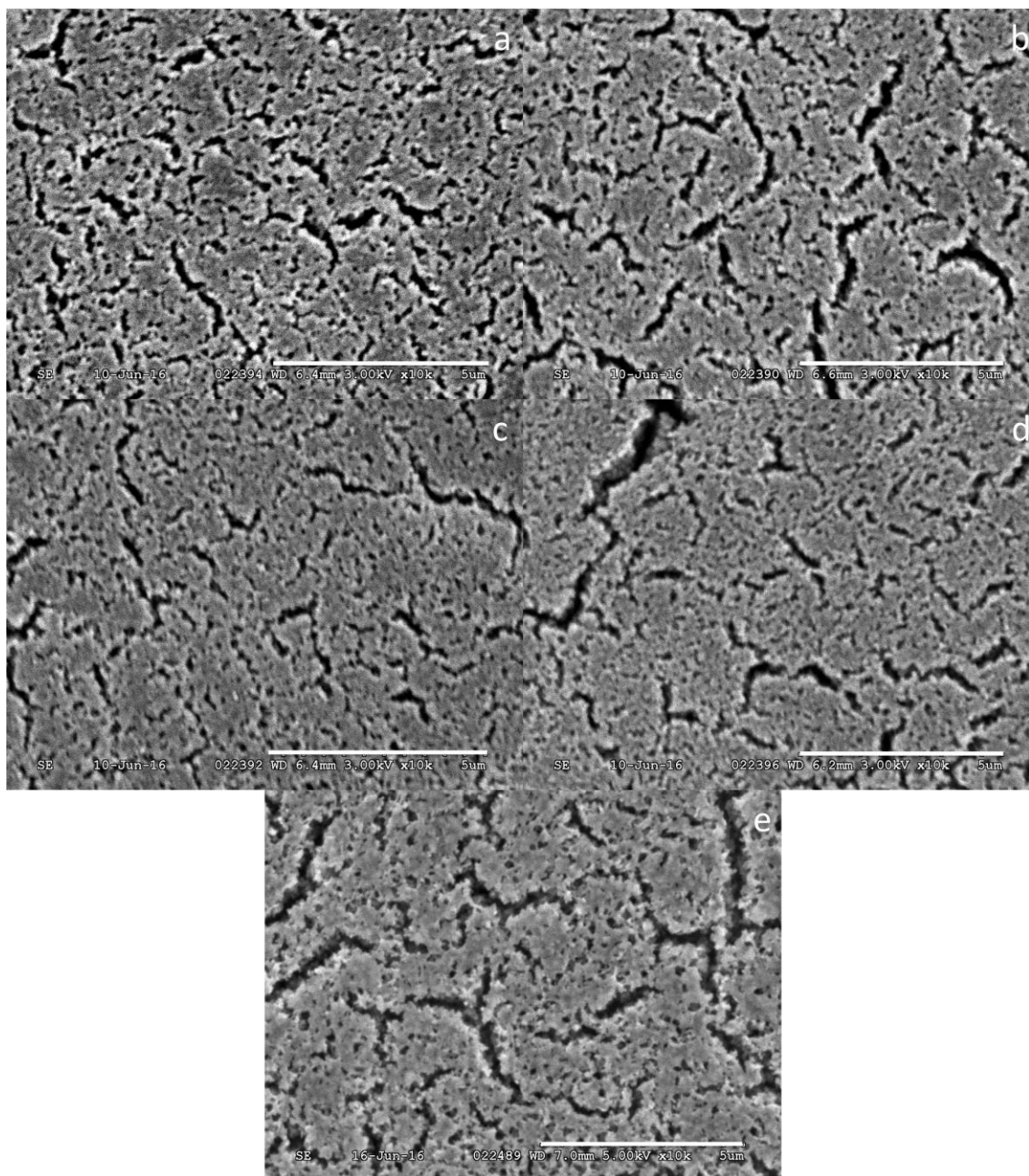


Figure 6.6 SEM micrographs of porous coating by 40% rosin: (a) No pretreatment; 150°C; (b) No pretreatment; 120°C; (c) Thermal oxidized; 150°C; (d) Thermal oxidized; 120°C; (e) Plasma oxidized; 120°C. Severer cracks were observed compared to porous coating with lower rosin content (30% rosin).

The surface morphologies of coated samples were illustrated using scanning electron microscopy. All five samples had various degree of cracking and flaws in micron length,

uniformly distributed on coated surfaces. All surfaces were homogeneous without a strong sign of phase separation. Compared to sample(f) described in Table 6.1, all five samples with a higher content of space-occupying material failed to achieve the surface with a higher porosity. Plasma oxidized substrate [Figure 6.6 (e)] did not have the evident advantage this time. No sharp difference between the surface morphologies of all five coated substrates. But both 150°C heat-treated samples with or without thermal oxidation were less cracked which could be considered as the comparative advantage specifically.

6.2.3 Sol-gel derived silica-titania porous coating by 50% rosin

The content of rosin as the space-occupying material was further increased to 50% as the attempt to build a porous coating in this group of the experiment. The formulation with only 30% titania in original sol was tried out again. Heat treatments at 120°C and 150°C were both applied on substrates with no pretreatment and substrates with thermal oxidation. The plasma oxidized substrate was still only heat-treated at 120°C rather than 150°C. All parameters in this group of experiments were listed in Table 6.3 in detail.

Table 6.3 Sol-gel derived silica-titania porous coating by 50% rosin

	Si / Ti (mol)	Si+Ti / Rosin (mol)	Pretreatment	Rotating speed (rpm)	Heating temperature /Time
a.	7:3	5:5	-	2000	150°C/1hr
b.	7:3	5:5	-	2000	120°C/1hr
c.	7:3	5:5	Thermal oxidation	2000	150°C/1hr
d.	7:3	5:5	Thermal oxidation	2000	120°C/1hr
e.	7:3	5:5	Plasma oxidation	2000	120°C/1hr

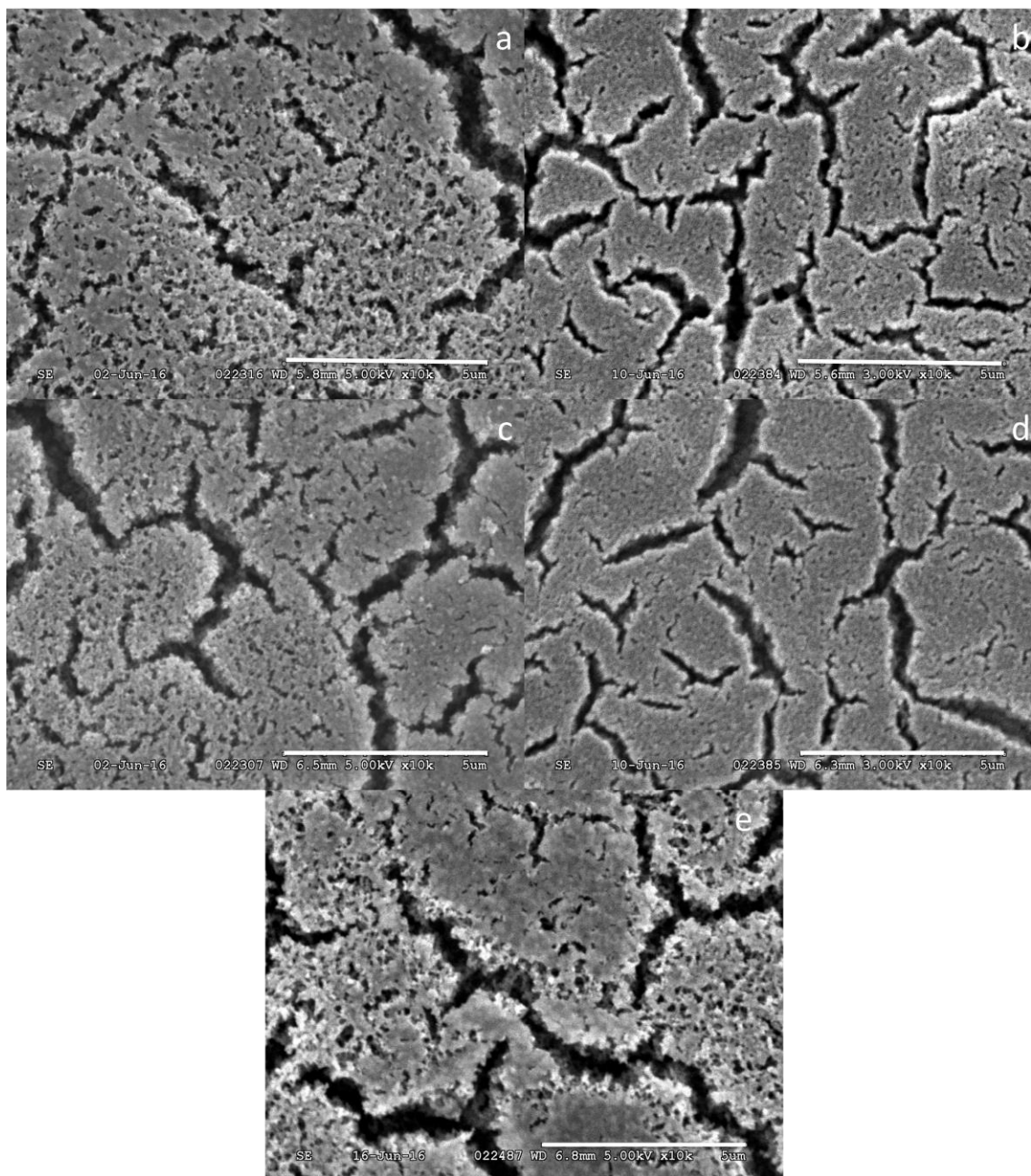


Figure 6.7 SEM micrographs of porous coating by 50% rosin: (a) No pretreatment; 150°C; (b) No pretreatment; 120°C; (c) Thermal oxidized; 150°C; (d) Thermal oxidized; 120°C; (e) Plasma oxidized; 120°C; Serious cracking was revealed on coated surface with highest rosin content (50% rosin).

SEM micrographs were taken to illustrate the surface morphology of the coated samples (Figure 6.7). All five surfaces resulted in critical cracking. Severe flaws in the length of

several microns and extremely tiny pores of nano-scale size were both revealed on the same coated surface. A higher proportion of space-occupying material didn't lead to a higher porosity but only the severer cracked surface. Sol-gel derived silica-titania coatings on titanium by 50% rosin were not proper to use as the bioactive coating for dental implants.

As suggested in above groups of experiments, coated samples with 30% rosin performed better with 120°C curing. Meanwhile, coated samples with 40% and 50% rosin had a more promising surface when curing at 150°C. The group of samples coated with 40% rosin was generally better performed with a more uniform surface and fewer flows. In summary, only certain sol-gel derived silica-titania porous coatings on titanium had the most proper surface morphologies and the higher chance of good bioactivity. When 30% rosin was used to space-occupying, plasma oxidized sample heat-treated at 120°C had the uniform micro-sized scaffold structure. As the content of space-occupying material increased to 40%, both samples without pretreatment and sample with thermal oxidation possessed the less-cracked porous surface under 150°C heat-treatment. All three formulations were further estimated about their mechanical characters and their bioactivities. Summarized details of these samples were listed in Table 6.4.

Table 6.4 Sol-gel derived coating with relative promising surface morphology

	Si / Ti (mol)	Si+Ti / Rosin (mol)	Pretreatment	Rotating speed (rpm)	Heating temperature /Time
I	7:3	6:4	-	2000	150°C/1hr
II	7:3	6:4	Thermal oxidation	2000	150°C/1hr
III	7:3	7:3	Plasma oxidation	2000	120°C/1hr

6.3 Mechanical properties of samples

Pencil hardness test was conducted to estimate the scratch resistances of the three coated surfaces. The 6H pencil produced a black line on each sample without leaving a scratch on the coated film under optical microscope observation. Contrastive images before and

after the 6H pencil scratch were also taken under an optical microscope with 500 magnifications as shown in Figure 6.8. Thus the scratch hardness end point could be considered as 6H. So all three samples exhibited pencil hardness harder than 6H.



Figure 6.8 Contrastive images of sample III before and after the 6H pencil scratch with 500 magnifications: a. before the scratch; b. after the scratch. The coated surfaces were harder than 6H since no obviously scratch mark was left on the surface.

Coatings adhesion on pure titanium substrates were assessed through the Elcometer 107 Cross Hutch Cutter according to ASTM D3359 standard. All three promising coatings achieved the highest adhesion rating of 5B which implied nil percent area of the lattices were dislodged by the removal of the adhesive tape during the testing (Figure 6.9). The results suggested that all three sol-gel derived surfaces were tightly attached to the titanium substrate with the excellent adhesion.



Figure 6.9 Comparative images of sample III before and after the cross hutch cutter test with 50 magnifications: a. before the test; b. after the test. The silica-titania surface was tightly attached to the titanium substrate.

Abrasion resistance test was also performed on all three coated samples and different cycles were conducted on each surface under the circumstances. Detailed numbers were listed in Table 6.5. Microscope images of every sample under each circumstance were taken (Figure 6.10; 6.11; 6.12) to visually demonstrate the abrasion resistance of each sample.

Table 6.5 Different abrasion cycles on each coated sample

	100 cycles	200 cycles	300 cycles	500 cycles
I	-	-	✓	✓
II	-	-	✓	✓
III	✓	✓	✓	-



Figure 6.10 Microscope images of sample I with 500 magnifications under cycles' abrasion: a. before abrasion; b. 300 cycles; c. 500 cycles. Most of the coating was rubbed out after 500 cycles abrasion.

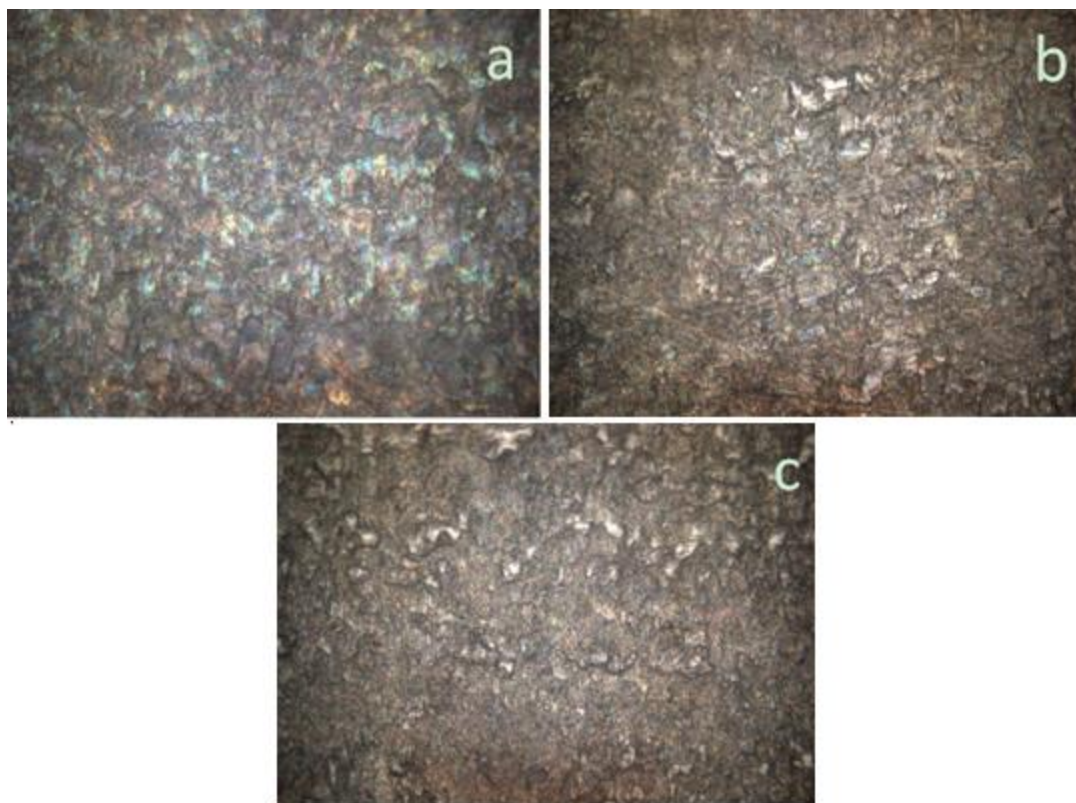


Figure 6.11 Microscope images of sample II with 500 magnifications under cycles' abrasion: a. before abrasion; b. 300 cycles; c. 500 cycles. Half of the coating was rubbed out after 500 cycles abrasion.

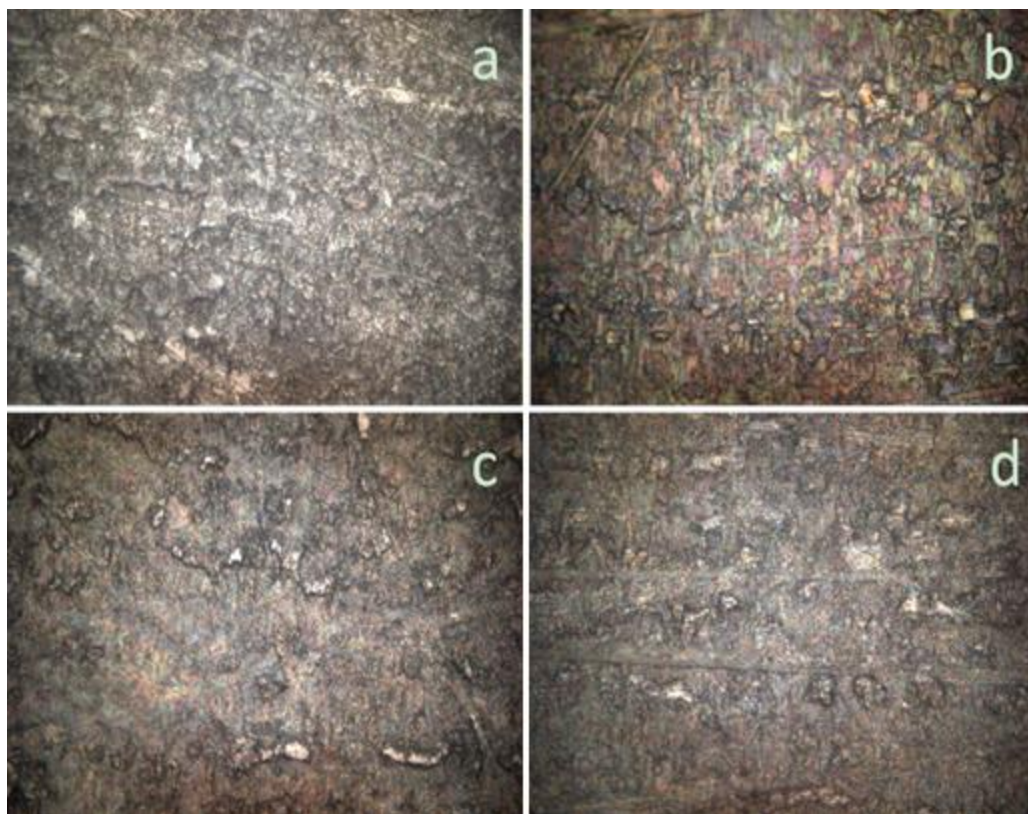


Figure 6.12 Microscope images of sample III with 500 magnifications under cycles' abrasion: a. before abrasion; b. 100 cycles; c. 200 cycles; d. 300 cycles. Most of the coating was rubbed out after only 200 cycles abrasion.

As shown in Figure 6.12, sample III was most sensitive to reiterative abrasion. Only a small portion of the surface texture was lost after 100 cycles and more stripe lost during the following abrasion analyses. The friction trace was plainly visible after 200 cycles abrasion. The sample I and sample II had the comparatively better resistances to abrasion. No abrasion mark was visible under naked eyes after 500 cycles abrasion on sample I and sample II. According to the microscope images in Figure 6.10 and Figure 6.11, the basic coated surface structures mostly maintained on the sample I and sample II substrates after 300 cycles abrasion. Sample II had the best abrasion resistance since only half the texture was lost after even 500 cycles abrasion.

6.4 Bioactivities of samples

The bioactivities of coated surfaces were illustrated by immersing the coated samples into 1.5SBF for different time periods. Commercially pure titanium (cp Ti) substrates without the sol-gel derived coating were also immersed in 1.5SBF for the same time ranges as the control group in this experiment. Although a thin layer of titanium dioxide might be performed on the titanium substrate through a natural air oxidation. All immersed samples were analyzed under the scanning electron microscopy (SEM) to estimate their abilities to form the bone-like calcium phosphate (CaP) on coated surfaces.

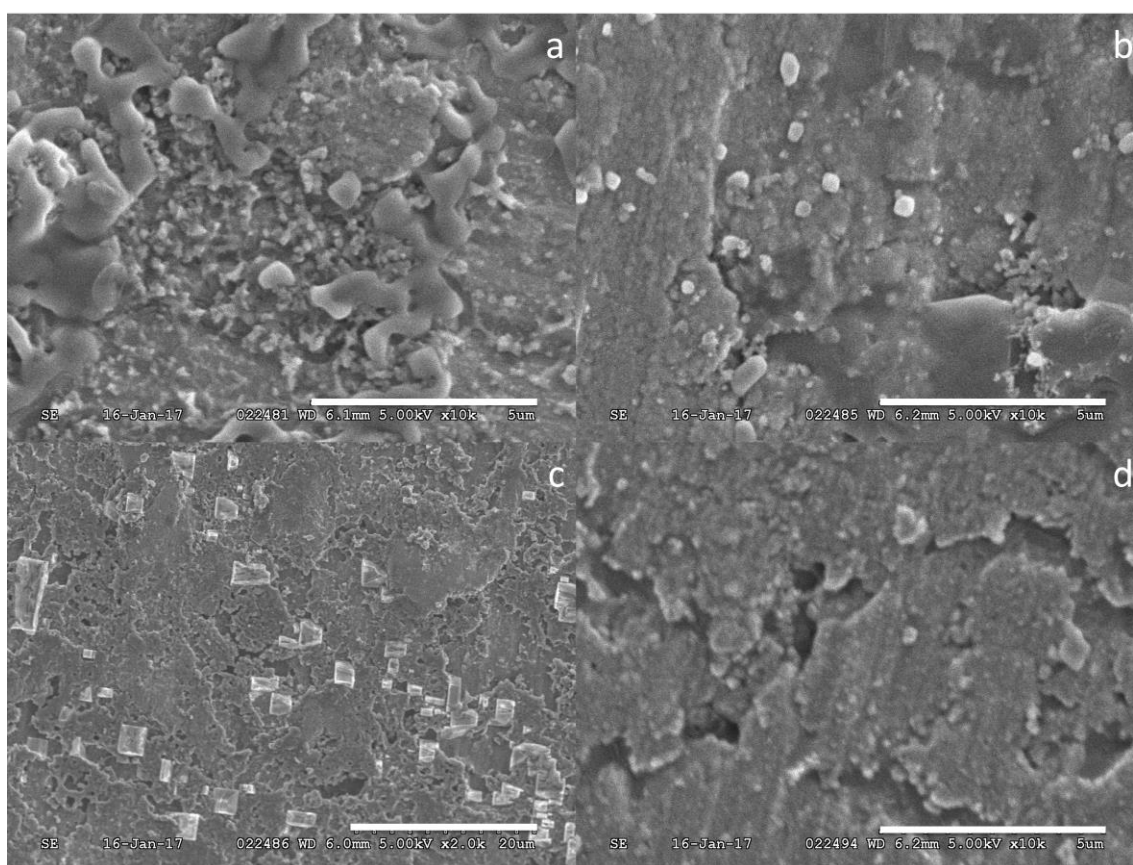


Figure 6.13 SEM micrographs of samples immersed in 1.5 SBF for 3 days: a. sample I; b. sample II; c. sample III; d. cp Ti substrate. More crystal deposits were found on coated silica-titania surfaces compared to the commercially pure titanium substrate.

Three samples coated through different procedures were incubated in 1.5SBF for 3 days with surface morphology shown in Figure 6.13. Porous surfaces on coated samples have already begun to display small mineral crystals by 3 days. The original porous coated surfaces were covered by a relatively continuous apatite film left by immersing fluids with small mineral crystals on it. The most definitive mineral crystals were already clearly found in sample III with magnification 2K. Only a few deposits were observed on commercially pure titanium substrate even with magnification 10K.

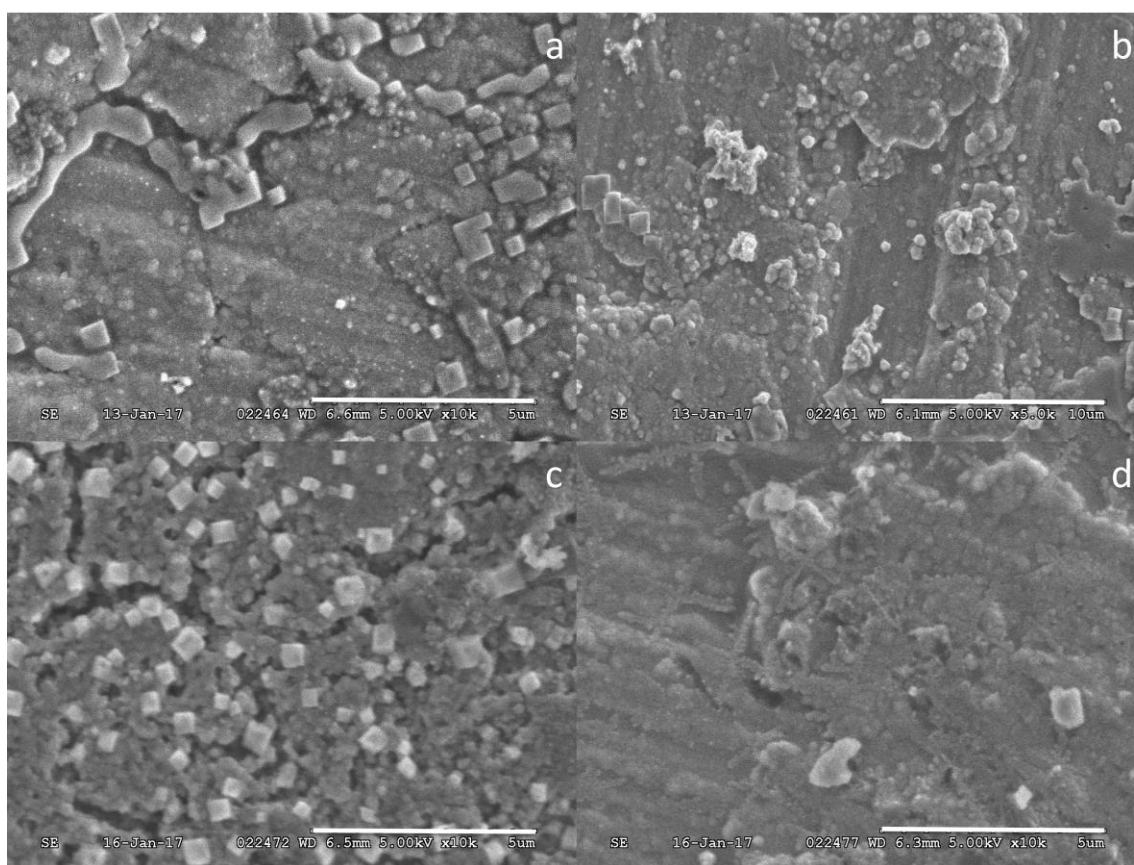


Figure 6.14 SEM micrographs of samples immersed in 1.5SBF for 10 days: a. sample I; b. sample II; c. sample III; d. cp Ti substrate. More mineral deposition were found on coated silica-titania surfaces compared to the commercially pure titanium substrate.

Immersion times of samples were extended to 10 days this time. Compared to samples incubated for only 3 days, the larger density of mineral crystal was grown and displayed

on sol-gel derived sample III coatings in this group with the most distinct deposits structure. No significant differences were found on sample I and sample II between 3 days and 10 days incubation. Mineral deposit was barely formed on the commercially pure titanium substrate.

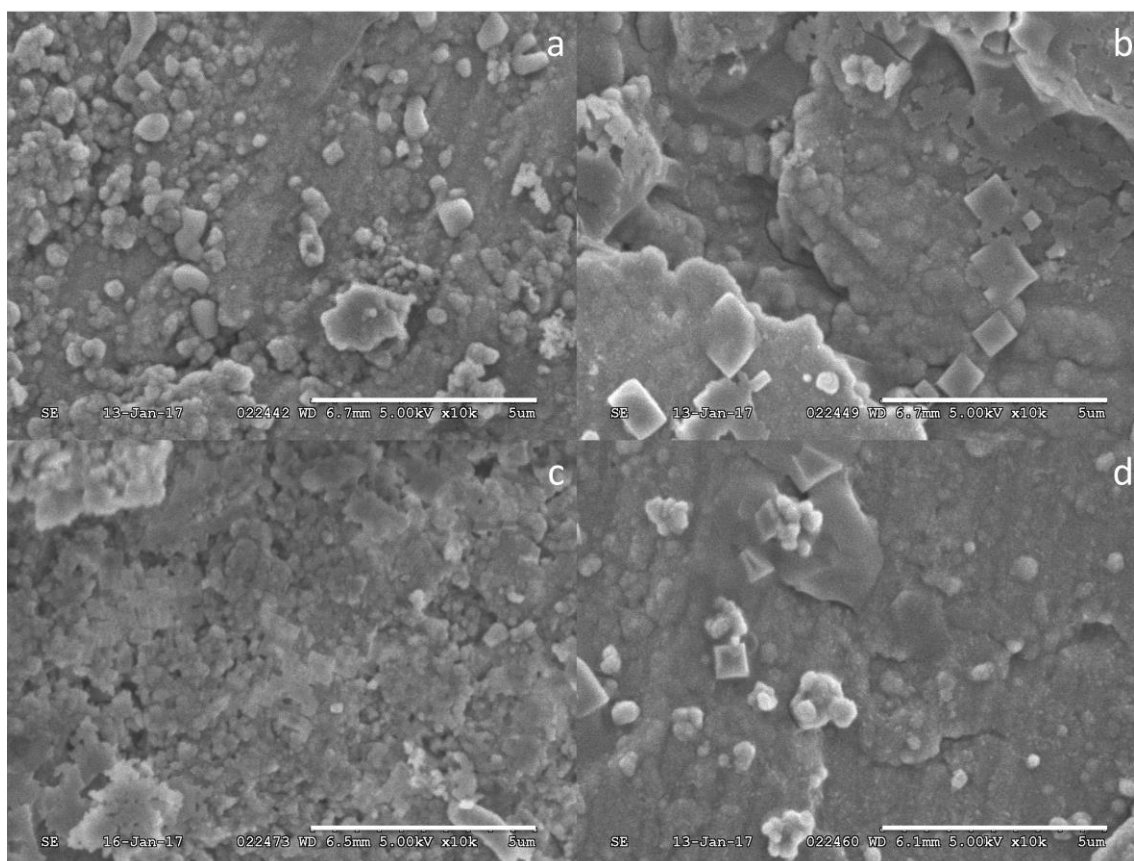


Figure 6.15 SEM micrographs of samples immersed in 1.5 SBF for 30 days: a. sample I; b. sample II; c. sample III; d. cp Ti substrate. More calcium phosphate was generated on coated silica-titania surfaces compared to the commercially pure titanium substrate.

All samples were treated in 1.5 SBF for 30 days and the formations of calcium phosphate (CaP) were evaluated under scanning electron microscopy. Plasma pre-treated sample III with 30% titania, 30% rosin was covered by a continuous mineral layer after 30 days incubation. A lot of mineral crystals was formed on sample I and a few clear deposits were displayed on sample II both over the longest immersion time as 30 days. The least

mineral crystals on all four tested samples were observed on the commercially pure titanium substrate as the control group.

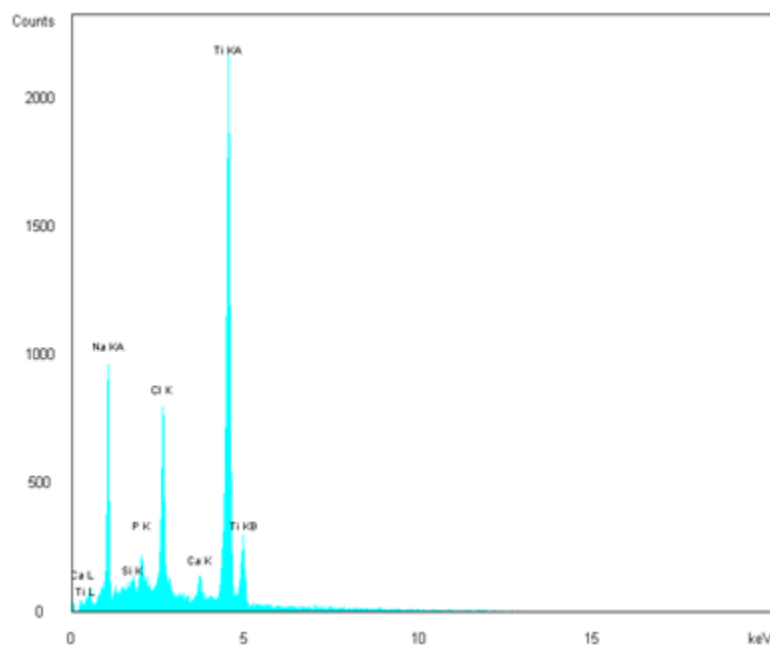


Figure 6.16 EDX analysis of the deposited mineral crystal on sample III after 10 days' incubation in 1.5SBF. The presence of calcium and phosphorus was detected. The low Ca/P atomic ratio (lower than 1.40) revealed the amorphous-stated calcium phosphate after 10 days incubation.

Energy dispersive x-ray spectroscopy (EDX) was performed to analyze the chemical composition of the mineral crystal on sample III with 10 days' incubation in 1.5SBF. Certain spots on the mineral crystal were chosen to detect and confirm their chemical composition on average. Titanium was detected at the highest level in all spots. Calcium and Phosphorus were also both detected at lower levels. There were also the presences of sodium and chlorine amongst the different spots. The findings confirmed the presences of Calcium and Phosphorus on the silica-titania coated surface and further revealed the amorphous-stated calcium phosphate after 10 days incubation. The calcium phosphate had the potential to be stabilized into crystalline apatite which is similar to bone apatite. Thus, the sol-gel derived porous coatings were able to induce the bone-like apatite during

the immersion in simulated body fluid with showed the proper bioactivities of the mixed silica-titania coatings.

Chapter 7

7 Concluding remarks and recommendations

7.1 Concluding remarks

The potential of sol-gel derived silica-titania coating on enhancing bioactivity was tested in this program using spin coating procedure. Rosin was applied as the space-holder material during the coating procedure and was then soaked off to leave a porous surface on the sol-gel derived coating. This coated porous silica-titania surface was aiming at improving the bioactivities of the substrates for the dental implants.

Glass microscope slides were experimented as the substrates at the very beginning to demonstrate the presumption of this coating procedure. Different experimental parameters during the procedure were tried out and were narrowed down to a manageable range for the following experiments. The sol-gel derived silica and titania coating was formed separately first on glass microscope slides both with rosin as the space occupying material. Evenly distributed pores were only found on the silica coating instead of the titania one. Two types of sols were mixed in different ratios at different times. The experimental parameters during the spin coating procedure like spinning speed, sintering temperature, curing time and soaking methods of rosin were all tested to search for the best result. Different proportions of the space-holder material were also tested to achieve a reasonable higher porosity on the coated surfaces. The illustrations of several groups of tests were achieved under the naked eye and the scanning electron microscopy. All experimental results showed that titania-first hydrolysis is the best way to hydrolyze two sols. Mixing after stirred aging also gave a better result than mixing before stirred aging. All mixed sols with titania content higher than 30% failed to create a porous hybrid coating. Porous surfaces arose with 30% rosin had a higher porosity than surfaces arose with 50% rosin. During the coating procedure, rotating speed as 2000rpm, 150°C heat-treatment for an hour and 10 seconds of 97% ethanol for rosin soaking off were applied as process parameters to achieve the desired results.

Aluminum was used secondly to compare the performance of the sol-gel derived silica-titania coating using a metal substrate. Different proportions of rosin were used again as the space-holder material to leave a porous surface on aluminum. As to the proportion of titania in the mixed silica-titania sol, 30%, 40%, and 50% were all tested out trying to contain more titania in a porous structure. Taken all together, no desired porous surface was created on aluminum. The corresponding outcomes of the experiments further illustrated that the highest proportion of titania with a desired porous surface was only up to 30%. Unlike the coating results on glass microscope slides, more contents of rosin did lead to a porous surface with a higher porosity. Compared to these coatings on glass microscope slides, the same sol formulations processed with the same spin-coating procedures performed distinct surfaces using aluminum as the substrate. Significant differences could be caused by different characteristics of the coated substrates.

Titanium was used for last as the substrate of the sol-gel derived silica-titania coating which had typically been used as the substrate for bone implants due to its strength and its highly inert titania layer once its inside one's body. Thermal oxidation and plasma oxidation were conducted on portions of titanium substrates respectively to improve the original surface morphology before the coating procedure (Le Guéhennec et al. 2007). The ratio of titania in the mixed sol was holding at 30% while the ratios of space-holder rosin were tried out from 30% to 50%. As discussed in previous contents, all titanium substrates with or without the pre-treatments were spin coated at 2000rpm and coated samples were cured in an air flow oven at either 150°C or 120°C for an hour. All coated surfaces were characterized by scanning electron microscopy (SEM) and three groups of samples with a relatively good surface morphology were selected for further detections. Commercially pure titanium substrate without any pretreatment and the thermally oxidized titanium substrate both achieved the best results with 40% space-holder rosin and 150°C curing. The plasma oxidized titanium substrates displayed the best performance with only 30% space-holder rosin and 120°C curing. The only group of samples with a scaffold-like structure and micro-sized pores was achieved through the plasma oxidization pretreatment. Mild rifts were observed on samples with thermal oxidation and samples with no pretreatment.

Some mechanical properties of the three samples were following demonstrated. All samples performed a higher hardness than 6H through the commercial pencil hardness test and they all achieved the highest adhesion rating of 5B according to ASTM D3359 standard through the Elcometer 107 Cross Hutch Cutter. Abrasion resistance test was also conducted through a rubbing tester on three samples. Plasma pre-treated samples were less abrasion resistant than other two samples with a significant damage after 200 cycles' abrasion. Basic textures were still left on the thermal oxidized titanium substrates and the no pre-treated titanium substrates after 300 cycles' abrasion. The thermal oxidized substrates performed a better remaining surface than the substrates without any pretreatments after 500 cycles' abrasion. Most mechanical properties were demonstrated through surface structure observations under the optical microscope with max 500 magnifications.

The bioactivities of the sol-gel derived porous silica-titania coatings on titanium substrate were illustrated by incubating coated samples into simulated body fluid *in vitro*. The uncoated commercially pure titanium substrates were also immersed under the same conditions as the blank control group. All coated samples displayed the higher densities of mineral deposition than uncoated titanium substrates. Most mineral crystals (even a continuous deposited film) were found in plasma oxidized samples after 30 days incubation, which gave the plasma oxidized samples the highest bioactivity in all coated samples. The relatively continuous apatite film with mineral crystals deposited on it could be helpful to promote the desired tissue attachment on the dental implants (Li et al. 1994).

7.2 Recommendations and limitations

Throughout this master project, the potential of a sol-gel derived porous silica-titania coating on titanium substrate was preliminary examined. The experimental parameters during the coating procedure have also been optimized. However, more experimental works were strongly suggested to be accomplished before this technology could be transferred to the clinic. Thus, the following recommendations were propounded for future works.

More detailed experimentation could be conducted to further evaluate the mechanical properties of these derived coatings. The thickness of the coating could be quantitatively measured to decide the effect of spin speed on the ultimate coating thickness (Jokinen et al. 1998). Coated surface roughness and surface porosity could also be quantitatively measured (AFM for example) instead of only the qualitative description (Poon and Bhushan 1995). The adhesion of the coated surface on titanium substrate could be further evaluated by screwing a coated screw-shaped titanium implant in and out the rat femur to make sure that no damage on the coated surface would be performed through the clinical surgery (Xia et al. 2012).

Other in vitro demonstrations on the biological performance of the coated surfaces should also be conducted before the future clinical in vivo studies. The cell attachment and proliferation on coated surface, cellular metabolic activity, and osteoinductive ability were all necessary to decide the biocompatibility of the sol-gel derived silica-titania porous coating (Kim et al. 2005).

The dip coating instead of the spin coating could be conducted to perform a evenner sol-gel derived coating surface. Since the spin coating was achieved by scattering the dropped sol through centrifugal force during the spin, the unevenly distributed surface could be observed sometimes. The dip coating procedure would be helpful to create a uniformly distributed surface on substrates and the thickness of the coating could be decided by the dipping speed and the dipping time (Jokinen et al. 1998).

Functional agents could be added into the silica-titania based sol-gel derived coating. Functional agents like calcium or silver could be added into the pores on the coated silica-titania surface. Or it could be added into the original silica-titania mixed sol formula to create a functionalized silica-titania based porous coating. Adding of functional agents like calcium oxide might further improve the biocompatibility and the osteoinductivity of titanium substrates (Catauro et al. 2014). Functional agents like silver might be utilized to create an antibacterial surface on dental implants (Babapour et al. 2011).

References

- Ääritalo, Virpi, Areva, Jokinen, Lindén, and Peltola. “Sol-Gel-Derived TiO₂–SiO₂ Implant Coatings for Direct Tissue Attachment. Part I: Design, Preparation and Characterization.” *Journal of Materials Science: Materials in Medicine* 18(9), 2007: 1863–73.
doi:10.1007/s10856-007-3062-1.
- Areva, Sami, Ääritalo, Tuusa, Jokinen, Lindén, and Peltola. “Sol-Gel-Derived TiO₂–SiO₂ Implant Coatings for Direct Tissue Attachment. Part II: Evaluation of Cell Response.” *Journal of Materials Science: Materials in Medicine* 18(8), 2007: 1633–42.
doi:10.1007/s10856-007-3064-z.
- Babapour, A, B Yang, S Bahang, and W Cao. “Low-Temperature Sol–gel-Derived Nanosilver-Embedded Silane Coating as Biofilm Inhibitor.” *Nanotechnology* 22(15), 2011: 155602. doi:10.1088/0957-4484/22/15/155602.
- Bradley, C. Donald. “Metal Alkoxides as Precursors for Electronic and Ceramic Materials.” *Chemical Reviews* 89(6), 1989: 1317–1322.
- Brett, P. M., J. Harle, V. Salih, R. Mihoc, I. Olsen, F. H. Jones, and M. Tonetti. “Roughness Response Genes in Osteoblasts.” *Bone* 35(1), 2004: 124–33.
doi:10.1016/j.bone.2004.03.009.
- Brinker, C. Jeffrey, and G.W. Scherer. *Sol-Gel Science: The Physics and Chemistry of Sol-Gel Processing*. Gulf Professional Publishing, 1990.
- Buser, D., R. K. Schenk, S. Steinemann, J. P. Fiorellini, C. H. Fox, and H. Stich. “Influence of Surface Characteristics on Bone Integration of Titanium Implants. A Histomorphometric Study in Miniature Pigs.” *Journal of Biomedical Materials Research* 25(7), 1991: 889–902. doi:10.1002/jbm.820250708.
- Catauro, M., F. Bollino, F. Papale, C. Ferrara, and P. Mustarelli. “Silica–polyethylene Glycol Hybrids Synthesized by Sol–gel: Biocompatibility Improvement of Titanium Implants by

- Coating.” *Materials Science and Engineering: C* 55 (October 2015): 118–25.
doi:10.1016/j.msec.2015.05.016.
- Catauro, M., S. P. Nunziante, F. Papale, and F. Bollino. “Preparation of 0.7SiO₂·0.3CaO/PCL Hybrid Layers via Sol–gel Dip Coating for the Surface Modification of Titanium Implants: Characterization, Bioactivity and Biocompatibility Evaluation.” *Journal of Sol-Gel Science and Technology* 76(2), 2015: 241–50. doi:10.1007/s10971-015-3771-8.
- Catauro, M., F. Papale, G. Roviello, C. Ferone, F. Bollino, M. Trifuoggi, and C. Aurilio. “Synthesis of SiO₂ and CaO Rich Calcium Silicate Systems via Sol-Gel Process: Bioactivity, Biocompatibility, and Drug Delivery Tests.” *Journal of Biomedical Materials Research. Part A* 102, no. 9 (September 2014): 3087–92. doi:10.1002/jbm.a.34978.
- Catauro, M., F. Bollino, and F. Papale. “Preparation, Characterization, and Biological Properties of Organic-Inorganic Nanocomposite Coatings on Titanium Substrates Prepared by Sol-Gel: Properties of Organic-Inorganic Coatings.” *Journal of Biomedical Materials Research Part A* 102(2), 2014: 392–99. doi:10.1002/jbm.a.34721.
- Catauro, M., F. Papale, and F. Bollino. “Characterization and Biological Properties of TiO₂/PCL Hybrid Layers Prepared via Sol–gel Dip Coating for Surface Modification of Titanium Implants.” *Journal of Non-Crystalline Solids* 415, 2015: 9–15.
doi:10.1016/j.jnoncrysol.2014.12.008.
- Choi, A. H., and B. Ben-Nissan. “Sol-Gel Production of Bioactive Nanocoatings for Medical Applications. Part II: Current Research and Development.” *Nanomedicine (London, England)* 2(1), 2007: 51–61. doi:10.2217/17435889.2.1.51.
- Cousins, B.G., H.E. Allison, P.J. Doherty, C. Edwards, M.J. Garvey, D.S. Martin, and R.L. Williams. “Effects of a Nanoparticulate Silica Substrate on Cell Attachment of *Candida Albicans*.” *Journal of Applied Microbiology* 102(3), 2007: 757–65. doi:10.1111/j.1365-2672.2006.03124.x.

- Craig, R. G., and R. Z. LeGeros. "Early Events Associated with Periodontal Connective Tissue Attachment Formation on Titanium and Hydroxyapatite Surfaces." *Journal of Biomedical Materials Research* 47(4), 1999: 585–94.
- Fiebach, Klemens, and Grimm. "Resins, Natural." In *Ullmann's Encyclopedia of Industrial Chemistry*, edited by Wiley-VCH Verlag GmbH & Co. KGaA. Weinheim, Germany: Wiley-VCH Verlag GmbH & Co. KGaA, 2000. doi:10.1002/14356007.a23_073.
- Fulzele, S. V., P. M. Satturwar, and A. K. Dorle. "Polymerized Rosin: Novel Film Forming Polymer for Drug Delivery." *International Journal of Pharmaceutics* 249(1–2), 2002: 175–84.
- Fulzele, S. V., P. M. Satturwar, and A. K. Dorle. "Study of the Biodegradation and in Vivo Biocompatibility of Novel Biomaterials." *European Journal of Pharmaceutical Sciences* 20(1), 2003: 53–61.
- He, G., B. Guo, H. Wang, C. Liang, L. Ye, Y. Lin, and X. Cai. "Surface Characterization and Osteoblast Response to a Functionally Graded Hydroxyapatite/Fluoro-Hydroxyapatite/Titanium Oxide Coating on Titanium Surface by Sol-Gel Method." *Cell Proliferation* 47(3), 2014: 258–66. doi:10.1111/cpr.12105.
- Hench, L. L. *An Introduction to Bioceramics*. World Scientific, 1993.
- Hinczewski, D. Saygin, M. Hinczewski, F.Z. Tepehan, and G.G. Tepehan. "Optical Filters from SiO₂ and TiO₂ Multi-Layers Using Sol-gel Spin Coating Method." *Solar Energy Materials and Solar Cells* 87(1–4), 2005: 181–96. doi:10.1016/j.solmat.2004.07.022.
- Horkavcová, D. P. Novák, I. Fialová, M. Černý, E. Jablonská, J. Lipov, T. Ruml, and A. Helebrant. "Titania Sol-Gel Coatings Containing Silver on Newly Developed TiSi Alloys and Their Antibacterial Effect." *Materials Science and Engineering: C* 76, 2017: 25–30. doi:10.1016/j.msec.2017.02.137.
- Hou, Nicholas Yue, Hiran Perinpanayagam, Mohammad Sayem Mozumder, and Jesse Zhu. "Novel Development of Biocompatible Coatings for Bone Implants." *Coatings* 5(4), 2015: 737–57. doi:10.3390/coatings5040737.

- McPherson, E., L. Dorr, T. Gruen, and M. Saberi. "Hydroxyapatite-Coated Proximal Ingrowth Femoral Stems. A Matched Pair Control Study." *Clinical Orthopaedics and Related Research*, (315), 1995: 223–30.
- Inoue, A.. "Stabilization of Metallic Supercooled Liquid and Bulk Amorphous Alloys." *Acta Materialia* 48(1), 2000: 279–306. doi:10.1016/S1359-6454(99)00300-6.
- Jokinen, M., M. Päätsi, H. Rahiala, T. Peltola, M. Ritala, and J. B. Rosenholm. "Influence of Sol and Surface Properties on in Vitro Bioactivity of Sol-Gel-Derived TiO₂ and TiO₂-SiO₂ Films Deposited by Dip-Coating Method." *Journal of Biomedical Materials Research* 42(2), 1998: 295–302.
- Kim, H., H. Kim, V. Salih, and J. Knowles. "Hydroxyapatite and Titania Sol-Gel Composite Coatings on Titanium for Hard Tissue Implants; Mechanical Andin Vitro Biological Performance." *Journal of Biomedical Materials Research* 72B(1), 2005: 1–8. doi:10.1002/jbm.b.30073.
- Kim, H., Y. Koh, L. Li, S. Lee, and H. Kim. "Hydroxyapatite Coating on Titanium Substrate with Titania Buffer Layer Processed by Sol–gel Method." *Biomaterials* 25(13), 2004: 2533–38. doi:10.1016/j.biomaterials.2003.09.041.
- Lakshmi, R.V., T. Bharathidasan, and B. Basu. "Superhydrophobic Sol–gel Nanocomposite Coatings with Enhanced Hardness." *Applied Surface Science* 257(24), 2011: 10421–26. doi:10.1016/j.apsusc.2011.06.122.
- Le Guéhennec, L., A. Soueidan, P. Layrolle, and Y. Amouriq. "Surface Treatments of Titanium Dental Implants for Rapid Osseointegration." *Dental Materials* 23(7), 2007: 844–54. doi:10.1016/j.dental.2006.06.025.
- Lee, C., S. Lim, G. Kim, D. Kim, D. Kim, H. Lee, and K. Lee. "Rosin Microparticles as Drug Carriers: Influence of Various Solvents on the Formation of Particles and Sustained-Release of Indomethacin." *Biotechnology and Bioprocess Engineering* 9(6), 2004: 476–481.

- Lee, C., S. Lim, G. Kim, D. Kim, J. Rhee, and K. Lee. "Rosin Nanoparticles as a Drug Delivery Carrier for the Controlled Release of Hydrocortisone." *Biotechnology Letters* 27(19), 2005: 1487–90. doi:10.1007/s10529-005-1316-x.
- Li, P., K. de Groot, and T. Kokubo. "Bioactive Ca₁₀(PO₄)₆(OH)₂-TiO₂ Composite Coating Prepared by Sol-Gel Process." *Journal of Sol-Gel Science and Technology* 7(1–2), 1996: 27–34. doi:10.1007/BF00401880.
- Li, P., and K. De Groot. "Calcium Phosphate Formation within Sol-Gel Prepared Titania in Vitro and in Vivo." *Journal of Biomedical Materials Research Part A* 27(12), 1993: 1495–1500.
- Li, P., I. Kangasniemi, K. de Groot, and T. Kokubo. "Bonelike Hydroxyapatite Induction by a Gel-Derived Titania on a Titanium Substrate." *Journal of the American Ceramic Society* 77(5), 1994: 1307–12. doi:10.1111/j.1151-2916.1994.tb05407.x.
- Li, P., C. Ohtsuki, T. Kokubo, K. Nakanishi, N. Soga, and K. de Groot. "The Role of Hydrated Silica, Titania, and Alumina in Inducing Apatite on Implants." *Journal of Biomedical Materials Research Part A* 28(1), 1994: 7–15.
- Li, P., C. Ohtsuki, T. Kokubo, K. Nakanishi, N. Soga, T. Nakamura, and T. Yamamuro. "Apatite Formation Induced by Silica Gel in a Simulated Body Fluid." *Journal of the American Ceramic Society* 75(8), 1992: 2094–2097.
- Liu, X, P Chu, and C Ding. "Surface Modification of Titanium, Titanium Alloys, and Related Materials for Biomedical Applications." *Materials Science and Engineering: R: Reports* 47(3–4), 2004: 49–121. doi:10.1016/j.mser.2004.11.001.
- Macwan, D. P., P. Dave, and S. Chaturvedi. "A Review on Nano-TiO₂ Sol-gel Type Syntheses and Its Applications." *Journal of Materials Science* 46(11), 2011: 3669–86. doi:10.1007/s10853-011-5378-y.
- Milella, E., F. Cosentino, A. Licciulli, and C. Massaro. "Preparation and Characterisation of Titania/Hydroxyapatite Composite Coatings Obtained by Sol-gel Process." *Biomaterials* 22(11), 2001: 1425–31. doi:10.1016/S0142-9612(00)00300-8.

- Murphy, W. L., D. H. Kohn, and D. J. Mooney. "Growth of Continuous Bonelike Mineral within Porous Poly (Lactide-Co-Glycolide) Scaffolds in Vitro," *Journal of biomedical materials research* 50(1), 2000: 50-58.
- Ohtsuki, C., T. Kokubo, and T. Yamamuro. "Mechanism of Apatite Formation on CaOSiO₂P₂O₅ Glasses in a Simulated Body Fluid." *Journal of Non-Crystalline Solids* 143, 1992: 84–92. doi:10.1016/S0022-3093(05)80556-3.
- Overgaard, S., K. Søballe, K. Josephsen, E. S. Hansen, and C. Bünger. "Role of Different Loading Conditions on Resorption of Hydroxyapatite Coating Evaluated by Histomorphometric and Stereological Methods." *Journal of Orthopaedic Research* 14(6), 1996: 888–94. doi:10.1002/jor.1100140607.
- Pardun, K., L. Treccani, E. Volkmann, G. Destri, G. Marletta, P. Streckbein, C. Heiss, and K. Rezwan. "Characterization of Wet Powder-Sprayed Zirconia/Calcium Phosphate Coating for Dental Implants: Mixed Surface Coatings with Firm Adhesion." *Clinical Implant Dentistry and Related Research* 17(1), 2015: 186–98. doi:10.1111/cid.12071.
- Peltola, T., M. Päätsi, H. Rahiala, I. Kangasniemi, and A. Yli-Urpo. "Calcium Phosphate Induction by Sol-Gel-Derived Titania Coatings on Titanium Substrates in Vitro." *Journal of Biomedical Materials Research* 41(3), 1998: 504–10.
- Poon, C. Y., and B. Bhushan. "Comparison of Surface Roughness Measurements by Stylus Profiler, AFM and Non-Contact Optical Profiler." *Wear* 190(1), 1995: 76–88.
- Satturwar, P. M., S. V. Fulzele, and A. K. Dorle. "Evaluation of Polymerized Rosin for the Formulation and Development of Transdermal Drug Delivery System: A Technical Note." *AAPs PharmsciTech* 6(4), 2005: E649–E654.
- Tanahashi, M., T. Yao, T. Kokubo, M. Minoda, T. Miyamoto, T. Nakamura, and T. Yamamuro. "Apatite Coating on Organic Polymers by a Biomimetic Process." *Journal of the American Ceramic Society* 77(11), 1994: 2805–8. doi:10.1111/j.1151-2916.1994.tb04508.x.

- Thomas, P., W. Stoks, and A. Buegman. *Abrasion Resistant Coatings*. United States Patent. US 6291054 B1, 2001
- Brunette, D. M. *Titanium in Medicine: Material Science, Surface Science, Engineering, Biological Responses, and Medical Applications*. Springer Science & Business Media, 2001.
- Tredwin, C. J., G. Georgiou, H. Kim, and J. C. Knowles. "Hydroxyapatite, Fluor-Hydroxyapatite and Fluorapatite Produced via the Sol-gel Method: Bonding to Titanium and Scanning Electron Microscopy." *Dental Materials* 29(5), 2013: 521–29. doi:10.1016/j.dental.2013.02.002.
- Velten, D., V. Biehl, F. Aubertin, B. Valeske, W. Possart, and J. Breme. "Preparation of TiO₂ Layers on Cp-Ti and Ti6Al4V by Thermal and Anodic Oxidation and by Sol-Gel Coating Techniques and Their Characterization." *Journal of Biomedical Materials Research Part A* 59(1), 2002: 18–28.
- Wang, W., Y. Ouyang, C. Poh. "Orthopaedic Implant Technology: Biomaterials from Past to Future." *Annals of the Academy of Medicine-Singapore* 40(5), 2011: 237.
- Webster, T. J., R. W. Siegel, and R. Bizios. "Osteoblast Adhesion on Nanophase Ceramics." *Biomaterials* 20(13), 1999: 1221–1227.
- Wen, C, W Xu, W Hu, and P Hodgson. "Hydroxyapatite/Titania Sol-gel Coatings on Titanium-zirconium Alloy for Biomedical Applications." *Acta Biomaterialia* 3(3), 2007: 403–10. doi:10.1016/j.actbio.2006.10.004.
- Wennerberg, A., C. Hallgren, C. Johansson, and S. Danelli. "A Histomorphometric Evaluation of Screw-Shaped Implants Each Prepared with Two Surface Roughnesses." *Clinical Oral Implants Research* 9(1), 1998: 11–19.
- Wong, M., J. Eulenberger, R. Schenk, and E. Hunziker. "Effect of Surface Topology on the Osseointegration of Implant Materials in Trabecular Bone." *Journal of Biomedical Materials Research* 29(12), 1995: 1567–75. doi:10.1002/jbm.820291213.

- Xia, W., K. Grandfield, A. Hoess, A. Ballo, Y. Cai, and H. Engqvist. "Mesoporous Titanium Dioxide Coating for Metallic Implants." *Journal of Biomedical Materials Research Part B: Applied Biomaterials* 100B(1), 2012: 82–93. doi:10.1002/jbm.b.31925.
- Yang, B., M. Uchida, H. Kim, X. Zhang, and T. Kokubo. "Preparation of Bioactive Titanium Metal via Anodic Oxidation Treatment." *Biomaterials* 25(6), 2004: 1003–10.
- Yoshida, K., K. Kamada, K. Sato, R. Hatada, K. Baba, and M. Atsuta. "Thin Sol-Gel-Derived Silica Coatings on Dental Pure Titanium Casting." *Journal of Biomedical Materials Research* 48(6), 1999: 778–785.
- Zinger, O., K. Anselme, A. Denzer, P. Habersetzer, M. Wieland, J. Jeanfils, P. Hardouin, and D Landolt. "Time-Dependent Morphology and Adhesion of Osteoblastic Cells on Titanium Model Surfaces Featuring Scale-Resolved Topography." *Biomaterials* 25(14), 2004: 2695–2711. doi:10.1016/j.biomaterials.2003.09.111.

Curriculum Vitae

Name: Yili Cheng

Post-secondary Education and Degrees: Sichuan University
Chengdu, Sichuan, China
2011-2015 B.E.

Western University
London, Ontario, Canada
2015-2017 M.E.Sc

Related Work Experience Teaching Assistant
Western University
2016-2017